Unfolding the resident–invader dynamics of similar strategies

Fabio Dercole [a,*], Stefan A.H. Geritz [b]

[a] *Department of Electronics, Information, and Bioengineering, Politecnico di Milano, Via Ponzio 34/5, 20133 Milano, Italy*
[b] *Department of Mathematics and Statistics, University of Helsinki, Finland*

We investigate the competition between two groups of similar agents in the restricted, but classical context of unstructured populations varying in continuous time in an isolated, homogeneous, and constant abiotic environment. Individual behavioral and phenotypic traits are quantified by one-dimensional strategies and intra- as well as inter-specific interactions are described in the vicinity of a stationary regime. Some known results are revisited: invasion by a new strategy generically implies the substitution of the former resident; and resident–invader coexistence is possible close to singular stra-tegies—the stationary points of the invasion fitness—and is generically protected—each of the two competing groups can invade the other. An (almost known) old conjecture is shown true: competition close to a singular strategy is "essentially Lotka–Volterra"—dominance of one strategy, protected coexistence at an intermediate equilibrium, and mutual exclusion are the generic outcomes. And the unfolding of the competition scenarios is completed with the analysis of three degenerate singular strategies—characterized by vanishing second-order fitness derivatives—near which resident–invader coexistence can be unprotected. Our approach is based on the series expansion of a generic demographic model, w.r.t. the small strategy difference between the two competing groups, and on known results on time-scale separation and bifurcation theories. The analysis is carried out up to third order and is extendable to any order. For each order, explicit genericity conditions under which higher orders can be neglected are derived and, interestingly, they are known prior to invasion. An important result is that degeneracies up to third-order are required to have more than one stable way of coexistence. Such degeneracies can be due to particular symmetries in the model formulation, and breaking the genericity conditions provides a direct way to draw biological interpretations. The developed body of theory is exemplified on a model for the evolution of cannibalism and on Lotka–Volterra competition models.

Keywords:
Bifurcations
Competition
Ecological modeling Invasion fitness
Lotka–Volterra
Singular perturbation
Singular strategies

* Corresponding author. Tel.: +39 02 2399 3484; fax: +39 02 2399 3412.
E-mail address: fabio.dercole@polimi.it (F. Dercole).

Published Journal Article available at: http://dx.doi.org/10.1016/j.jtbi.2015.11.032

1. Introduction

Many systems, both natural and artificial, are regulated by the competition between groups of similar agents. E.g., the struggle for life between a resident and a similar mutant phenotype for the same environmental niche is the basis of the Darwinian concept of natural selection (Mayr, 1982; Maynard-Smith, 1993); marginal innovations characterize the battle for market share in many economic sectors (Grossman and Helpman, 1991; Ziman, 2000); similar strategies produced by imperfect imitation, learning or cultural transmission challenge each other in both real-life and virtual social networks and define the behavioral schemes of artificial intelligence (Sutton and Barto, 1998; Gintis, 2000; Hofbauer and Sigmund, 2003).

The performance of an *invader* strategy x_2 against a *resident* strategy x_1 is universally called the *invasion fitness* of the invader and is typically quantified by a function, that we denote $\lambda(x_1, x_2)$, measuring the initial rate of growth shown by the invader population when introduced at very small density (Metz et al., 1992). Positive/negative fitness thus indicates invasion/extinction of the invader. Typically, the best performing strategy takes over the others (Gause, 1934; Hardin, 1960; Geritz, 2005; Meszéna et al., 2005; Dercole and Rinaldi, 2008) (see Fig. 1a and b). This leads to evolutionary steps in the resident strategy in the direction of the invasion fitness gradient $\partial_{x_2}\lambda(x_1, x_2)|_{x_2=x_1}$ (Metz et al., 1996; Dieckmann and Law, 1996), i.e., in the direction that is advantageous for the invader (Fig. 1b). However, there are *singular* strategies x near which selection is not directional and allows the coexistence of similar strategies (Fig. 1c), the prerequisite for *evolutionary branching* (Metz et al., 1996; Geritz et al., 1997, 1998). These are strategies x where the fitness gradient vanishes at $x_1 = x$ and the resident–invader dynamics are ruled by the "curvatures" of the fitness landscape (i.e., by the fitness second-derivatives w.r.t. resident and invader strategies).

Resident–invader coexistence between nearly singular strategies is typically *protected*—each of the two types can invade the other, so that no one can take over the other (Fig. 1c). This is well known since from the first classification of singular strategies (Metz et al., 1996; Geritz et al., 1997, 1998), though the arrange-ment of the internal attractors of the resident–invader dynamics has been poorly investigated. Restricting to stationary coexistence, we show that competition between similar strategies works as in the classical model of Lotka (1920) and Volterra (1926): either one type dominates and leads to a stable monomorphic equilibrium (Fig. 1a and b), or coexistence is protected, with a unique stable internal equilibrium (Fig. 1c), or the two types mutually exclude each other, with a unique internal saddle equilibrium separating the basins of attraction of the two monomorphic equilibria (Fig. 1d).

Although this result may seem rather intuitive and has been surmised since Metz et al. (1996) and Geritz et al. (1997, 1998) (see also Durinx et al., 2008, where the result is shown for a particular class of single-species physiologically structured population models), its formal derivation is rather involved, as will be seen in the next sections, and its implications are broad. If, for example, an innovative strategy is able to coexist with the established ones, then we know a priori that, generically (the genericity condition turns out to be the nonvanishing fitness cross-derivative, see Fig. 1c), it cannot take over the similar residents, even if its relative abundance is arbitrarily increased. Moreover, the coexistence equilibrium being unique, there is only one way in which evolution can proceed after branching.

Resident–invader *unprotected* coexistence—coexistence that is stable together with at least one of the monomorphic equilibria—is possible close to a singular strategy characterized by degeneracies in the curvatures of the fitness landscape. The two most simple configurations are depicted in Fig. 1e and f. We show that these are the only possible competition scenarios if fitness degeneracies do not involve the third-order derivatives at the singular strategy. Note that in Fig. 1f there is only one stable equilibrium of

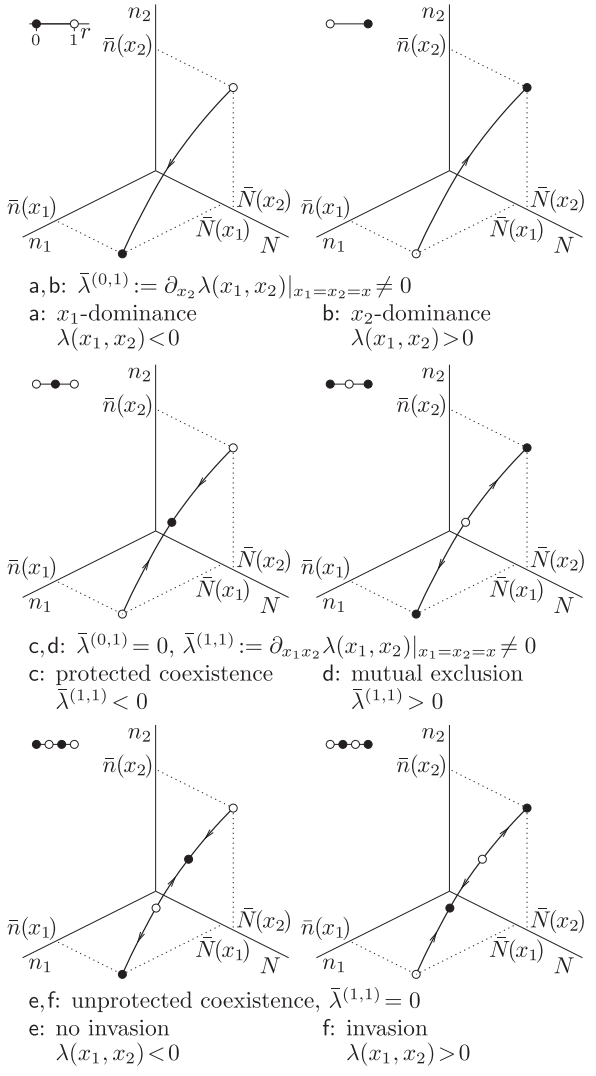

Fig. 1. Competition scenarios of the resident–invader dynamics between two similar strategies x_1 (resident, density n_1) and x_2 (invader, density n_2), possibly interacting with other resident populations (densities in vector N, graphically represented as one-dimensional). Strategies x_1 and x_2 are thought to be close to a reference strategy x, that is nonsingular in cases a and b, and singular (i.e., $\bar{\lambda}^{(0,1)}=0$) in cases c–f. The singular strategy x is generic in cases c and d (i.e., $\bar{\lambda}^{(1,1)}\neq 0$), and degenerate in cases e and f. In the absence of invader, the resident populations coexist at the stable equilibrium $(\bar{n}(x_1),\bar{N}(x_1))$. After resident substitution, the new residents coexist at $(\bar{n}(x_2),\bar{N}(x_2))$. The dynamics of the relative density of the invader, $r := n_2/(n_1+n_2)$, are schematically represented in the top-left of each panel. The sketches of the r-dynamics will be used to identify the six scenario in Section 4.

coexistence, so that, again, there is no ambiguity on about how evolution may proceed. And more in general, we show that fitness degeneracies up to order $k \geq 1$ are required to have up to k internal equilibria in the resident–invader competition dynamics.

In this paper we restrict the analysis to the stationary coexistence between two similar strategies involved in intra- as well as inter-specific interactions, and we place our analysis in the classical framework in which most of theoretical ecology and evolution have been developed. That is: unstructured and asexual populations varying in continuous time in an isolated, homogeneous, and constant abiotic environment, with individual behavioral and phenotypic traits quantified by scalar (i.e., one-dimensional) continuous strategies. This is also the classical framework for the game-theoretical view of economics and social sciences, where individuals are natural or artificial agents (e.g., human beings, robots, segments of computer code, and commercial products) playing different strategies in a market or in a social network.

We unfold the competition scenarios between two sufficiently similar strategies x_1 (resident) and x_2 (invader) that can generically occur: (1) away from singularity, thus reobtaining the "invasion implies substitution principle" (Geritz, 2005; Meszéna et al., 2005; Dercole and Rinaldi, 2008); (2) close to a generic singular strategy, proving that competition between similar strategies is "essentially Lotka–Volterra"; and (3) close to degenerate singular strategies characterized by trivial configurations (e.g., vanishing) second-order fitness derivatives. Analogous results are expected to hold for the case of structured populations, where the total population density is partitioned into physiological classes, e.g., according to age or stage, living in heterogeneous habitats, and for the case of multi-dimensional (vector-valued) strategies. However, the derivation is much more involved and will be addressed separately.

We do not investigate the evolutionary dynamics resulting from repeated invasions, locally to the singular strategy. The evolutionary scenarios are well known only locally to generic singular strategies (Geritz et al., 1997, 1998), whereas nothing is basically known for degenerate fitness configurations. In particular, unexpected evolutionary scenarios are possible when the evolutionary dynamics are dominated by third- (or higher-) orders in the fitness expansion, e.g., evolutionary branching has been numerically observed by Doebeli and Ispolatov (2010) locally to an attracting evolutionary stable strategy (convergence-stable ESS). This remains an open problem in the modeling framework of Adaptive Dynamics (AD; Metz et al., 1996; Dieckmann and Law, 1996; Geritz et al., 1997, 1998; Dercole and Rinaldi, 2008), that we will address separately, but we note that our analyses of the underlying competition scenarios are suited for that purpose, too.

The methodological approach is based on the series expansion of a generic demographic model with respect to the small difference between the resident and invader strategies. As a result, the sum of the resident and invader population densities, as well as the abundances of the other interacting populations, change faster than the resident–invader relative densities ($1-r$ and r in Fig. 1). Because of this separation of time scales, the slow dynamics of the invader relative density are essentially one-dimensional and can be studied in isolation (see the sketches of the r-axis in Fig. 1). Moreover, by exploiting a specific structure relating the derivatives w.r.t. the resident strategies of the populations' growth rates (recently introduced by Dercole, 2015), all our results are expressed in terms of quantities to be evaluated at the resident monomorphic equilibrium (i.e., at $(\overline{n}(x_1), \overline{N}(x_1))$ in Fig. 1), before the invasion occurs. This is important in applications, where all such quantities can be interpreted biologically or economically and experimentally estimated without waiting for the appearance of the invader strategy.

The competition scenarios that are generically possible in the above mentioned situations (1)–(3) are classified, together with the *bifurcation* boundaries (Kuznetsov, 2004; Meijer et al., 2009) separating them in the plane (x_1, x_2) of the resident and invader strategies. In case (1), the first-order expansion is enough to fully characterize the resident–invader dynamics, provided, as expected, the slope of the invasion fitness does not vanish, whereas case (2) requires a second-order expansion and, as genericity conditions, a nonvanishing fitness cross-derivative (i.e., the second-derivative $\overline{\lambda}^{(1,1)}$ in Fig. 1) and unequal second-order pure-derivatives. These two conditions were already shown to discriminate the classification of singular strategies (Metz et al., 1996; Geritz et al., 1997, 1998). In addition, we show that a nonvanishing fitness cross-derivative is the genericity condition under which coexistence is protected whenever it occurs between nearly singular strategies. This result attributes quite an important role to the fitness cross-derivative, that can be geometrically thought as determining the fitness sign (positive/negative for invasion/extinction of the invader) when the competing strategies x_1 and x_2 are locally perturbed from the singular value x in opposite directions. That is, a negative/positive $\lambda^{(1,1)}$ (see Fig. 1c and d) gives a positive/negative fitness for $x_1 = x-\varepsilon$, $x_2 = x+\varepsilon$, ε small.

As for nongeneric singular strategies, we consider all possible degeneracies related to particular configurations of the second-order fitness derivatives. That is: case (3.1) of equal pure-derivatives (and nonvanishing cross-derivative), characterized by two colliding singular strategies; case (3.2) of vanishing cross-derivative (and nonvanishing pure-derivatives), showing that unprotected coexistence is indeed possible for nearby resident and invader strategies; case (3.3) in which the above degeneracies occurs together, which implies that all second-order fitness derivatives vanish, so that the resident–invader dynamics are fully determined by third-order terms in the expansion. The latter double degeneracy (codimension-two, in the jargon of bifurcation theory) is definitely less important in applications, but yet interesting because the evolutionary scenarios at these singular strategies are also ruled by third-order conditions that still need to be explored.

Higher-order degeneracies can also be analyzed by means of our approach, by simply breaking the genericity conditions at one order, e.g., due to particular symmetries in the model formulation, and proceeding to the next order expansion. Also worth to note is that, within a given assumed degeneracy (cases (3.1)–(3.3)), we assume a *generic* demographic model. This means that each time our results hold under a certain condition, we assume that condition as generically satisfied. However, if this is not the case, because of the peculiarity of a specific model, again our approach can go through, to the analysis of the leading order. One example for all: Lotka–Volterra competition models are nongeneric. Because the per-capita growth rates of the two competing stra-tegies are linearly density dependent, they cannot show unpro-tected coexistence (there cannot be more than one internal equi-librium in the resident–invader dynamics). Given the popularity of Lotka–Volterra competition models in ecological theory, they are specifically analyzed in the example section.

The main significance of this paper resides in the proposed methodological approach and in the analysis of degenerate singular strategies (cases (3.1)–(3.3) above), as cases (1) and (2) has been long known or conjectured. An important result emerging from our analysis is that some specific degeneracies in the third-order derivatives of the model equations are required in order to have more than one stable way of coexistence between the two competing strategies. Thus, even though coexistence can be unprotected under second-order degeneracies, there is generically only one way in which evolution can proceed after branching. The

analytic expressions of the third-order degeneracies yielding two stable coexistence equilibria are not easily interpretable but, again, can be experimentally tested prior to invasion.

Another interesting result can be drawn by complementing our local analysis (strategies x_1 and x_2 in the vicinity of a reference strategy x) with the global analysis of Priklopil (2012) of the boundaries, in the strategy plane (x_1, x_2), of the region allowing coexistence. We can indeed conclude that the competition scenarios that we see locally to a degenerate singular strategy do also occur in the vicinity of a generic, though nearly degenerate singu-larity, but require a small finite difference between the resident and invader strategies. For example, we can generically expect unpro-tected coexistence close to a singular strategy with small (negative) fitness cross-derivative (see Fig. 1c and e and f). This justifies the extra effort required for unfolding the competition scenarios that are possible locally to degenerate singular strategies.

The paper is organized as follows. We start by introducing in Section 2.1 the basic notation and assumptions of our demographic model and, in Section 2.2, the fast and slow variables that are useful for the analysis. Then, in Section 2.3, we exploit the time-scale separation and derive the approximation of the (one-dimensional) invader relative dynamics up to third order in the difference between resident and invader strategies. Most computations have been handled symbolically, so part of the proof relies on the output of a *Mathematica* script that is attached as online Supplementary Data. Some intermediate results are reported in Appendices A and B.

In Section 3, the classification of the competition scenarios is organized in the three levels of genericity corresponding to cases (1), (2), and (3.1)–(3.3) above: away from singularity (Section 3.1), close to a generic singular strategy (Section 3.2), and close to (codimension-one and -two) degenerate singular strategies (Sections 3.1–3.3). Sections 3.1–3.3 are essentially analytic and can be skipped by the non-interested reader (though the opening of Section 3 is worth reading). The results are summarized (with emphasis on geometrical and biological interpretation) in Section 4, that can be used as a practical guide to the classification of competition scenarios.

Section 5 is dedicated to two examples. The first is a model proposed in the literature to study the evolution of cannibalism (Dercole and Rinaldi, 2002; Dercole, 2003), in which all studied degenerate singular strategies occur for suitable values of the model parameters. The second particularizes our analysis to the case of Lotka–Volterra competition models. In particular, we show that all degenerate singular strategies (vanishing fitness cross-derivative) are further degenerate than generically expected, and this indeed prevents the possibility of unprotected coexistence. However, in the presence of any non-Lotka–Volterra interaction, e. g., resident and invader prey are preyed upon by a predator with Holling-type-II functional response (see, e.g., Dercole et al., 2003), the model turns out to be generic (in respect of our analysis), even if resident–invader competition is Lotka–Volterra.

Section 6 closes the paper with first a discussion of the presented results in the light of those already available in the literature (mainly in the original papers Metz et al., 1996; Geritz et al., 1997, 1998, but also in Geritz, 2005; Meszéna et al., 2005, and in Durinx et al., 2008) and then a vision on the future directions for the analysis of resident–invader and evolutionary dynamics.

2. Methods

2.1. Basic notation and assumptions

We consider two similar competing populations with abundances measured by densities $n_1(t)$ and $n_2(t)$ at time t, whose individuals only differ in the value of a one-dimensional strategy (or trait) x that takes value x_1 in population 1 and x_2, arbitrarily close to x_1, in population 2. We refer to populations 1 and 2 as the *resident* and the *invader*, respectively, and allow them to interact with P other populations of the same or different type (or species), with densities packed in the vector $N(t)\in\mathbb{R}^P$ and corresponding strategies (finitely different from x_1 and x_2 in the case of populations of the resident and invader type) not explicitly pointed out. We study the demographic dynamics of the community in the $(2+P)$−dimensional space (n_1, n_2, N) (see Fig. 1, where the N-axis represents a P-dimensional subspace). Note that strategies x_1 and x_2 play the role of constant parameters. Since populations 1 and 2 are each composed of individuals of the same type, their percapita growth rates $\dot{n}_1/n_1$ and $\dot{n}_2/n_2$ can be expressed through a unique function suitably operating on the densities (n_1, n_2, N) and on the strategies (x_1, x_2). This can be done using the so-called *fit-ness generating function* (or g-function, Vincent and Brown, 2005) $g(n_1, n_2, N, x_1, x_2, x')$ that gives the per-capita growth rates of a population of strategy x' with infinitesimally small density, in an environment where strategies x_1 and x_2 are present with densities n_1 and n_2 and all other populations are present according to the density vector N. Then, $\dot{n}_1/n_1$ and $\dot{n}_2/n_2$ are given by the g-function evaluated for $x'=x_1$ and $x'=x_2$, respectively (see Section 5 for specific examples). Packing the population growth rates $\dot{N}$ in the vector-valued function F, the demographic dynamics of the community read:

$$\dot{n}_1 = n_1\, g(n_1, n_2, N, x_1, x_2, x_1), \tag{1a}$$

$$\dot{n}_2 = n_2\, g(n_1, n_2, N, x_1, x_2, x_2), \tag{1b}$$

$$\dot{N} = F(n_1, n_2, N, x_1, x_2). \tag{1c}$$

Model (1) is henceforth called the *resident–invader* model.

In order to define reasonable population dynamics, we assume that functions g and F enjoy the four basic properties described below. The first three are trivial, whereas the fourth one is more involved and has been recently shown in Dercole (2015) to be a consequence of the natural way in which ecological models are written in terms of individual strategies. Here and in the rest of the paper, we assume smoothness and use lists of integer superscripts to indicate the position of the arguments w.r.t. which we take derivatives and the order of differentiation (this is the notation used by *Mathematica* for derivatives and should facilitate the inspection of the *Mathematica* scripts accompanying the paper), e. g., $g^{(1,0,0,0,0,0)}$ and $g^{(0,0,1,0,0,0)}$ are the first-order partial derivatives of g w.r.t. n_1 and N, so, while the first is a real number, the second is a P-dimensional row vector; $g^{(2,0,0,0,0,0)}$, $g^{(1,0,1,0,0,0)}$, and $g^{(0,0,2,0,0,0)}$ are examples of second-order derivatives, a real number, a P-dimensional row vector, and tensor operator from $\mathbb{R}^P\times\mathbb{R}^P$ into $\mathbb{R}$, respectively,

P1 : $g(n_1, 0, N, x_1, x_2, x') = g_1(n_1, N, x_1, x')$,
$F(n_1, 0, N, x_1, x_2) = F_1(n_1, N, x_1)$,

for suitable functions g_1 and F_1. The per-capita growth rate of a strategy x', as well as those of the populations in N, are not affected by the strategy x_2 of an absent population:

P2 : $g(n_1, n_2, N, x, x, x') = g(\alpha(n_1+n_2), (1-\alpha)(n_1+n_2), N, x, x, x')$,
$F(n_1, n_2, N, x, x) = F(\alpha(n_1+n_2), (1-\alpha)(n_1+n_2), N, x, x)$,

for any $0\le\alpha\le 1$. Any partitioning of the total density (n_1+n_2) into two populations with same strategy x must result in the same per-capita growth rate for strategy x' and for the populations in N.

P3 : $g(n_1, n_2, N, x_1, x_2, x') = g(n_2, n_1, N, x_2, x_1, x')$,
$F(n_1, n_2, N, x_1, x_2) = F(n_2, n_1, N, x_2, x_1)$.

The order in which populations 1 and 2 are considered is irrelevant.

$$\text{P4}: g^{(0,0,0,d_1,0,0)}(n_1,n_2,N,x,x,x') = \sum_{i_1=1}^{d_1} \phi_{d_1,i_1}(n_1+n_2,N,x,x')n_1^{i_1},$$

$$g^{(0,0,0,d_1,d_2,0)}(n_1,n_2,N,x,x,x') = \sum_{i_1=1}^{d_1}\sum_{i_2=1}^{d_2} \phi_{d_1,d_2,i_1,i_2}(n_1+n_2,N,x,x')n_1^{i_1}n_2^{i_2},$$

$$F^{(0,0,0,d_1,0)}(n_1,n_2,N,x,x) = \sum_{i_1=1}^{d_1} \psi_{d_1,i_1}(n_1+n_2,N,x)n_1^{i_1},$$

$$F^{(0,0,0,d_1,d_2)}(n_1,n_2,N,x,x) = \sum_{i_1=1}^{d_1}\sum_{i_2=1}^{d_2} \psi_{d_1,d_2,i_1,i_2}(n_1+n_2,N,x)n_1^{i_1}n_2^{i_2},$$

for suitable functions ϕ_{d_1,i_1}, ϕ_{d_1,d_2,i_1,i_2}, ψ_{d_1,i_1}, and ψ_{d_1,d_2,i_1,i_2}, d_1, $d_2 \geq 1$. This follows from a generalization of the principle of *mass-action*, according to which function g (resp. F) describes the interactions of a target individual with strategy x' (resp. belonging to a population in N) through pairwise encounters with other individuals, which are, in turn, involved in other interactions (Dercole, 2015). When considering identical resident and invader strategies, $x_1 = x_2 = x$, the sensitivity (i.e., the derivative) of the growth rate g (resp. F) w.r.t. x at fourth or fifth argument is proportional to the density of the corresponding individuals, n_1 or n_2, whose strategy is being perturbed by the derivative, with a proportionality coefficient that can be density-dependent only as a function of the total density n_1+n_2. Moreover, due to nonlinear density dependencies in g (resp. F), higher powers of n_1 and n_2 may appear in further derivatives (up to the order d_1 and d_2 of differentiation).

Properties P1–P4 can be combined to produce further relations among g-derivatives that will be taken into account in our computations (in particular in the Supplementary Data). Specifically:

$$\text{P1,2a}: g^{(l_1,l_2,0,0,0,0)}(n_1,n_2,N,x,x,x') = g_1^{(l_1+l_2,0,0,0)}(n_1+n_2,N,x,x'),$$
$$F^{(l_1,l_2,0,0,0)}(n_1,n_2,N,x,x) = F_1^{(l_1+l_2,0,0)}(n_1+n_2,N,x),$$

i.e., n_1- and n_2-perturbations simply perturb the total density (n_1+n_2) if the two populations have the same strategy x:

$$\text{P1,2b}: \sum_{i=0}^{d}\binom{d}{i} g^{(l_1,l_2,0,i,d-i,0)}(n_1,n_2,N,x,x,x') = g_1^{(l_1+l_2,0,d,0)}(n_1+n_2,N,x,x'),$$

$$\sum_{i=0}^{d}\binom{d}{i} F^{(l_1,l_2,0,i,d-i)}(n_1,n_2,N,x,x) = F_1^{(l_1+l_2,0,d)}(n_1+n_2,N,x),$$

$d \geq 1$, obtained by x-differentiating P1,2a:

$$\text{P1,3}: g(0,n_2,N,x_1,x_2,x') = g_1(n_2,N,x_2,x'),$$
$$F(0,n_2,N,x_1,x_2) = F_1(n_2,N,x_2).$$

$$\text{P1,4}: g_1^{(0,0,d,0)}(n,N,x,x') = \sum_{i=1}^{d} \phi_{d,i}(n,N,x,x')n^i,$$

$$F_1^{(0,0,d)}(n,N,x) = \sum_{i=1}^{d} \psi_{d,i}(n,N,x)n^i.$$

$$\text{P1,2,4}: \sum_{i=i_1}^{d-i_2}\binom{d}{i}\phi_{i,d-i,i_1,i_2}(n,N,x,x') = \binom{i_1+i_2}{i_1}\phi_{d,i_1+i_2}(n,N,x,x'),$$

$$\sum_{i=i_1}^{d-i_2}\binom{d}{i}\psi_{i,d-i,i_1,i_2}(n,N,x) = \binom{i_1+i_2}{i_1}\psi_{d,i_1+i_2}(n,N,x),$$

for each $i_1, i_2 \geq 1$ with $i_1+i_2 \leq d \geq 2$, obtained by substituting P4 and P1,4 into P1,2b (with $l_1 = l_2 = 0$) and by balancing same (n_1,n_2)−monomials at the left- and right-hand sides. In particular,

$$\begin{aligned}
&d=2,\ i_1=1,\ i_2=1 \quad \text{gives } 2\phi_{1,1,1,1} = 2\phi_{2,2},\\
&d=3,\ i_1=1,\ i_2=1 \quad \text{gives } 3\phi_{1,2,1,1} + 3\phi_{2,1,1,1} = 2\phi_{3,2},\\
&d=3,\ i_1=1,\ i_2=2 \quad \text{gives } 3\phi_{1,2,1,2} = 3\phi_{3,3},\\
&d=3,\ i_1=2,\ i_2=1 \quad \text{gives } 3\phi_{2,1,2,1} = 3\phi_{3,3},
\end{aligned}$$

thus linking the functions ϕ's with two sum indexes to those characterized by a single sum index, and similarly for functions ψ's.

$$\text{P3,4a}: g^{(0,0,0,0,0,d_2,0)}(n_1,n_2,N,x,x,x') = \sum_{i_2=1}^{d_2} \phi_{d_2,i_2}(n_1+n_2,N,x,x')n_2^{i_2},$$

$$F^{(0,0,0,0,0,d_2)}(n_1,n_2,N,x,x) = \sum_{i_2=1}^{d_2} \psi_{d_2,i_2}(n_1+n_2,N,x)n_2^{i_2}.$$

$$\text{P3,4b}: \phi_{d_1,d_2,i_1,i_2} = \phi_{d_2,d_1,i_2,i_1},$$
$$\psi_{d_1,d_2,i_1,i_2} = \psi_{d_2,d_1,i_2,i_1}.$$

$$\text{P1}-4: \quad \phi_{1,1,1,1} = \phi_{2,2},\quad \phi_{2,1,1,1} = \phi_{1,2,1,1} = \tfrac{1}{3}\phi_{3,2},$$
$$\phi_{2,1,2,1} = \phi_{1,2,1,2} = \phi_{3,3},\quad \psi_{1,1,1,1} = \psi_{2,2},$$
$$\psi_{2,1,1,1} = \psi_{1,2,1,1} = \tfrac{1}{3}\psi_{3,2},\quad \psi_{2,1,2,1} = \psi_{1,2,1,2} = \psi_{3,3},$$

obtained by exploiting P3,4b in the examples of P1,2,4. Moreover, further derivatives w.r.t. N and x' can be added to all properties.

Examples of property P4 are

$$g^{(0,0,0,1,0,0)} = \phi_{1,1}\, n_1,\quad g^{(0,0,0,1,1,0)} = \phi_{2,2}\, n_1 n_2,\quad g^{(0,0,0,2,0,0)} = \phi_{2,1}\, n_1 + \phi_{2,2}\, n_1^2$$

(where arguments have been omitted for brevity), to which derivatives w.r.t. (n_1,n_2) apply as follows:

$$\begin{aligned}
g^{(1,0,0,1,0,0)} &= \phi_{1,1} + \phi_{1,1}^{(1,0,0,0)} n_1,\\
g^{(0,1,0,1,0,0)} &= \phi_{1,1}^{(1,0,0,0)} n_1,\\
g^{(1,1,0,1,0,0)} &= \phi_{1,1}^{(1,0,0,0)} + \phi_{1,1}^{(2,0,0,0)} n_1,\\
g^{(1,0,0,1,1,0)} &= \phi_{2,2}\, n_2 + \phi_{2,2}^{(1,0,0,0)} n_1 n_2,\\
g^{(1,0,0,2,0,0)} &= \phi_{2,1} + (\phi_{2,1}^{(1,0,0,0)} + 2\phi_{2,2}) n_1 + \phi_{2,2}^{(1,0,0,0)} n_1^2
\end{aligned}$$

(analogous examples hold for function F).

As anticipated in the Introduction, we consider the (simplest, but most typical) case of stationary coexistence. In particular, we assume that for all values of the strategy x_1 that we consider, the resident population (population 1) coexists with the other populations accounted for by vector N at a strictly positive and (hyperbolically) stable equilibrium of the model ((1a) and (1c)), with $n_2 = 0$. Denoting the equilibrium densities with functions $\overline{n}(x_1)$ and $\overline{N}(x_1)$, we thus have

$$0 = g_1(\overline{n}(x_1), \overline{N}(x_1), x_1, x_1), \tag{2a}$$

$$0 = F_1(\overline{n}(x_1), \overline{N}(x_1), x_1) \tag{2b}$$

(see property P1 above). Note that the hyperbolicity of the resident equilibrium (i.e., nonzero real part of all associated eigenvalues) and the similarity between the resident and invader populations ($x_1 \simeq x_2$), guarantee that the invader population (population 2) is also able to coexist with populations N at the strictly positive (and hyperbolically stable) equilibrium $(\overline{n}(x_2), \overline{N}(x_2))$ of model ((1b) and (1c)) with $n_1 = 0$. In other words, the resident–invader model (1) admits the two monomorphic equilibria $(\overline{n}(x_1), 0, \overline{N}(x_1))$ and $(0, \overline{n}(x_2), \overline{N}(x_2))$ (see Fig. 1) for all the pairs (x_1,x_2) that we consider.

One of the most important concept in evolutionary biology is that of *invasion fitness* (Metz et al., 1992), defined as the exponential rate of growth initially shown by the invader population when introduced at very small density in the resident community

at equilibrium, i.e.,

$$\lambda(x_1,x_2) \coloneqq g_1(\overline{n}(x_1),\overline{N}(x_1),x_1,x_2). \tag{3}$$

A positive fitness means that the invader population indeed invades the resident community, at least temporary, while innovative strategies with a negative fitness go extinct (as it is implied by our analysis in Section 3 and previously proven in Geritz et al. (2002), invasion followed by eventual extinction—see, e.g., Mylius and Diekmann (2001) and Dercole et al. (2002)—requires a non-hyperbolic resident equilibrium).

Technically, $\lambda(x_1,x_2)$ is the eigenvalue (from which the symbol λ in lieu of the traditionally used s) of the monomorphic equilibrium $(\overline{n}(x_1),0,\overline{N}(x_1))$ of model (1) corresponding to the (unique) eigenvector with nonzero n_2 component (see Fig. 1). So, the sign of $\lambda(x_1,x_2)$ tells the (local) stability of the equilibrium, all other eigenvalues having negative real part by the hyperbolic stability of the resident equilibrium. Similarly, $\lambda(x_2,x_1)$ is the eigenvalue of the monomorphic equilibrium $(0,\overline{n}(x_2),\overline{N}(x_2))$ corresponding to the eigenvector with nonzero n_1 component.

The invasion fitness gives only local information on the resident–invader dynamics. The eventual fate of the invader population depends, in principle, on the full nonlinearity of the demographic model (1). What can be said based only on invasion considerations, i.e., without looking in the interior of the resident–invader demographic state space, has puzzled theoretical biologists since from the advent of the phenotypic approaches to evolutionary biology. A major role is played by the so-called *selection gradient*, $\lambda^{(0,1)}(x_1,x_1)$, i.e., the slope of the fitness landscape at the resident strategy in the direction of the invader strategy. The evolution of the resident strategy has been postulated in the direction of the selection gradient, grounded on the principle that invasion always (or, better, generically) implies substitution (see Fig. 1b), and this type of evolutionary dynamics has been called "canonical" (Dieckmann and Law, 1996; Dercole and Rinaldi, 2008), as it also agrees with quantitative genetics considerations (Bulmer, 1980). But the principle became a theorem only much later (Geritz, 2005; Meszéna et al., 2005; Dercole and Rinaldi, 2008) and, as already mentioned in the Introduction, it is revisited in Section 2.2 and also in Section 3.1. Whereas the unfolding of resident–invader coexistence, whether protected or not, based on information prior to invasion, remained incomplete. In Section 3 we show how suitable evaluations of the g-function g_1 (and of function F_1, see property P1) at the resident equilibrium are sufficient to fully characterize the resident–invader dynamics for x_1 sufficiently close to x_2.

2.2. A useful change of variables and parameters

Following Meszéna et al. (2005) and Dercole and Rinaldi (2008), we introduce the sum s of the resident and invader densities and the relative density of invaders $r \in [0,1]$ as new variables, i.e.,

$$s = n_1+n_2, \quad r \coloneqq \frac{n_2}{n_1+n_2}, \tag{4a}$$

with invertible transformations given by

$$n_1 = (1-r)s, \quad n_2 = rs. \tag{4b}$$

We also introduce polar coordinates in the parameter plane of the resident and invader strategies, i.e., we set

$$x_1 = x+\varepsilon\cos\theta, \quad x_2 = x+\varepsilon\sin\theta \tag{5}$$

(see Fig. 2), where x is a reference strategy close to x_1 and x_2, that will be assumed to be nonsingular in Section 3.1 and singular in Sections 3.2 and 3.3. In other words, x is the strategy around which we study the competition between similar strategies and θ (obviously different from $\frac{1}{4}\pi$ and $\frac{5}{4}\pi$) gives the direction of perturbation of point (x_1,x_2) from (x,x). Our aim is to determine the

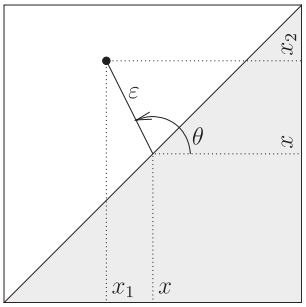

Fig. 2. Polar coordinates in the plane of resident and invader strategies.

competition scenarios in the limit $\varepsilon \to 0$ for any given θ, i.e., for sufficiently similar strategies x_1 and x_2 along each possible ray emanating from x.

Due to the symmetry of model (1) w.r.t. the diagonal $x_1 = x_2$ (see property P3), we only need to consider the region of the strategy plane above the diagonal, where

$$\tfrac{1}{4}\pi < \theta < \tfrac{5}{4}\pi \quad \text{and} \quad x_2-x_1 = \varepsilon(\sin\theta-\cos\theta) > 0. \tag{6}$$

The resident–invader dynamics for (x_1,x_2) below the diagonal can be obtained from those corresponding to the symmetric point (x_2,x_1) above the diagonal, by also exchanging n_1 with n_2.

In the new variables (4) and parameters (5), we can write model (1) as

$$\begin{aligned}\dot{s} &= \dot{n}_1+\dot{n}_2\\ &= n_1\, g(n_1,n_2,N,x+\varepsilon\cos\theta,x+\varepsilon\sin\theta,x+\varepsilon\cos\theta)\\ &\quad + n_2\, g(n_1,n_2,N,x+\varepsilon\cos\theta,x+\varepsilon\sin\theta,x+\varepsilon\sin\theta)\\ &= s\, g(s,0,N,x,x,x)+O(\varepsilon),\end{aligned} \tag{7a}$$

$$\begin{aligned}\dot{r} &= \frac{\dot{n}_2(n_1+n_2)-n_2(\dot{n}_1+\dot{n}_2)}{(n_1+n_2)^2}\\ &= \frac{n_1n_2}{(n_1+n_2)^2}\, g(n_1,n_2,N,x+\varepsilon\cos\theta,x+\varepsilon\sin\theta,x+\varepsilon\sin\theta)\\ &\quad - \frac{n_1n_2}{(n_1+n_2)^2}\, g(n_1,n_2,N,x+\varepsilon\cos\theta,x+\varepsilon\sin\theta,x+\varepsilon\cos\theta)\\ &= \varepsilon(\sin\theta-\cos\theta)r(1-r)g^{(0,0,0,0,0,1)}(s,0,N,x,x,x)+O(\varepsilon^2),\end{aligned} \tag{7b}$$

$$\dot{N} = F(n_1,n_2,N,x+\varepsilon\cos\theta,x+\varepsilon\sin\theta) = F(s,0,N,x,x,x)+O(\varepsilon), \tag{7c}$$

where the right-hand sides have been ε-expanded around $\varepsilon = 0$ (i.e., $x_1 = x_2 = x$), property P2 has been exploited, and the big-O notation collects higher-order terms.

From Eqs. (7), we see that s and N are "fast" variables, converging if $\varepsilon = 0$ to the resident equilibrium, $\overline{n}(x)$ and $\overline{N}(x)$, respectively, on the time scale of time t, whereas r is a "slow" variable, whose dynamics develop on the time scale of the new time variable $\tau = \varepsilon t$. We also see that $r=0$ and $r=1$ are constant solutions for r (also for small but finite ε), corresponding to the two monomorphic equilibria.

Well-known results on time-scale separation (see Hoppensteadt, 1966; Fenichel, 1979, for the original contributions and Hek, 2010, for a survey oriented to ecology), say that, thanks to the hyperbolicity of the resident equilibrium, the dynamics of model (7) for sufficiently small ε are equivalent to the so-called "singular" ones (not to be confused with the singularity of strategies!), obtained for $\varepsilon = 0$. That is, the fast segment

$$\dot{s} = s\, g(s,0,N,x,x,x), \quad \dot{N} = F(s,0,N,x,x,x), \quad r(t) = r(0), \quad t \geq 0, \tag{8a}$$

along which s and N converge to $\overline{n}(x)$ and $\overline{N}(x)$ at constant r, concatenated with the slow segment ruled by

$$\frac{\mathrm{d}r}{\mathrm{d}\tau} \frac{1}{(\sin\theta-\cos\theta)r(1-r)} = g^{(0,0,0,0,0,1)}(\overline{n}(x),0,\overline{N}(x),x,x,x) = \lambda^{(0,1)}(x,x), \tag{8b}$$

with constant $s(\tau)=\overline{n}(x)$ and $N(\tau)=\overline{N}(x)$, $\tau\geq 0$ (the factor $(\sin\theta-\cos\theta)r(1-r)$ has been moved to the left-hand side just for typesetting convenience).

From Eq. (8b) we immediately get the "invasion implies substitution" theorem: invasion with nonzero selection gradient, i.e., positive $\lambda^{(0,1)}(x,x)$ and $(\sin\theta-\cos\theta)$ $(x_2>x_1$, recall (6)), or negative $\lambda^{(0,1)}(x,x)$ and $(\sin\theta-\cos\theta)$ $(x_2<x_1)$, implies the substitution of the resident type ($r(\tau)\to 1$ for any $r(0)\in(0,1)$).

In order to shorten the notation, in the next sections, we will omit the arguments of functions g and F, by indicating with a "bar" the evaluations at $(\overline{n}(x),0,\overline{N}(x),x,x,x)$ and at $(\overline{n}(x),0,\overline{N}(x),x,x)$, respectively, otherwise we assume evaluations at (n_1,n_2,N,x,x,x) and (n_1,n_2,N,x,x). Similarly, we will write $\overline{\phi}^{(l,m,0,q)}_{d_1,i_1}$, $\overline{\phi}^{(l,m,0,q)}_{d_1,d_2,i_1,i_2}$, $\overline{\psi}^{(l,m,0)}_{d_1,i_1}$, and $\overline{\psi}^{(l,m,0)}_{d_1,d_2,i_1,i_2}$ for $\phi^{(l,m,0,q)}_{d_1,i_1}(\overline{n}(x),\overline{N}(x),x,x)$, $\phi^{(l,m,0,q)}_{d_1,d_2,i_1,i_2}(\overline{n}(x),\overline{N}(x),x,x)$, $\psi^{(l,m,0,q)}_{d_1,i_1}(\overline{n}(x),\overline{N}(x),x)$, and $\psi^{(l,m,0,q)}_{d_1,d_2,i_1,i_2}(\overline{n}(x),\overline{N}(x),x)$ when using property P4 of Section 2.1, $\overline{\lambda}^{(d,q)}$ for $\lambda^{(d,q)}(x,x)$, and $\overline{n}^{(d)}$ and $\overline{N}^{(d)}$ for $\overline{n}^{(d)}(x)$ and $\overline{N}^{(d)}(x)$. For example, we have $\overline{g}^{(0,0,0,0,0,1)}=\overline{\lambda}^{(0,1)}$ and $\overline{g}^{(1,0,0,1,0,0)}=\overline{\phi}_{1,1}+\overline{\phi}^{(1,0,0,0)}_{1,1}\overline{n}$.

Our aim is that of writing the expansion of Eq. (7b) in terms of "bar"-evaluations, i.e., evaluations prior to invasion at the resident equilibrium (note that "bar"-evaluations only require functions g_1 and F_1 of property P1). We will see that this is indeed possible thanks to properties P1–P4, property P4 in particular.

2.3. Time-scale separation

When the selection gradient $\overline{\lambda}^{(0,1)}$ vanishes, the singular slow equation becomes $\mathrm{d}r/\mathrm{d}\tau=0$ and is not informative on the dynamics of model (7) for small ε. And expanding the right-hand side of Eq. (7b) up to second-order is not useful, because the ε-term in the right-hand side does not disappear (though $g^{(0,0,0,0,0,1)}(s,0,N,x,x,x)$ vanishes on the fast time scale), so that the singular slow segment cannot be studied in the time $\tau=\varepsilon^2 t$.

The proper way to perform the time-scale separation when $\overline{\lambda}^{(0,1)}=0$ is that of keeping ε small but finite during the fast segment and then take the limit $\varepsilon\to 0$ in the slow one. For small $\varepsilon>0$, the equilibrium of the fast variables s and N is given by suitable functions $s_f(r,\varepsilon,\theta)$ and $N_f(r,\varepsilon,\theta)$ of the slow variable $r\in[0,1]$, which also depend on the scaling parameter ε and on the perturbation angle θ. For given (ε,θ), $\{s_f(r,\varepsilon,\theta),N_f(r,\varepsilon,\theta),\ r\in[0,1]\}$ is the r-parametrization of the one-dimensional "fast-equilibrium manifold", connecting the two monomorphic equilibria (see Fig. 3 (left)), i.e.,

$$s_f(0,\varepsilon,\theta)=\overline{n}(x+\varepsilon\cos\theta)=\overline{n}(x_1),\quad N_f(0,\varepsilon,\theta)=\overline{N}(x+\varepsilon\cos\theta)=\overline{N}(x_1),$$

$$s_f(1,\varepsilon,\theta)=\overline{n}(x+\varepsilon\sin\theta)=\overline{n}(x_2),\quad N_f(1,\varepsilon,\theta)=\overline{N}(x+\varepsilon\sin\theta)=\overline{N}(x_2).$$

For $\varepsilon\to 0$ the fast-equilibrium manifold degenerates into the straight segment connecting $(\overline{n},0,\overline{N})$ and $(0,\overline{n},\overline{N})$ (see Fig. 3 (right)) and composed of a continuum of (critically) stable equilibria of model (7).

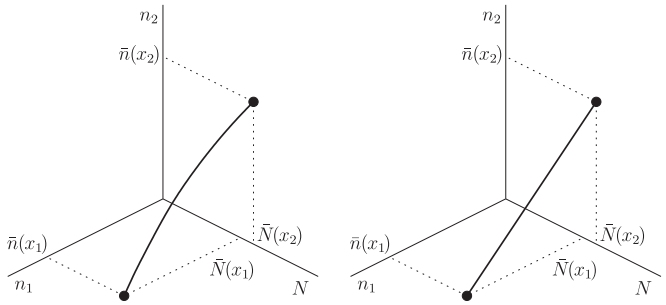

Fig. 3. The fast-equilibrium manifold in the state space (n_1,n_2,N) for small $\varepsilon>0$ (sketched in the left panel) and for $\varepsilon=0$ (right).

Time-scale separation (Hoppensteadt, 1966; Fenichel, 1979; Hek, 2010) and the hyperbolicity of the resident equilibrium guarantee that, for sufficiently small ε, the slow dynamics of model (7) are equivalent to those restricted to the fast-equilibrium manifold (more precisely, the slow dynamics of model (7) for small ε develop on the so-called "Fenichel invariant manifold," that shares equilibria and equivalent global dynamics with the fast-equilibrium manifold). We can therefore ε-expand the right-hand side of (7b) after using the substitutions

$$n_1=(1-r)s_f(r,\varepsilon,\theta),\quad n_2=r\,s_f(r,\varepsilon,\theta),\quad N=N_f(r,\varepsilon,\theta). \tag{9}$$

Note that this is different from expanding before the substitution (as we did in (7b) up to first-order), since we now take the ε-perturbation of the fast-equilibrium manifold into account (i.e., we take g-derivatives also w.r.t. n_1, n_2, and N to be multiplied by the derivatives of s_f and N_f w.r.t. ε).

The resulting expansion, up to order k, can be rearranged according to the following structure:

$$\begin{aligned}\dot{r}\,\frac{1}{(\sin\theta-\cos\theta)r(1-r)}=\\ R_{0,1}(\theta)\varepsilon+\ R_{0,2}(\theta)\varepsilon^2+R_{0,3}(\theta)\varepsilon^3+\cdots+R_{0,k}(\theta)\varepsilon^k\\ +\big(R_{1,2}(\theta)\varepsilon^2+\ R_{1,3}(\theta)\varepsilon^3+\cdots+R_{1,k}(\theta)\varepsilon^k\big)r\\ +\big(R_{2,3}(\theta)\varepsilon^3+\cdots+R_{2,k}(\theta)\varepsilon^k\big)r^2\\ +\cdots\\ +R_{k-1,k}(\theta)\varepsilon^k\,r^{k-1}+O(\varepsilon^{k+1}),\end{aligned} \tag{10}$$

where the functions $R_{i,j}$, $i<j$, up to $j=3$ are reported in Table 1 (their derivation can be checked, up to $j=4$, in the Supplementary Data).

First note that the right-hand side of (10) is a polynomial expression in r. This is due to property P4 of Section 2.1, that expresses the g-derivative

$$g^{(0,0,m,d_1,d_2,q)}((1-r)\overline{n},r\overline{n},\overline{N},x,x,x)$$

as an r-polynomial of degree d_1+d_2 with coefficients that depend on the resident equilibrium $(\overline{n},\overline{N})$ and on "bar"-evaluations of the functions $\phi^{(0,m,0,q)}_{d_1,d_2,i_1,i_2}$; and similarly for the F-derivative

$$F^{(0,0,m,d_1,d_2)}((1-r)\overline{n},r\overline{n},\overline{N},x,x).$$

Second note that the terms of order k in the right-hand side of (10) form an r-polynomial with degree less or equal to $(k-1)$ (i.e., the functions $R_{i,j}$ are defined for $i<j$). In other words, r-powers with degree k only appear if we ε-expand up to order greater than k. This is the crucial property on which all our results in the next section are based. It is due to the structure of Eq. (7b), where the difference between the invader and resident per-capita growth rates is taken, i.e., two evaluations of function g that only differ in the last argument. Thus, only the derivatives of g with at least one order of differentiation w.r.t. the invader strategy matter in Eq. (7b), the other simply cancel in the difference. Relevant derivatives of order k can therefore be only up to order $k-1$ jointly w.r.t. arguments one-to-five, and each of such differentiations can contribute at most one degree in r (again due to property P4).

Functions $R_{i,j}$ collect the coefficients of r^i among the terms of order j in the ε-expansion (10) ($i<j$). They depend on the reference strategy x (not shown as an argument; it is needed to evaluate the resident equilibrium $(\overline{n},\overline{N})$ and the "bar"-evaluations of functions g and F, as well as ϕ's and ψ's) and on the perturbation angle θ ($\cos\theta$ and $\sin\theta$ appear due to the ε-derivatives of $x_1=x+\varepsilon\cos\theta$ and $x_2=x+\varepsilon\sin\theta$), and are therefore known prior to invasion.

Whenever possible, the functions $R_{i,j}$ are expressed in Table 1 in terms of invasion fitness derivatives, taking into account that by the fitness definition we have

$$\overline{\lambda}^{(1,0)}=\overline{g}^{(1,0,0,0,0,0)}\overline{n}^{(1)}+\overline{g}^{(0,0,1,0,0,0)}\overline{N}^{(1)}+\overline{g}^{(0,0,0,1,0,0)}, \tag{11a}$$

Table 1
Functions $R_{i,j}(\theta)$, $i<j$. Note that $R_{1,3}$ and $R_{2,3}$ (with a star over the equal sign in their definition) cannot be expressed only in terms of invasion fitness derivatives and involve the $(P+1)\times(P+1)$ nonsingular matrix M defined at the bottom ($\tilde{M}$ is the adjugate matrix, i.e., the transpose of the matrix of cofactors of M).

$$R_{0,1}(\theta) := \overline{\lambda}^{(0,1)}$$

$$R_{0,2}(\theta) := \cos\theta\,\overline{\lambda}^{(1,1)} + \tfrac{1}{2}(\sin\theta + \cos\theta)\overline{\lambda}^{(0,2)}$$

$$R_{1,2}(\theta) := (\sin\theta - \cos\theta)\overline{\lambda}^{(1,1)}$$

$$R_{0,3}(\theta) := \tfrac{1}{2}\cos^2\theta\,\overline{\lambda}^{(2,1)} + \tfrac{1}{2}\cos\theta(\sin\theta + \cos\theta)\overline{\lambda}^{(1,2)} + \tfrac{1}{6}(1+\sin\theta\cos\theta)\overline{\lambda}^{(0,3)}$$

$$R_{1,3}(\theta) \overset{*}{:=} \cos\theta(\sin\theta - \cos\theta)\overline{\lambda}^{(2,1)} + \tfrac{1}{2}(\sin^2\theta - \cos^2\theta)\overline{\lambda}^{(1,2)} - \tfrac{1}{2}(\sin\theta - \cos\theta)^2 \times\left(\frac{1}{\det M}\left(\overline{g}^{(0,0,1,0,0,1)}\tilde{F}^{(1,0,0,0,0)} + \overline{g}^{(1,0,0,0,0,1)}\tilde{g}^{(1,0,0,0,0,0)}\right)\left(\overline{\lambda}^{(0,2)} + \overline{\phi}_{2,1}\,\overline{n}\right) + \frac{1}{\det M}\left(\overline{g}^{(0,0,1,0,0,1)}\tilde{F}^{(0,0,1,0,0)} + \overline{g}^{(1,0,0,0,0,1)}\tilde{g}^{(0,0,1,0,0,0)}\right)\overline{\psi}_{2,1}\,\overline{n} - \overline{\phi}_{2,1}^{(0,0,0,1)}\overline{n}\right)$$

$$R_{2,3}(\theta) \overset{*}{:=} \tfrac{1}{2}(\sin^2\theta - \cos^2\theta)\left(\overline{\lambda}^{(2,1)} + \overline{\lambda}^{(1,2)}\right) - R_{1,3}(\theta)$$

$$M := \begin{bmatrix} \overline{g}^{(1,0,0,0,0,0)} & \overline{g}^{(0,0,1,0,0,0)} \\ \overline{F}^{(1,0,0,0,0)} & \overline{F}^{(0,0,1,0,0)} \end{bmatrix}, \quad \tilde{M} := \begin{bmatrix} \tilde{g}^{(1,0,0,0,0,0)} & \tilde{g}^{(0,0,1,0,0,0)} \\ \tilde{F}^{(1,0,0,0,0)} & \tilde{F}^{(0,0,1,0,0)} \end{bmatrix}, \quad M\tilde{M} = \det M\, I_{1+P}$$

$$\overline{\lambda}^{(0,1)} = \overline{g}^{(0,0,0,0,0,1)}, \tag{11b}$$

$$\overline{\lambda}^{(2,0)} = \overline{g}^{(2,0,0,0,0,0)}(\overline{n}^{(1)})^2 + 2\overline{g}^{(1,0,1,0,0,0)}\overline{n}^{(1)}\overline{N}^{(1)} + 2\overline{g}^{(1,0,0,1,0,0)}\overline{n}^{(1)} + \overline{g}^{(1,0,0,0,0,0)}\overline{n}^{(2)} + \overline{g}^{(0,0,2,0,0,0)}[\overline{N}^{(1)},\overline{N}^{(1)}] + 2\overline{g}^{(0,0,1,1,0,0)}\overline{N}^{(1)} + \overline{g}^{(0,0,1,0,0,0)}\overline{N}^{(2)} + \overline{g}^{(0,0,0,2,0,0)}, \tag{11c}$$

$$\overline{\lambda}^{(1,1)} = \overline{g}^{(1,0,0,0,0,1)}\overline{n}^{(1)} + \overline{g}^{(0,0,1,0,0,1)}\overline{N}^{(1)} + \overline{g}^{(0,0,0,1,0,1)}, \tag{11d}$$

$$\overline{\lambda}^{(0,2)} = \overline{g}^{(0,0,0,0,0,2)}, \tag{11e}$$

and similarly for higher-order derivatives. In particular, we use λ-derivatives with at least one order of differentiation w.r.t. the invader strategy, since pure-derivatives w.r.t. the resident strategy can be eliminated by exploiting the identity $\lambda(x,x)=0$ (invasion is neutral when resident and invader are identical; see Eqs. (2a) and (3)), e.g.,

$$\overline{\lambda}^{(1,0)} = -\overline{\lambda}^{(0,1)}, \quad \overline{\lambda}^{(2,0)} = -2\,\overline{\lambda}^{(1,1)} - \overline{\lambda}^{(0,2)}. \tag{12}$$

When it is not possible to express a function $R_{i,j}$ only in terms of fitness derivatives (see, e.g., functions $R_{1,3}$ and $R_{2,3}$), a star is added over the equal sign in the definition, and we will use this notation for all relevant quantities throughout the paper. These are the quantities that explicitly depends on the $(P+1)\times(P+1)$ matrix M, defined in Table 1 and shown to be nonsingular (in Appendix A) by the hyperbolicity of the resident equilibrium. Of course the expressions for the star-quantities greatly simplify in the special case in which the resident and invader populations have no other intra- or inter-specific interaction, i.e., the case $P=0$. The simplified expressions of functions $R_{1,3}$ and $R_{2,3}$ can be easily obtained from those derived for $P>0$ assuming that the resident populations in N do not affect the dynamics of the resident and invader types, i.e., setting

$$\overline{g}^{(l,0,m,d,0,q)} = 0 \text{ (implying } \overline{\phi}^{(0,m,0,q)} = 0),\ m>0, \tag{13a}$$

$$\det M = \overline{g}^{(1,0,0,0,0,0)}\det\overline{F}^{(0,0,1,0,0)}, \tag{13b}$$

$$\tilde{g}^{(1,0,0,0,0,0)} = \det\overline{F}^{(0,0,1,0,0)}, \tag{13c}$$

$$\tilde{g}^{(0,0,1,0,0,0)} = 0 \tag{13d}$$

and then removing the argument N from the resulting expressions. The result for function $R_{1,3}$ ($R_{2,3}$ is expressed in terms of $R_{1,3}$, see Table 1) is reported below for the reader's convenience

$$R_{1,3}(\theta) \overset{*}{:=} \cos\theta(\sin\theta - \cos\theta)\overline{\lambda}^{(2,1)} + \frac{1}{2}(\sin^2\theta - \cos^2\theta)\overline{\lambda}^{(1,2)} - \frac{1}{2}(\sin\theta - \cos\theta)^2\left(\frac{\overline{g}^{(1,0,0,0,0,1)}}{\overline{g}^{(1,0,0,0,0,0)}}\left(\overline{\lambda}^{(0,2)} + \overline{\phi}_{2,1}\,\overline{n}\right) - \overline{\phi}_{2,1}^{(0,0,0,1)}\overline{n}\right) \quad (P=0), \tag{14}$$

where $\overline{g}^{(1,0,0,0,0,0)} < 0$ is the condition for the hyperbolic stability of the resident equilibrium $\overline{n}(x)$ (note that, after dropping the argument N, g has five arguments in (14), (n_1,n_2,x_1,x_2,x'), and $\phi_{2,1}$ has three, (n,x,x')).

The expressions of the x-derivatives of the resident equilibrium $(\overline{n}(x),\overline{N}(x))$ that appear in (3) can be expressed in terms of "bar"-evaluations of the functions g and F (by differentiation of Eqs. (2) w.r.t. x_1 at $x_1=x$) and this is done in Appendix A (see Table A1 for the general case $P>0$ and Table A2 for the case $P=0$).

Finally, the expressions of the ε-derivatives of the fast-equilibrium manifold $\{s_f(r,\varepsilon,\theta),\ N_f(r,\varepsilon,\theta),\ r\in[0,1]\}$, that are needed for computing the expansion (10) and the functions $R_{i,j}$, are computed in Appendix B (see Table B1 for $P>0$ and Table B2 for $P=0$). They characterize the ε-perturbations of the fast-equilibrium manifold from the zero-order solution $(s_f(r,0,\theta),\ N_f(r,0,\theta)) = (\overline{n},\overline{N})$, corresponding to the straight segment of Fig. 3 (right). They are also polynomial expressions in r (again due to property P4), with degree equal to the order of differentiation and coefficients that are ultimately functions of the reference strategy x and of the perturbation angle θ.

3. Analysis

We now unfold the resident–invader dynamics, based on the expansion (10) and on time-scale separation (under the hyperbolicity of the resident equilibrium). For a given perturbation angle θ and in the limit of small ε ($\varepsilon\to 0$), the fast variables s and N converge to $s_f(r,\varepsilon,\theta)$ and $N_f(r,\varepsilon,\theta)$ and we can study the slow dynamics of r by means of Eq. (10). During the slow dynamics, the resident and invader densities n_1 and n_2 track the $(1-r)$ and r fractions of $s=s_f(r,\varepsilon,\theta)$, while $N=N_f(r,\varepsilon,\theta)$.

If the first-order term in (10) does not vanish, i.e., when the reference strategy x is nonsingular, we can study the slow dynamics in the time scale of time $\tau=\varepsilon t$ and this is quickly done in Section 3.1 (reobtaining the "invasion implies substitution" theorem already discussed in Section 2.2). Otherwise, when x is singular and generic, i.e., without assuming any degeneracy in the second-order terms in Eq. (10), we must consider the slow time $\tau=\varepsilon^2 t$ (Section 3.2). The nongeneric cases, involving degeneracies in the second-order derivatives of the invasion fitness, are unfolded in Section 3.3, and some require a third-order analysis in the slow time $\tau=\varepsilon^3 t$. The genericity conditions that are assumed or violated case by case are progressively labeled with a G prefix.

In all cases, the dynamics of model (7) for sufficiently small ε are equivalent to those obtained in the limit $\varepsilon\to 0$. Since the fast-equilibrium manifold $\{s_f(r,\varepsilon,\theta),N_f(r,\varepsilon,\theta),\ r\in[0,1]\}$ introduced in Section 2.3 is one-dimensional, the asymptotic limits of the slow-dynamics can only be the monomorphic equilibria at $r=0$ and $r=1$, or internal equilibria at $\overline{r}\in(0,1)$. Moreover, since the k-th-order in the right-hand side of (10) is an r-polynomial with degree $k-1$, model degeneracies up to order $k>0$ are needed to have up to k internal equilibria.

When several resident–invader competition scenarios are possible for different values on the angle θ, the bifurcation boundaries (Kuznetsov, 2004; Meijer et al., 2009) separating neighboring scenarios are computed in the plane of the strategies (x_1,x_2). Bifurcation curves necessarily emanate from the point (x,x), otherwise they are irrelevant in our local analysis for $\varepsilon\to 0$ (see Priklopil, 2012 for cases with small but finite ε). They are described in terms of ε-expansions of their polar parametrization $\theta=\theta(\varepsilon)$,

where $\theta(0)$ (in the interval (6)) gives the tangent direction at $\varepsilon=0$, while the first nonvanishing derivative $\theta^{(k)}(0)$, $k\geq 1$, determines the curvature (whether θ increases or decreases when moving away from $\varepsilon=0$ starting in the $\theta(0)$−direction).

3.1. Away from singularity

In the time scale of time $\tau=\varepsilon t$, Eq. (10) becomes

$$\frac{\mathrm{d}r}{\mathrm{d}\tau}\frac{1}{(\sin\theta-\cos\theta)r(1-r)}=\overline{\lambda}^{(0,1)}+O(\varepsilon). \tag{15}$$

From (15) we obtain that invasion with

$$G_1:=\overline{\lambda}^{(0,1)}\neq 0 \tag{G1}$$

by a sufficiently similar invader implies (under the hyperbolicity of the resident equilibrium) the substitution of the resident type. More precisely, for sufficiently small ε, strategy x_2 (resp. x_1) dominates the competition if $\lambda(x_1,x_2)=\overline{\lambda}^{(0,1)}(x_2-x_1)+O(\varepsilon)$ is positive (resp. negative). In fact, recalling (x_2-x_1) from (6), we have $\mathrm{d}r/\mathrm{d}\tau$ positive (resp. negative) for all $r\in(0,1)$, i.e., r is

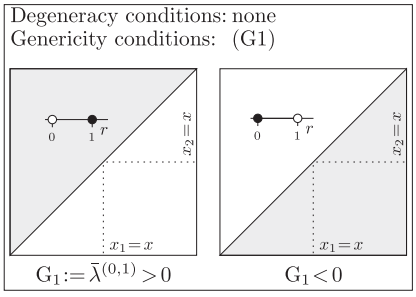

Fig. 4. The two competition scenarios that are generically possible away from singularity.

increasing (resp. decreasing) and asymptotically tends to one (resp. zero). The two cases are graphically represented in Fig. 4.

3.2. Close to a generic singular strategy

If $G_1=0$, i.e., if x is a singular strategy, then, in the time scale of time $\tau=\varepsilon^2 t$, Eq. (10) becomes

$$\begin{aligned}\frac{\mathrm{d}r}{\mathrm{d}\tau}\frac{1}{(\sin\theta-\cos\theta)r(1-r)}&=R_{0,2}(\theta)+R_{1,2}(\theta)r+O(\varepsilon)\\&=\cos\theta\,\overline{\lambda}^{(1,1)}+\frac{1}{2}(\sin\theta+\cos\theta)\overline{\lambda}^{(0,2)}\\&\quad+(\sin\theta-\cos\theta)\overline{\lambda}^{(1,1)}\,r+O(\varepsilon).\end{aligned} \tag{16}$$

As expected from the analysis of Section 2.3, the right-hand side at $\varepsilon=0$ is linear in r. This implies that the resident–invader competition scenarios that are generically possible for $x_1<x_2$ (recall (6)) close to a singular strategy are the four classical Lotka–Volterra scenarios: x_2- (resp. x_1-) dominance if the right-hand side of (16) at $\varepsilon=0$ is positive (resp. negative) at both $r=0$ and $r=1$, protected coexistence at an intermediate $\overline{r}\in(0,1)$ if the right-hand side is positive at $r=0$ and negative at $r=1$, mutual exclusion if it is negative at $r=0$ and positive at $r=1$ (symmetrically, the competition scenarios for $x_1>x_2$ are obtained by exchanging x_1 with x_2 and n_1 with n_2).

The above analysis fails when θ is such that the second-order terms $R_{0,2}(\theta)$ and $R_{1,2}(\theta)$ both vanish, so that higher-order terms matter. Within the θ-interval in (6), this is possible if and only if $\overline{\lambda}^{(1,1)}=0$ together with either $\theta=\frac{3}{4}\pi$ or $\overline{\lambda}^{(0,2)}=0$ (see Table 1). This means that the unfolding of the resident–invader dynamics close to a singular strategy x is fully determined (i.e., for any given θ in interval (6) and $\varepsilon\to 0$) by the second-order fitness derivatives if and only if

$$G_{2,1}:=\overline{\lambda}^{(1,1)}\neq 0. \tag{G2.1}$$

The fitness cross-derivative $\overline{\lambda}^{(1,1)}$ thus fully characterizes the genericity of a singular strategy. If and only if it is nonzero, we can neglect third- and higher-order fitness derivatives.

Which of the four Lotka–Volterra scenarios occurs for a given θ and $\varepsilon\to 0$ depends on θ and, of course, on the values of the fitness derivatives $\overline{\lambda}^{(1,1)}$ and $\overline{\lambda}^{(0,2)}$. The boundaries separating the four scenarios in the strategy plane (x_1,x_2) correspond to bifurcation curves involving the equilibria of Eq. (16). Only two bifurcations are generically possible by varying θ from $\frac{1}{4}\pi$ to $\frac{5}{4}\pi$, namely the so-called *transcritical* bifurcations at which the internal equilibrium collides (and exchanges stability) with one of the two monomorphic equilibria. They are mathematically characterized by the fact that the right-hand side of Eq. (16) (including higher-order terms!) changes sign at $r=0$ and $r=1$, respectively.

Recalling the structure of Eq. (10) and that $R_{0,1}(\theta):=\overline{\lambda}^{(0,1)}=G_1=0$ at the singular strategy x, the point (ε,θ) of the (x_1,x_2)-plane is on the transcritical bifurcation curve involving the monomorphic equilibrium at $r=0$ if

$$R_{0,2}(\theta)+R_{0,3}(\theta)\varepsilon+\cdots+R_{0,k}(\theta)\varepsilon^{k-2}+\cdots=0.$$

The bifurcation curve $\theta=\theta_{\mathrm{T2}}(\varepsilon)$ is hence implicitly defined by imposing

$$R_{0,2}(\theta_{\mathrm{T2}}(\varepsilon))+R_{0,3}(\theta_{\mathrm{T2}}(\varepsilon))\varepsilon+\cdots+R_{0,k}(\theta_{\mathrm{T2}}(\varepsilon))\varepsilon^{k-2}+\cdots=0 \tag{17}$$

for any small ε. Along the curve $\theta=\theta_{\mathrm{T2}}(\varepsilon)$ the invader density n_2 is vanishing at the internal equilibrium (i.e., the bifurcating equilibrium is $(n_1,n_2,N)=(\overline{n}(x_1),0,\overline{N}(x_1))$. By evaluating (17) and its ε-derivatives at $\varepsilon=0$, and solving for $\theta_{\mathrm{T2}}(0)$ and for the derivatives $\theta^{(k)}_{\mathrm{T2}}(0)$, $k\geq 1$, we can fully characterize the bifurcation curve locally to $\varepsilon=0$ ($\varepsilon<0$ can be used in the expansion $\theta_{\mathrm{T2}}(\varepsilon)=\theta_{\mathrm{T2}}(0)+\theta^{(1)}_{\mathrm{T2}}(0)\varepsilon+\cdots$ to characterize the curve below the diagonal $x_1=x_2$). For example, up to $k=1$, we have

$$R_{0,2}(\theta_{\mathrm{T2}}(0))=0,\quad R^{(1)}_{0,2}(\theta_{\mathrm{T2}}(0))\theta^{(1)}_{\mathrm{T2}}(0)+R_{0,3}(\theta_{\mathrm{T2}}(0))=0, \tag{18}$$

from which we obtain (taking also the second relation in (12) into account)

$$\tan\theta_{\mathrm{T2}}(0)=-\frac{2\overline{\lambda}^{(1,1)}+\overline{\lambda}^{(0,2)}}{\overline{\lambda}^{(0,2)}}=\frac{\overline{\lambda}^{(2,0)}}{\overline{\lambda}^{(0,2)}},\quad \theta^{(1)}_{\mathrm{T2}}(0)=-\frac{R_{0,3}(\theta_{\mathrm{T2}}(0))}{R^{(1)}_{0,2}(\theta_{\mathrm{T2}}(0))} \tag{19}$$

(we always consider an arctan with values in our interval (6) of interest). Note that $R^{(1)}_{0,2}(\theta_{\mathrm{T2}}(0))$ is nonzero under condition (G2.1) ($R^{(1)}_{0,2}(\theta_{\mathrm{T2}}(0))=0$ is equivalent to $\tan\theta_{\mathrm{T2}}(0)=\overline{\lambda}^{(0,2)}/(2\overline{\lambda}^{(1,1)}+\overline{\lambda}^{(2,0)})=-\overline{\lambda}^{(0,2)}/\overline{\lambda}^{(2,0)}$, which gives a $\frac{1}{2}\pi$ difference w.r.t. the first equation in (19)), and this guarantees that the bifurcation does take place when moving (x_1,x_2) across the bifurcation curve (this is technically called the *transversality* of the bifurcation). Indeed, $R_{0,2}(\theta_{\mathrm{T2}}(0))=0$ (from (18)) and a nonzero $R^{(1)}_{0,2}(\theta_{\mathrm{T2}}(0))$ implies that the right-hand side of Eq. (16) at $r=0$ changes sign for small ε when θ moves across $\theta_{\mathrm{T2}}(0)$.

At the transcritical bifurcation at $r=1$, the right-hand side of Eq. (16) vanishes along the curve $\theta=\theta_{\mathrm{T1}}(\varepsilon)$ (the resident density n_1 is vanishing at the internal equilibrium, the bifurcating equilibrium being $(n_1,n_2,N)=(0,\overline{n}(x_2),\overline{N}(x_2))$), i.e.,

$$\begin{aligned}&R_{0,2}(\theta_{\mathrm{T1}}(\varepsilon))+R_{0,3}(\theta_{\mathrm{T1}}(\varepsilon))\varepsilon+\cdots+\quad R_{0,k}(\theta_{\mathrm{T1}}(\varepsilon))\varepsilon^{k-2}+\cdots\\&+R_{1,2}(\theta_{\mathrm{T1}}(\varepsilon))+R_{1,3}(\theta_{\mathrm{T1}}(\varepsilon))\varepsilon+\cdots+\quad R_{1,k}(\theta_{\mathrm{T1}}(\varepsilon))\varepsilon^{k-2}+\cdots\\&\qquad+R_{2,3}(\theta_{\mathrm{T1}}(\varepsilon))\varepsilon+\cdots+\quad R_{2,k}(\theta_{\mathrm{T1}}(\varepsilon))\varepsilon^{k-2}+\cdots\\&\qquad\qquad+\cdots\\&\qquad\qquad\qquad+R_{k-1,k}(\theta_{\mathrm{T1}}(\varepsilon))\varepsilon^{k-2}+\cdots\\&\qquad\qquad\qquad\qquad+\cdots=0\end{aligned} \tag{20}$$

for any small ε, from which we derive

$$R_{0,2}(\theta_{\mathrm{T1}}(0))+R_{1,2}(\theta_{\mathrm{T1}}(0))=0, \tag{21a}$$

$$\left(R^{(1)}_{0,2}(\theta_{\mathrm{T1}}(0))+R^{(1)}_{1,2}(\theta_{\mathrm{T1}}(0))\right)\theta^{(1)}_{\mathrm{T1}}(0)+R_{0,3}(\theta_{\mathrm{T1}}(0)) +R_{1,3}(\theta_{\mathrm{T1}}(0))+R_{2,3}(\theta_{\mathrm{T1}}(0))=0, \tag{21b}$$

i.e.,

$$\tan\theta_{\mathrm{T1}}(0)=\frac{\overline{\lambda}^{(0,2)}}{\overline{\lambda}^{(2,0)}},\quad \theta^{(1)}_{\mathrm{T1}}(0)=-\frac{R_{0,3}(\theta_{\mathrm{T1}}(0))+R_{1,3}(\theta_{\mathrm{T1}}(0))+R_{2,3}(\theta_{\mathrm{T1}}(0))}{R^{(1)}_{0,2}(\theta_{\mathrm{T1}}(0))+R^{(1)}_{1,2}(\theta_{\mathrm{T1}}(0))}. \tag{22}$$

Again, $R^{(1)}_{0,2}(\theta_{\mathrm{T1}}(0))+R^{(1)}_{1,2}(\theta_{\mathrm{T1}}(0))\neq 0$ is the transversality condition for the bifurcation and is implied by (G2.1) ($R^{(1)}_{0,2}(\theta_{\mathrm{T1}}(0))+R^{(1)}_{1,2}(\theta_{\mathrm{T1}}(0))=0$ is equivalent to $\tan\theta_{\mathrm{T1}}(0)=(2\overline{\lambda}^{(1,1)}+\overline{\lambda}^{(2,0)})/\overline{\lambda}^{(0,2)}=-\overline{\lambda}^{(2,0)}/\overline{\lambda}^{(0,2)}$, which gives a $\frac{1}{2}\pi$ difference w.r.t. the first equation in (22)).

Note that $\theta_{\mathrm{T2}}(0)$ and $\theta_{\mathrm{T1}}(0)$ are symmetric angles w.r.t. the anti-diagonal $x_1+x_2=2x$ (the $\theta=\frac{3}{4}\pi$ direction), which is of no surprise due to the symmetry of model (1) w.r.t. the diagonal $x_1=x_2$. If the equilibrium at $r=0$ bifurcates at point (x_1,x_2), then the equilibrium at $r=1$ does the same at the symmetric point (x_2,x_1), so the bifurcation curve of the equilibrium at $r=1$ is simply obtained by mirroring the curve for the equilibrium at $r=0$ w.r.t. the diagonal (this also implies $\theta^{(1)}_{\mathrm{T2}}(0)=\theta^{(1)}_{\mathrm{T1}}(0)$, that can be easily verified, and more in general that $\theta^{(k)}_{\mathrm{T2}}(0)=(-1)^{k-1}\theta^{(k)}_{\mathrm{T1}}(0)$, $k\geq 1$).

Also the type of transcritical bifurcation, namely the fact that the internal equilibrium involved in the bifurcation is stable or not (*non-catastrophic* and *catastrophic* cases, respectively), can be formalized. In fact, if the slope w.r.t. r of the right-hand side of (16) at the bifurcation ($r=0$ or $r=1$; small ε) is negative (resp. positive), then the internal equilibrium ($\bar{r}\in(0,1)$) present at one side of the bifurcation is attracting (resp. repelling) orbits originating at nearby values of r (this is clear when picturing the right-hand side of (16) as a function of r locally to $r=0$ or $r=1$). Thus, the slope at $\varepsilon=0$ being $R_{1,2}(\theta_{\mathrm{T2}}(0))$ at $r=0$ and $R_{1,2}(\theta_{\mathrm{T1}}(0))$ at $r=1$ (and recalling (6)), we conclude that under (G2.1) the transcritical bifurcations are of the same type: non-catastrophic (resp. catastrophic) if the fitness cross-derivative is negative (resp. positive).

A concise summary of the above analysis is presented in Fig. 5, which classifies the competition scenarios that are possible close to a generic singular strategy. Genericity requires (G2.1) together with $\theta_{\mathrm{T2}}(0)$ and $\theta_{\mathrm{T1}}(0)$ being different from $\frac{1}{4}\pi$ and $\frac{5}{4}\pi$, i.e.,

$$G_{2,2}:=\overline{\lambda}^{(1,1)}+\overline{\lambda}^{(0,2)}=\tfrac{1}{2}\left(\overline{\lambda}^{(0,2)}-\overline{\lambda}^{(2,0)}\right)\neq 0 \tag{G2.2}$$

($\tan\theta_{\mathrm{T2}}(0)\neq 1$ in (19)). Note that $G_{2,2}$ is the x_1-derivative of the selection gradient $\overline{\lambda}^{(0,1)}(x_1,x_1)$ at the singular strategy x. That is, we also assume that the selection gradient changes sign with nonzero slope at the singularity. Thus, negative/positive $G_{2,2}$ means that selection favors larger/smaller strategy values when x_1 is smaller than x, and smaller/larger strategy values when x_1 is larger than x (convergence/divergence to/from the singular strategy in a one-dimensional adaptive dynamics; as we will see in Section 3.3.1, the case of vanishing $G_{2,2}$ corresponds to a bifurcation of singularity itself).

In Fig. 5, the cases with negative/positive $G_{2,2}$ are depicted in the first/second row of panels, all others conditions being equal. Note that the cases with positive $G_{2,2}$ can be easily obtained from the corresponding cases with negative $G_{2,2}$ by reversing the stability of all equilibria (boundary at $r=0$ and $r=1$ and internal) and, consequently, the type of transcritical bifurcations. Further note that, locally to point (x,x) (small ε), the two transcritical bifurcation curves define a cone where resident–invader protected coexistence (resp. mutual exclusion) occurs if the fitness cross-derivative is negative (resp. positive).

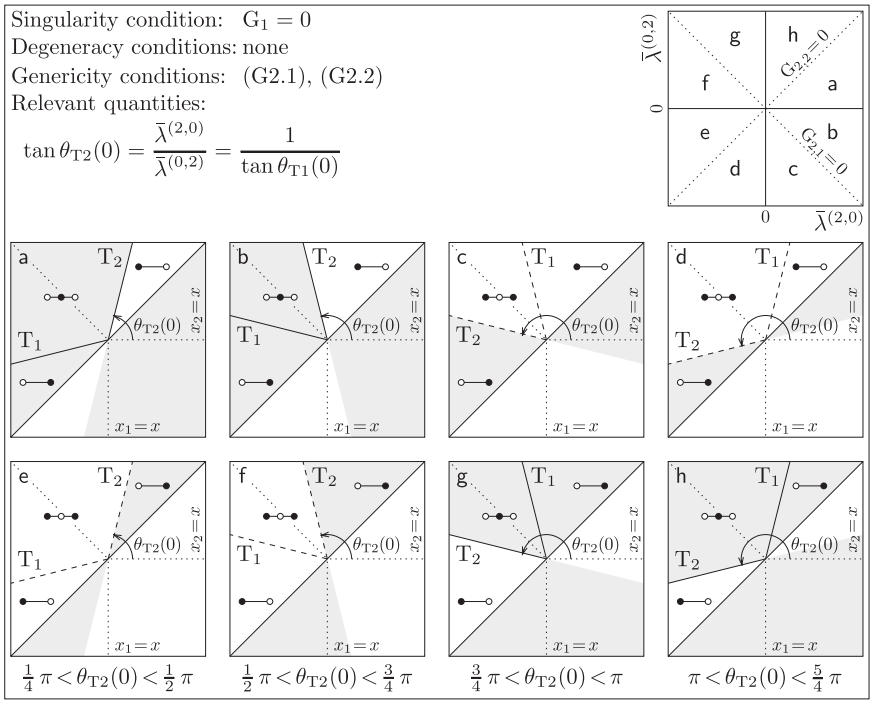

Fig. 5. Classification of the competition scenarios that are possible close to a generic singular strategy x. $G_{2,1}<0$ in cases g–b clockwise (stability of the internal equilibrium); $G_{2,1}>0$ in cases c–f (instability of the internal equilibrium). $G_{2,2}<0$ in cases a–d (selection favors larger/smaller strategy values when x_1 is smaller/larger than x); $G_{2,2}>0$ in cases e–h. The top-right panel (adapted from Geritz et al., 1998) shows how the competition scenarios classify in terms of the fitness second pure-derivatives at the singularity.

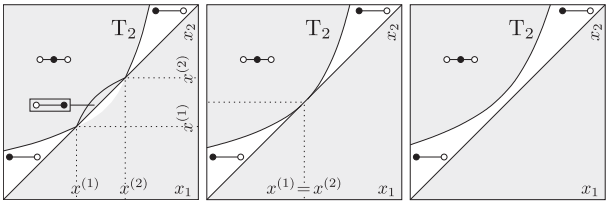

Fig. 6. Unfolding of the saddle-node bifurcation of singular strategies. Two singular strategies $x^{(1)}$ and $x^{(2)}$ of class h ($G_{2,2}>0$, $G_{3,1}<0$) and a ($G_{2,2}<0$, $G_{3,1}<0$) (compare the PIP locally to $x^{(1)}$ and $x^{(2)}$ and those of cases h and a in Fig. 5) collide and disappear. At the bifurcation, the competition scenario is that of the left panel in Fig. 7.

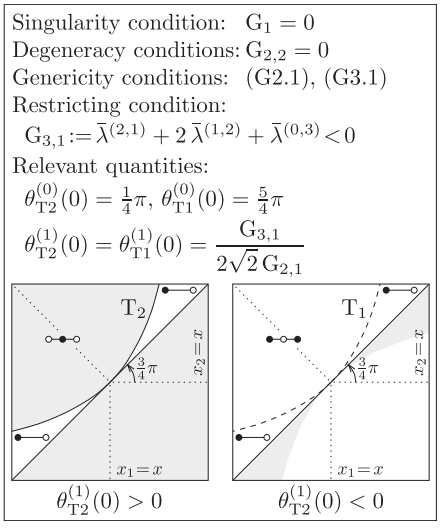

Fig. 7. Classification of the competition scenarios that are generically possible close to a saddle-node singular strategy x. Only the cases with $G_{3,1}<0$ are shown (selection favors smaller strategy values on both sides of x); the cases with $G_{3,1}>0$ can be obtained by reversing the stability of all equilibria.

3.3. Close to degenerate singular strategies

3.3.1. Saddle-node singular strategy

In this section we analyze the degenerate (codimension-one) case in which (G2.1) is met at the singular strategy x, but $G_{2,2}=0$. The analysis of Section 3.2 still holds true, except for the fact that the selection gradient, $\lambda^{(0,1)}(x_1,x_1)$, generically has the same sign for x_1 close to x. The sign is that of the quadratic coefficient of the selection gradient around x, that we expect to be nonzero, i.e.,

$$G_{3,1} := \bar{\lambda}^{(2,1)} + 2\bar{\lambda}^{(1,2)} + \bar{\lambda}^{(0,3)} \neq 0. \tag{G3.1}$$

Thus, selection favors larger (resp. smaller) strategy values on both sides of x if $G_{3,1}$ is positive (resp. negative).

This correspond to a saddle-node (or fold) bifurcation of singular strategies, i.e., the collision and disappearance of two singular strategies—typically one attracting and one repelling the nearby adaptive dynamics—as $G_{2,2}$ goes through zero due to gradual changes in some model parameters (see Fig. 6). At the bifurcation (central panel in Fig. 6), the saddle-node singular strategy (the merging of the two colliding singularities) is generically unstable, attracting/repelling from below and repelling/attracting from above if $G_{3,1}$ is positive/negative.

Fig. 7 shows the two competition scenarios that are possible for $G_{3,1}<0$ (the two cases with $G_{3,1}>0$ can be obtained by reversing the stability of all equilibria and the type of transcritical bifurcation). The transcritical bifurcation curves involving the two monomorphic equilibria, $r=0$ and $r=1$, are tangent to the diagonal $x_1=x_2$ at point (x,x). In fact, as $G_{2,2}$ vanishes, one of the angles $\theta_{T2}(0)$ and $\theta_{T1}(0)$ approaches $\frac{1}{4}\pi$, the other $\frac{5}{4}\pi$ (recall (19), (22), and (G2.2)). When $G_{2,2}=0$, we can arbitrarily set $\theta_{T2}(0)=\frac{1}{4}\pi$ and $\theta_{T1}(0)=\frac{5}{4}\pi$, with

$$\theta^{(1)}_{T2}(0)=\theta^{(1)}_{T1}(0)=\frac{G_{3,1}}{2\sqrt{2}\,G_{2,1}}\neq 0 \tag{23}$$

(see (19)) and Table 1; the alternative choice would switch the sign of the right-hand side in (23), but would still represent the same bifurcation curves). If $\theta^{(1)}_{T2}(0)\gtrless 0$ (left/right panel in Fig. 7), the curve T_2 develops above/below the diagonal (recall that curves T_2 and T_1 are symmetric w.r.t. the diagonal). The case with $\theta^{(1)}_{T2}(0)>0$ is assumed in the unfolding of Fig. 6.

3.3.2. Vanishing fitness cross-derivative

Symmetrically, we now analyze the (codimension-one) case in which (G2.2) is met at the singular strategy x, but $G_{2,1}=0$. Note that, by taking the second relation in (12) with $\bar{\lambda}^{(1,1)}=0$ into account, (G2.2) can now be written as $\bar{\lambda}^{(0,2)}\neq 0$. Geometrically, this is the case approaching which—along with gradual changes in some model parameters—the cone of resident–invader coexistence closes up ($\theta_{T2}(0)=\theta_{T1}(0)=\frac{3}{4}\pi$ in Eqs. (19) and (22).

Note that the analysis of Section 3.2 still holds true in the limit $\varepsilon\to 0$ if $\theta\neq\frac{3}{4}\pi$. In fact, $\theta\neq\frac{3}{4}\pi$ and (G2.2) guarantee that in Eq. (16) the second-order term $R_{0,2}(\theta)=\frac{1}{2}(\sin\theta+\cos\theta)\bar{\lambda}^{(0,2)}$ does not vanish. Moreover, $R_{1,2}(\theta)=0$ under $G_{2,1}=0$ (see Table 1), so that the right-hand side of (16) is constant at $\varepsilon=0$ and x_1- (resp. x_2-) dominance is the outcome for $R_{0,2}(\theta)<0$ (resp. $R_{0,2}(\theta)>0$).

Only if $\theta=\frac{3}{4}\pi$, we have to consider the third-order terms in the expansion (10) and look at the following equation in the time scale of time $\tau=\varepsilon^3 t$:

$$\frac{dr}{d\tau}\frac{1}{\sqrt{2}\,r(1-r)}=\bar{R}_{0,3}+\bar{R}_{1,3}\,r+\bar{R}_{2,3}\,r^2+O(\varepsilon), \tag{24}$$

where the bar over functions $R_{i,j}$ (and their derivatives) hereafter stands for evaluation at $\theta=\frac{3}{4}\pi$ under $G_{2,1}=0$. The evaluations that are used below are summarized in Table 2 (note that $\bar{R}_{1,3}=-\bar{R}_{2,3}$, the only two quantities that cannot be expressed only in terms of invasion fitness derivatives, are also displayed in the special case $P=0$, see Eq. (14)).

The $O(\varepsilon)$-terms in Eq. (24) can be neglected in the limit $\varepsilon\to 0$ provided the third-order terms $\bar{R}_{0,3}$, $\bar{R}_{1,3}$, and $\bar{R}_{2,3}$ do not all vanish, a requirement that reduces to one of the two following conditions:

$$G_{3,2} := 12\,\bar{R}_{0,3}=3\,\bar{\lambda}^{(2,1)}+\bar{\lambda}^{(0,3)}\neq 0 \tag{G3.2}$$

or

$$G_{3,3} := \bar{R}_{1,3}=-\bar{R}_{2,3}\neq 0 \tag{G3.3}$$

(see Table 2).

Table 2
Quantities $\bar{R}^{(k)}_{i,j}$, $i<j$, $k\geq 0$ (see Table 1).

$$\bar{R}^{(1)}_{0,2}=-\frac{\sqrt{2}}{2}\bar{\lambda}^{(0,2)},\quad \bar{R}^{(2)}_{0,2}=0$$

$$\bar{R}_{0,3}=\tfrac{1}{12}\left(3\,\bar{\lambda}^{(2,1)}+\bar{\lambda}^{(0,3)}\right),\quad \bar{R}^{(1)}_{0,3}=\tfrac{1}{2}\left(\bar{\lambda}^{(2,1)}+\bar{\lambda}^{(1,2)}\right)$$

$$\bar{R}_{1,3}=-\bar{R}_{2,3}\overset{*}{=}-\bar{\lambda}^{(2,1)}+\bar{\phi}^{(0,0,0,1)}_{2,1}\bar{n}$$
$$-\frac{1}{\det M}\left(\bar{g}^{(0,0,1,0,0,1)}\tilde{F}^{(1,0,0,0,0)}+\bar{g}^{(1,0,0,0,0,1)}\tilde{g}^{(1,0,0,0,0,0)}\right)\left(\bar{\lambda}^{(0,2)}+\bar{\phi}_{2,1}\,\bar{n}\right)$$
$$-\frac{1}{\det M}\left(\bar{g}^{(0,0,1,0,0,1)}\tilde{F}^{(0,0,1,0,0)}+\bar{g}^{(1,0,0,0,0,1)}\tilde{g}^{(0,0,1,0,0,0)}\right)\bar{\psi}_{2,1}\,\bar{n}\;(P>0)$$

$$\bar{R}_{1,3}=-\bar{R}_{2,3}\overset{*}{=}-\bar{\lambda}^{(2,1)}+\bar{\phi}^{(0,0,1)}_{2,1}\bar{n}-\frac{\bar{g}^{(1,0,0,0,1)}}{\bar{g}^{(1,0,0,0,0)}}\left(\bar{\lambda}^{(0,2)}+\bar{\phi}_{2,1}\,\bar{n}\right)\quad(P=0)$$

$$\bar{R}_{0,4}=-\frac{\sqrt{2}}{24}\left(\bar{\lambda}^{(3,1)}+\bar{\lambda}^{(1,3)}\right)$$

A little thought on the stationary solutions of Eq. (24) at $\varepsilon=0$ (the roots $\bar r$ of the parabola $\overline R_{0,3}+\overline R_{1,3}\bar r(1-\bar r)$) shows that there can only be either none or two internal solutions $\bar r\in(0,1)$: none (one negative solution and one positive solution $\bar r>1$) if $\overline R_{0,3}$ and $\overline R_{1,3}$ have same sign; two (resp. none) if $\overline R_{0,3}$ and $\overline R_{1,3}$ have opposite sign and the solutions are real (resp. complex). Thus, in the limit $\varepsilon\to 0$, only x_1- or x_2-dominance, or unprotected coexistence, are possible under the genericity condition (G3.2) or (G3.3).

The analysis of the transcritical bifurcation at $r=0$ starts again from Eq. (17), but now the two conditions in (18) give

$$\theta_{\mathrm{T}2}(0)=\frac{3}{4}\pi,\quad \theta^{(1)}_{\mathrm{T}2}(0)=-\frac{\overline R_{0,3}}{\overline R^{(1)}_{0,2}}=\frac{3\,\bar\lambda^{(2,1)}+\bar\lambda^{(0,3)}}{6\sqrt{2}\,\bar\lambda^{(0,2)}}=\frac{G_{3,2}}{6\sqrt{2}\,G_{2,2}},\tag{25}$$

where $\overline R^{(1)}_{0,2}\neq 0$ under (G2.2) assures the transversality of the bifurcation. The type of the bifurcation is determined by the sign of $\overline R_{1,3}=G_{3,3}\neq 0$ (the slope w.r.t. r of the right-hand side of (24) at $r=0$ and $\varepsilon=0$), negative (resp. positive) for the non-catastrophic (resp. catastrophic) case. Similarly, the analysis at $r=1$ (see (21a), where $R_{1,2}(\theta)=0$ under $G_{2,1}=0$) gives

$$\theta_{\mathrm{T}1}(0)=\frac{3}{4}\pi,\quad \theta^{(1)}_{\mathrm{T}1}(0)=-\frac{\overline R_{0,3}+\overline R_{1,3}+\overline R_{2,3}}{\overline R^{(1)}_{0,2}}=\theta^{(1)}_{\mathrm{T}2}(0)$$

(recall that $\overline R_{1,3}+\overline R_{2,3}=0$ and the symmetry between the two bifurcation curves), $\overline R^{(1)}_{0,2}\neq 0$ assures transversality, and the type of the bifurcation is determined by the sign of $\overline R_{1,3}+2\,\overline R_{2,3}=-\overline R_{1,3}$ (the r-slope of the right-hand side of (24) at $r=1$), i.e., the two bifurcations have opposite type.

To prove that there indeed are two distinct transcritical bifurcations, and to say which one comes first when θ is increased, we need to compute the second-order derivative $\theta^{(2)}_{\mathrm{T}2}(0)=-\theta^{(2)}_{\mathrm{T}1}(0)$ locally characterizing the deviations of the bifurcation curves from the curve at constant curvature $\theta=\frac{3}{4}\pi+\theta^{(1)}_{\mathrm{T}2}(0)\varepsilon$. The computation of $\theta^{(2)}_{\mathrm{T}2}(0)$ involves up to fourth-order terms in the expansion (10) (see Supplementary Data) and the result is

$$\begin{aligned}\theta^{(2)}_{\mathrm{T}2}(0)=-\theta^{(2)}_{\mathrm{T}1}(0)&=-\frac{\overline R^{(2)}_{0,2}\left(\theta^{(1)}_{\mathrm{T}2}(0)\right)^2+2\,\overline R^{(1)}_{0,3}\,\theta^{(1)}_{\mathrm{T}2}(0)+2\,\overline R_{0,4}}{\overline R^{(1)}_{0,2}}\\&=\frac{\left(\bar\lambda^{(2,1)}+\bar\lambda^{(1,2)}\right)\theta^{(1)}_{\mathrm{T}2}(0)-\frac{\sqrt2}{12}\left(\bar\lambda^{(3,1)}+\bar\lambda^{(1,3)}\right)}{\frac{\sqrt2}{2}\bar\lambda^{(0,2)}}\end{aligned}\tag{26}$$

(note that $\overline R^{(2)}_{0,2}=0$ under $G_{2,1}=0$ and recall. (G2.2)). Thus, substituting $\theta^{(1)}_{\mathrm{T}2}(0)$ from (25) into (26), we have two distinct transcritical bifurcations if the genericity condition

$$G_4:=\left(\bar\lambda^{(2,1)}+\bar\lambda^{(1,2)}\right)\frac{G_{3,2}}{6\sqrt2\,G_{2,2}}-\frac{\sqrt2}{12}\left(\bar\lambda^{(3,1)}+\bar\lambda^{(1,3)}\right)\neq 0\tag{G4}$$

is satisfied. Generically, we expect $\theta^{(1)}_{\mathrm{T}2}(0)=\theta^{(1)}_{\mathrm{T}1}(0)$ to be nonzero by (G3.2), so the two bifurcation curves are bended to the same side of the anti-diagonal $x_1+x_2=2x$. Otherwise (when $\theta^{(1)}_{\mathrm{T}2}(0)=\theta^{(1)}_{\mathrm{T}1}(0)=0$), the curvature is determined by $\theta^{(2)}_{\mathrm{T}2}(0)=-\theta^{(2)}_{\mathrm{T}1}(0)$, i.e., under (G4) the curves are locally bended symmetrically w.r.t. the anti-diagonal.

Having now up to two internal equilibria, we also need to analyze the possible saddle-node bifurcation at which they collide and disappear. The saddle-node conditions are

$$\begin{aligned}&R_{0,2}(\theta)+R_{0,3}(\theta)\varepsilon+\cdots+R_{0,k}(\theta)\varepsilon^{k-2}+\cdots\\&\quad+\left(R_{1,3}(\theta)\varepsilon+\cdots+R_{1,k}(\theta)\varepsilon^{k-2}+\cdots\right)\bar r\\&\quad+\left(R_{2,3}(\theta)\varepsilon+\cdots+R_{2,k}(\theta)\varepsilon^{k-2}+\cdots\right)\bar r^2\\&\qquad+\cdots+\left(R_{k-1,k}(\theta)\varepsilon^{k-2}+\cdots\right)\bar r^{k-1}\\&\qquad\qquad+\cdots=0,\end{aligned}\tag{27a}$$

which says that $\bar r$ is an equilibrium of Eq. (10) (in which $R_{0,1}(\theta)$ and $R_{1,2}(\theta)$ are now null by assumption), and its $\bar r-$derivative

$$\begin{aligned}&R_{1,3}(\theta)\varepsilon+\cdots+R_{1,k}(\theta)\varepsilon^{k-2}+\cdots\\&+2\left(R_{2,3}(\theta)\varepsilon+\cdots+R_{2,k}(\theta)\varepsilon^{k-2}+\cdots\right)\bar r\\&\quad+\cdots\\&\quad+(k-1)\left(R_{k-1,k}(\theta)\varepsilon^{k-2}+\cdots\right)\bar r^{k-2}\\&\qquad+\cdots=0,\end{aligned}\tag{27b}$$

which imposes the saddle-node (the zero slope of the right-hand side of (10) w.r.t. r at $\bar r$). They implicitly defines two functions $\bar r(\varepsilon)$ and $\theta_{\mathrm F}(\varepsilon)$ that satisfy Eqs. (27) for any small ε and, respectively, identify the saddle-node equilibrium and the bifurcation curve. Evaluating (27) and their ε-derivatives at $\varepsilon=0$, and solving for $\bar r(0)$ and $\theta_{\mathrm F}(0)$ and for their derivatives $\bar r^{(k)}(0)$ and $\theta^{(k)}_{\mathrm F}(0)$, $k\geq 1$, we can fully characterize both functions locally to $\varepsilon=0$. Up to $k=1$, we have

$$\begin{aligned}&0=R_{0,2}(\theta_{\mathrm F}(0)),\\&0=R^{(1)}_{0,2}(\theta_{\mathrm F}(0))\theta^{(1)}_{\mathrm F}(0)+R_{0,3}(\theta_{\mathrm F}(0))+R_{1,3}(\theta_{\mathrm F}(0))\bar r(0)+R_{2,3}(\theta_{\mathrm F}(0))\bar r(0)^2,\\&0=R_{1,3}(\theta_{\mathrm F}(0))+2\,R_{2,3}(\theta_{\mathrm F}(0))\bar r(0),\end{aligned}$$

from which we obtain

$$\bar r(0)=\frac12,\quad \theta_{\mathrm F}(0)=\frac34\pi,\quad \theta^{(1)}_{\mathrm F}(0)=-\frac{\overline R_{0,3}+\overline R_{1,3}/4}{\overline R^{(1)}_{0,2}}=\theta^{(1)}_{\mathrm{T}2}(0)+\frac{G_{3,3}}{2\sqrt2\,G_{2,2}}.\tag{28}$$

Note that, under (G3.3), the curvature of the saddle-node bifurcation curve is different from that of the transcritical bifurcations and that, when $\varepsilon\to 0$, the saddle-node equilibrium tends to $\frac12$, i.e., the two colliding equilibria are indeed internal and characterized by the same proportion of resident and invader densities. Further note that we generically expect

$$G_{3,4}:=4\,\overline R_{0,3}+\overline R_{1,3}=\tfrac13 G_{3,2}+G_{3,3}\neq 0,\tag{G3.4}$$

otherwise the curvature of the bifurcation curve is determined by fourth-order terms in the expansion (10).

For completeness, we should check the transversality of the bifurcation, that is however granted by the fact that the right-hand side of (10) is locally a parabola for small ε (second- and third-orders matter), so that two internal equilibria do collide and disappear when θ moves across the bifurcation curve. Precisely, the second $\bar r-$derivative of the left-hand side of (27a) at $(\bar r,\theta)=(\frac12,\frac34\pi)$ is given by $2\overline R_{2,3}\,\varepsilon+O(\varepsilon^2)$, that is nonzero under (G3.3) along the bifurcation curve for small $\varepsilon>0$. Finally, note that the saddle-node bifurcation is always catastrophic, since it involves the disappearance of a stable equilibrium.

We can now summarize the classification of the competition scenarios that are possible close to the (codimension-one) singular strategies characterized by the degeneracy $G_{2,1}=0$ (vanishing fitness cross-derivative) and by the genericity conditions (G2.2), (G3.2)–(G3.4), and (G4). This is done graphically in Fig. 8, where only the cases where $G_{2,2}$ is negative, i.e., those in which selection favors larger/smaller invader strategies when the resident x_1 is smaller/larger than x (convergence to the singular strategy in a one-dimensional adaptive dynamics), are reported. The cases with positive $G_{2,2}$ can be obtained by reversing the stability of all equilibria (boundary at $r=0$ and $r=1$ and internal) and, consequently, the type of transcritical bifurcations.

3.3.3. *Vanishing all second-order fitness derivatives*

In this section we analyze the (codimension-two) case in which $G_{2,1}=G_{2,2}=0$, i.e., the fitness cross-derivative $\bar\lambda^{(1,1)}$ and the pure-derivatives $\bar\lambda^{(2,0)}$ and $\bar\lambda^{(0,2)}$ all vanish (recall the second relation in (12)). Geometrically, this is the case approaching which—along

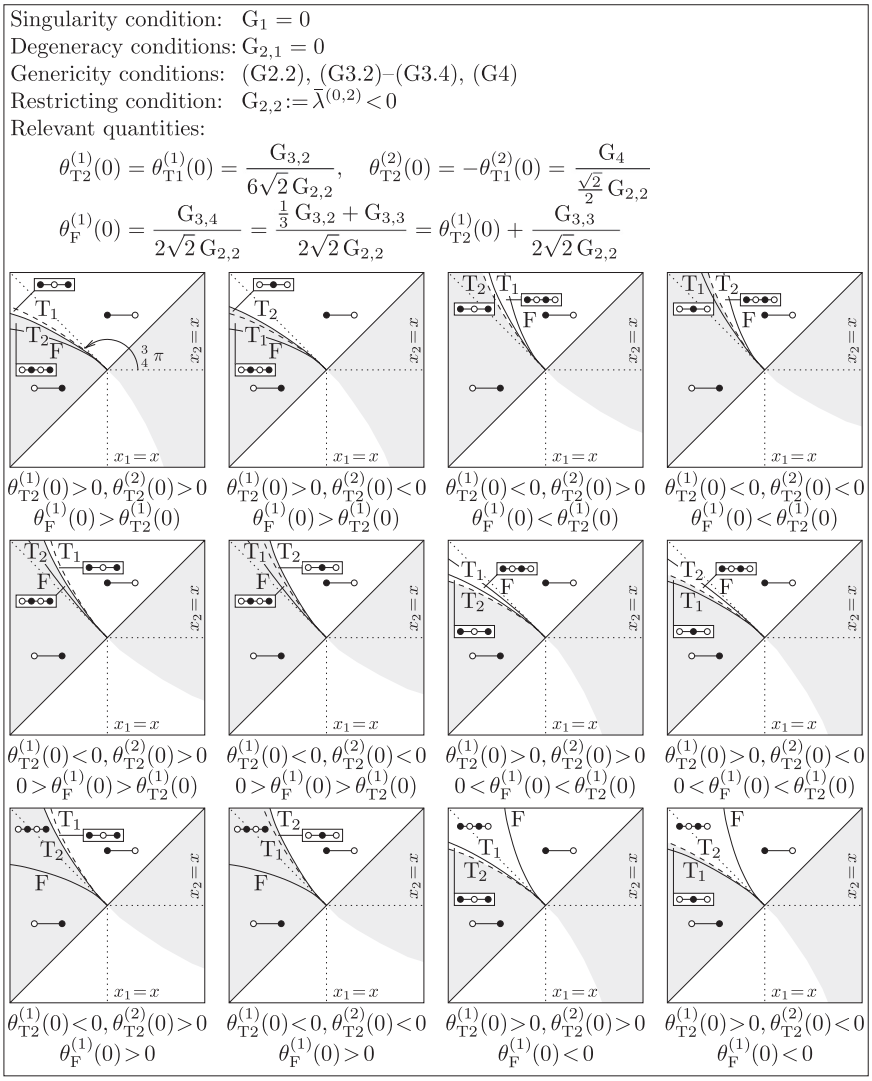

Fig. 8. Classification of the competition scenarios that are generically possible close to a singular strategy x with vanishing fitness cross-derivative. Only the cases with $G_{2,2} < 0$ are shown (selection favors larger/smaller strategy values when x_1 is smaller/larger than x); the cases with $G_{2,2} > 0$ can be obtained by reversing the stability of all equilibria.

with gradual changes in some model parameters—the cone of resident–invader coexistence degenerates on a saddle-node bifurcation between singular strategies.

In the time scale of time $\tau = \varepsilon^3 t$, Eq. (10) becomes

$$\frac{\mathrm{d}r}{\mathrm{d}\tau}\frac{1}{(\sin\theta - \cos\theta)r(1-r)} = R_{0,3}(\theta) + R_{1,3}(\theta)r + R_{2,3}(\theta)r^2 + O(\varepsilon). \tag{29}$$

In the limit $\varepsilon \to 0$, there can be, depending on θ, none, one, or two internal equilibria, so that x_1- or x_2-dominance, as well as protected and unprotected coexistence and mutual exclusion are possible. Cases with more than two internal equilibria require r-powers with degree higher than two, and are therefore ruled out as long as the third-order terms $R_{0,3}(\theta)$, $R_{1,3}(\theta)$, and $R_{2,3}(\theta)$ do not all vanish.

Note that $R_{1,3}$ and $R_{2,3}$ can be written as

$$R_{1,3}(\theta) = \tfrac{1}{2}(\sin\theta - \cos\theta)^2\overline{R}_{1,3} + \tfrac{1}{2}(\sin^2\theta - \cos^2\theta)\left(\bar{\lambda}^{(2,1)} + \bar{\lambda}^{(1,2)}\right), \tag{30a}$$

$$R_{2,3}(\theta) = -\tfrac{1}{2}(\sin\theta - \cos\theta)^2\overline{R}_{1,3}, \tag{30b}$$

so that the genericity condition (G3.3) (where now $\bar{\lambda}^{(0,2)} = 0$) implies that $R_{2,3}$ is nonzero for all θ in interval (6). If (G3.3) is not satisfied, then $R_{2,3}$ is null and, provided

$$G_{3,5} := \bar{\lambda}^{(2,1)} + \bar{\lambda}^{(1,2)} \neq 0, \tag{G3.5}$$

$R_{1,3}$ vanishes only for $\theta = \frac{3}{4}\pi$, at which $R_{0,3} = \overline{R}_{0,3}$ is nonzero under (G3.2) (see Table 2). Thus, condition " (G3.3) (or G3.2) and (G3.5)" is sufficient (even though not necessary) for dropping the $O(\varepsilon)$-terms in Eq. (29).

As for the transcritical bifurcation at $r=0$, Eq. (17) now becomes

$$R_{0,3}(\theta_{T2}(\varepsilon)) + \cdots + R_{0,k}(\theta_{T2}(\varepsilon))\varepsilon^{k-3} + \cdots = 0,$$

so that the tangent direction to the bifurcation curve is obtained by solving

$$R_{0,3}(\theta_{T2}(0)) = 0. \tag{31}$$

We find Eq. (31) more convenient to solve for the deviation

$$\Delta\theta_{T2}(0) := \theta_{T2}(0) - \tfrac{3}{4}\pi. \tag{32}$$

We proceed as follows. Substituting (32) into Eq. (31), we can rearrange terms as

$$3\,\bar{\lambda}^{(2,1)} + 6(1-C)\bar{\lambda}^{(1,2)} + (3-2\,C)\bar{\lambda}^{(0,3)} = -6(\pm\sqrt{C(1-C)})(\bar{\lambda}^{(2,1)} + \bar{\lambda}^{(1,2)}), \tag{33}$$

where $C := \cos^2\Delta\theta_{T2}(0)$ and $\pm\sqrt{1-C}$ has been written in place of

$\sin\Delta\theta_{T2}(0)$. Then, squaring both sides, we can get rid of the $\pm$ ambiguity and solve the second-order equation $a\,C^2+b\,C+c=0$, with

$$\tfrac{1}{4}a := 9\left(\bar\lambda^{(2,1)}+\bar\lambda^{(1,2)}\right)^2+\left(3\,\bar\lambda^{(1,2)}+\bar\lambda^{(0,3)}\right)^2, \tag{34a}$$

$$-\tfrac{1}{12}b := 3\left(\bar\lambda^{(2,1)}+\bar\lambda^{(1,2)}\right)^2+\left(3\,\bar\lambda^{(1,2)}+\bar\lambda^{(0,3)}\right)\left(\bar\lambda^{(2,1)}+2\,\bar\lambda^{(1,2)}+\bar\lambda^{(0,3)}\right) \tag{34b}$$

$$\tfrac{1}{9}c := \left(\bar\lambda^{(2,1)}+2\,\bar\lambda^{(1,2)}+\bar\lambda^{(0,3)}\right)^2. \tag{34c}$$

Obviously, only the positive solutions

$$C^{\pm}=(-b\pm\sqrt{b^2-4ac})/(2a)\quad\text{with } 0<C^{\pm}<1$$

are feasible, and for those we set $\cos\Delta\theta^{\pm}_{T2}(0)=\sqrt{C^{\pm}}$ (a negative cosine corresponds to an angle $\theta_{T2}(0)$ out of our interval (6) of interest). For each feasible solution, which one of the two sign alternatives solves (33) gives the sign of $\sin\Delta\theta^{\pm}_{T2}(0)$.

Looking at the coefficients a, b, and c in (34c), we see that the quadratic expression geometrically represents a upword parabola ($a>0$ under (G3.5)) with positive height at $C=0$ ($c>0$ under (G3.1)) and at $C=1$ ($a+b+c=G_{3,2}^2$). Moreover, the discriminant $b^2-4\,a\,c$ results in $432\,G_{3,5}^2\,G_{3,6}$, with (generically)

$$G_{3,6} := 3\left(\bar\lambda^{(1,2)}\right)^2-2\left(2\,\bar\lambda^{(2,1)}+\bar\lambda^{(1,2)}\right)\bar\lambda^{(0,3)}-\left(\bar\lambda^{(0,3)}\right)^2\neq 0 \tag{G3.6}$$

(see Supplementary Data), so that, if the discriminant is positive, there are either two solutions $C^{\pm}\in(0,1)$ or none; no solution if the discriminant is negative.

We therefore conclude that, under (G3.1), (G3.2), (G3.5), (G3.6), there are either two or no transcritical bifurcation curves of the equilibrium at $r=0$, emanating from point (x,x) in the $(x_1,x_2)-$plane with directions given by $\theta^{\pm}_{T2}(0)=\frac{3}{4}\pi+\Delta\theta^{\pm}_{T2}(0)$. Similar to Section 3.3.2, the transversality of the bifurcations is assured by

$$G^{\pm}_{3,7} := R^{(1)}_{0,3}(\theta^{\pm}_{T2}(0))=\tfrac{1}{3}\,\sin\Delta\theta^{\pm}_{T2}(0)\cos\,\Delta\theta^{\pm}_{T2}(0)\left(3\bar\lambda^{(1,2)}+\bar\lambda^{(0,3)}\right)$$
$$-\tfrac{1}{2}(\sin^2\Delta\theta^{\pm}_{T2}(0)-\cos^2\Delta\theta^{\pm}_{T2}(0))G_{3,5}\neq 0 \tag{G3.7}$$

(under which the right-hand side of Eq. (29) at $r=0$ changes sign for small ε when θ moves across the bifurcation curves) and the bifurcation type is determined by the sign of $R_{1,3}(\theta^{\pm}_{T2}(0))$, negative (resp. positive) for the non-catastrophic- (resp. catastrophic) case. Generically, we expect

$$G^{\pm}_{3,8} := R_{1,3}(\theta^{\pm}_{T2}(0))$$
$$=\cos^2\Delta\theta^{\pm}_{T2}(0)G_{3,3}-\sin\,\Delta\theta^{\pm}_{T2}(0)\cos\,\Delta\theta^{\pm}_{T2}(0)G_{3,5}\neq 0 \tag{G3.8}$$

(see Supplementary Data for the computations).

As for the transcritical bifurcation at $r=1$, the condition for the tangent direction now becomes (from Eq. (17))

$$R_{0,3}(\theta_{T1}(0))+R_{1,3}(\theta_{T1}(0))+R_{2,3}(\theta_{T1}(0))=0. \tag{35}$$

Obviously (due to the symmetry of model (1) w.r.t. the diagonal $x_1=x_2$), Eq. (35) again yields (33), where now $C := \cos^2\Delta\theta_{T1}(0)$ and $\mp\sqrt{1-C}$ has been written in place of $\sin\Delta\theta_{T1}(0)$ (note the opposite sign in front of the square root), $\Delta\theta_{T1}(0) := \theta_{T1}(0)-\frac{3}{4}\pi$. Thus, we have the same feasible solutions for $\cos\Delta\theta_{T2}(0)$ and $\cos\Delta\theta_{T1}(0)$, but with opposite sine, i.e., opposite angle deviations from $\frac{3}{4}\pi$. There is therefore a transcritical bifurcation curve of the equilibrium at $r=1$ for each one involving the equilibrium at $r=0$, emanating from point (x,x) in the $(x_1,x_2)-$plane with symmetric direction w.r.t. the anti-diagonal, i.e., $\theta^{\pm}_{T1}(0)=\frac{3}{4}\pi+\Delta\theta^{\pm}_{T1}(0)=\frac{3}{4}\pi-\Delta\theta^{\pm}_{T2}(0)$.

The transversality of the bifurcations is assured by

$$R^{(1)}_{0,3}(\theta^{\pm}_{T1}(0))+R^{(1)}_{1,3}(\theta^{\pm}_{T1}(0))+R^{(1)}_{2,3}(\theta^{\pm}_{T1}(0))\neq 0$$

(under which the right-hand side of Eq. (29) at $r=1$ changes sign for small ε when θ moves across the bifurcation curves), the left-hand side of which turns out to be the opposite of $R^{(1)}_{0,3}(\theta^{\pm}_{T2}(0))$ in (G3.7). The bifurcation type is determined by the sign of $R_{1,3}(\theta^{\pm}_{T1}(0))+2\,R_{2,3}(\theta^{\pm}_{T1}(0))$, that turns out to be the opposite of $R_{1,3}(\theta^{\pm}_{T2}(0))$ in (G3.8) (see Supplementary Data). Thus, the transcritical bifurcation at $r=1$ with direction $\theta^{\pm}_{T1}(0)$ generically takes place and has opposite type of the corresponding bifurcation at $r=0$ with direction $\theta^{\pm}_{T2}(0)$.

We last have to analyze the possible saddle-node bifurcations involving two internal equilibria of Eq. (29) in the limit $\varepsilon\to 0$. The saddle-node conditions (27) now give

$$0=R_{0,3}(\theta_F(0))+R_{1,3}(\theta_F(0))\bar r(0)+R_{2,3}(\theta_F(0))\bar r(0)^2, \tag{36a}$$

$$0=R_{1,3}(\theta_F(0))+2\,R_{2,3}(\theta_F(0))\bar r(0), \tag{36b}$$

i.e., being $R_{2,3}(\theta_F(0))$ nonzero under (G3.3) (see (6) and (30b)),

$$0=\left(R_{1,3}(\theta_F(0))\right)^2-4\,R_{0,3}(\theta_F(0))R_{2,3}(\theta_F(0)),$$

which imposes the linear condition

$$\left(G_{3,5}^2+G_{3,3}\left(-G_{3,3}+2\,\bar\lambda^{(1,2)}+\frac{2}{3}\bar\lambda^{(0,3)}\right)\right)C=G_{3,5}^2+G_{3,3}\,G_{3,1} \tag{37}$$

on $C := \cos^2\Delta\theta_F(0)$, $\Delta\theta_F(0) := \theta_F(0)-\frac{3}{4}\pi$ (see Supplementary Data). Thus, if C results in $(0,1)$, then we have two bifurcation curves emanating from point (x,x) in the $(x_1,x_2)-$plane with directions $\frac{3}{4}\pi+\Delta\theta_F(0)$ and $\frac{3}{4}\pi-\Delta\theta_F(0)$, symmetric w.r.t. the anti-diagonal, where $\sin\Delta\theta_F(0)=\sqrt{1-C}>0$). And $R_{2,3}(\theta_F(0))\neq 0$ under (G3.3) assures the transversality of the bifurcations.

Of course, we expect the coefficients of Eq. (37) to be nonzero and unequal:

$$G_{3,9} := G_{3,5}^2+G_{3,3}\,G_{3,1}\neq 0, \tag{G3.9}$$

$$G_{3,10} := G_{3,5}^2+G_{3,3}\left(-G_{3,3}+2\,\bar\lambda^{(1,2)}+\frac{2}{3}\bar\lambda^{(0,3)}\right)\neq 0, \tag{G3.10}$$

$$G_{3,11} := \frac{G_{3,9}-G_{3,10}}{G_{3,3}}=G_{3,1}+G_{3,3}-2\,\bar\lambda^{(1,2)}-\frac{2}{3}\bar\lambda^{(0,3)}\neq 0, \tag{G3.11}$$

so that C is defined and different from 0 and 1 (i.e., we generically expect $0<\Delta\theta_F(0)<\frac{1}{2}\pi$ whenever $\Delta\theta_F(0)$ is defined). Finally note that the angles of the saddle-node bifurcations cannot coincide, locally to (x,x), with the angles of transcritical bifurcations, otherwise, comparing Eqs. (31), (35), and (36a), we see that this would require the saddle-node equilibrium to be at either $\bar r=0$ or $\bar r=1$, but then (36b) would contradict (G3.8).

As done in the previous sections, we graphically summarize the classification of the competition scenarios that are possible close to the (codimension-two) singular strategies characterized by the degeneracies $G_{2,1}=G_{2,2}=0$ (vanishing all second-order fitness derivatives) and by the genericity conditions (G3.1)–(G3.3), (G3.5)–(G3.11). As in Fig. 7, we display in Figs. 9 and 10 only the cases where $G_{3,1}<0$ is negative (selection favoring smaller strategies on both sides of x).

4. Summary of the results

We now summarize our results in a recipe-like style, ready to be used. This section can be considered as the statement of a theorem, the proof of which is contained in the analyses of Section 3. For each of the considered cases, where the reference strategy x is (1) nonsingular, (2) close to generic singularity, (3.1–3.3) close to degenerate (codimension-one and -two) singular strategies, we addressed the following two questions (with reference to Fig. 2):

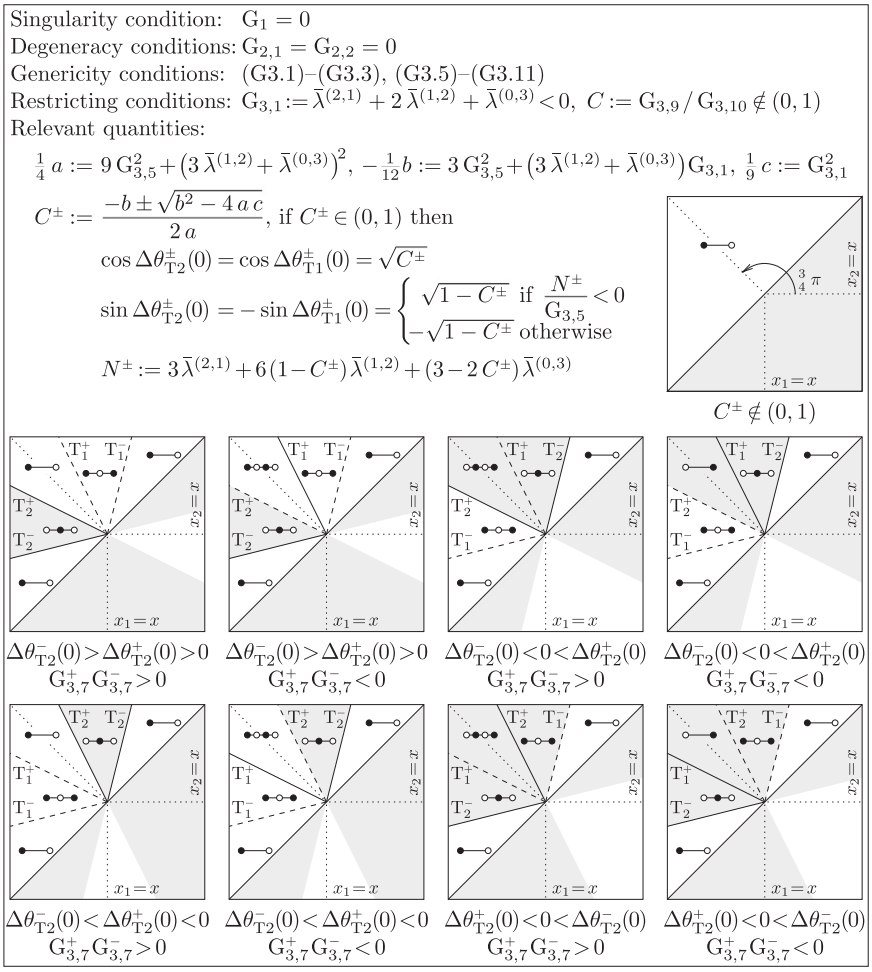

Fig. 9. Classification of the competition scenarios that are generically possible close to a singular strategy x with vanishing second-order fitness derivatives. Only the cases with $G_{3,1} < 0$ (selection favors smaller strategy values on both sides of x) and $C \notin (0, 1)$ (no saddle-node bifurcations) are shown. The cases with $G_{3,1} > 0$ can be obtained by reversing the stability of all equilibria. The cases with $C = \cos^2 \Delta\theta_F(0) \in (0, 1)$ (two saddle-node bifurcations) are reported in Fig. 10.

- What is the competition scenario that occurs for a given perturbation angle θ, in the interval $\frac{1}{4}\pi < \theta < \frac{5}{4}\pi$, and for sufficiently small ε (i.e., in the limit $\varepsilon \to 0$)?
- If different scenarios occur for different θ (and small ε), then what is the structure and shape of the bifurcation boundaries separating them locally to point (x,x) in the plane of the strategies (x_1, x_2)?

Each case assumes some degeneracy and genericity conditions, under which the answers are given (degeneracies are stated in terms of failing genericity conditions). All genericity conditions, except the hyperbolicity of the resident equilibrium $(\overline{n}(x), \overline{N}(x))$ (which is always assumed), are reported for the reader's convenience in Table 3 (those that cannot be expressed only in terms of invasion fitness derivatives have a star over the equal sign in their definition; the $(P+1) \times (P+1)$ nonsingular matrix M involved in $G_{3,3}$ for $P > 0$ is defined in Table 1).

Note that we do not discuss the competition scenarios and the relative bifurcation boundaries if a finite distance ε from the reference strategy x is required. Also, we do not discuss (if not occasionally, e.g., later in Fig. 6) the unfolding of cases (1)–(3) along with gradual changes in some model parameters. The latter topics are definitely interesting but are left out to limit the length of the paper. They can be dealt with by complementing our local analysis with the global results of Priklopil (2012) on the boundaries in the plane (x_1, x_2) of the region allowing coexistence.

Figs. 4–10 display the classification of the competition scenarios that are possible close to the reference strategy x in cases (1), (2), (3.1–3.3). They contain all information to answer the two above questions: the assumed degeneracy and genericity conditions and the relevant quantities to discriminate among subcases (see Table 4 for the graphical and symbolical notation). Each scenario is identified by the sketch of the resident–invader (slow) dynamics on the one-dimensional axis of the relative invader density, $r \in [0, 1]$ (r-sketches in the following). The dynamics of model (1), in the state space of the resident–invader densities, are qualitatively displayed in Fig. 1 for each of the involved r-sketches.

Fig. 4 illustrates the"invasion implies substitution" theorem (Geritz, 2005; Meszéna et al., 2005; Dercole and Rinaldi, 2008). Invasion away from singularity, i.e., positive invasion fitness (point (x_1, x_2) in the gray area) under (G1), implies the extinction of the resident type (r converges to 1, provided ε is sufficiently small). Conversely, the invader goes extinct if the invasion fitness is negative (r converges to 0 if point (x_1, x_2) lies in the white area). The diagram of the fitness sign is known in evolutionary biology as the *pairwise invasibility plot* (PIP) and is always drawn in Figs. 4–10, locally to the reference strategy x, in gray/white for the positive/negative sign. Another common diagram (not shown), the *mutual invasibility plot* (MIP), is obtained by the superposition of the PIP with its mirror image along the diagonal. Due to the symmetry of the resident–invader model (1), points in the gray–gray areas of the MIP are characterized by mutant invasion

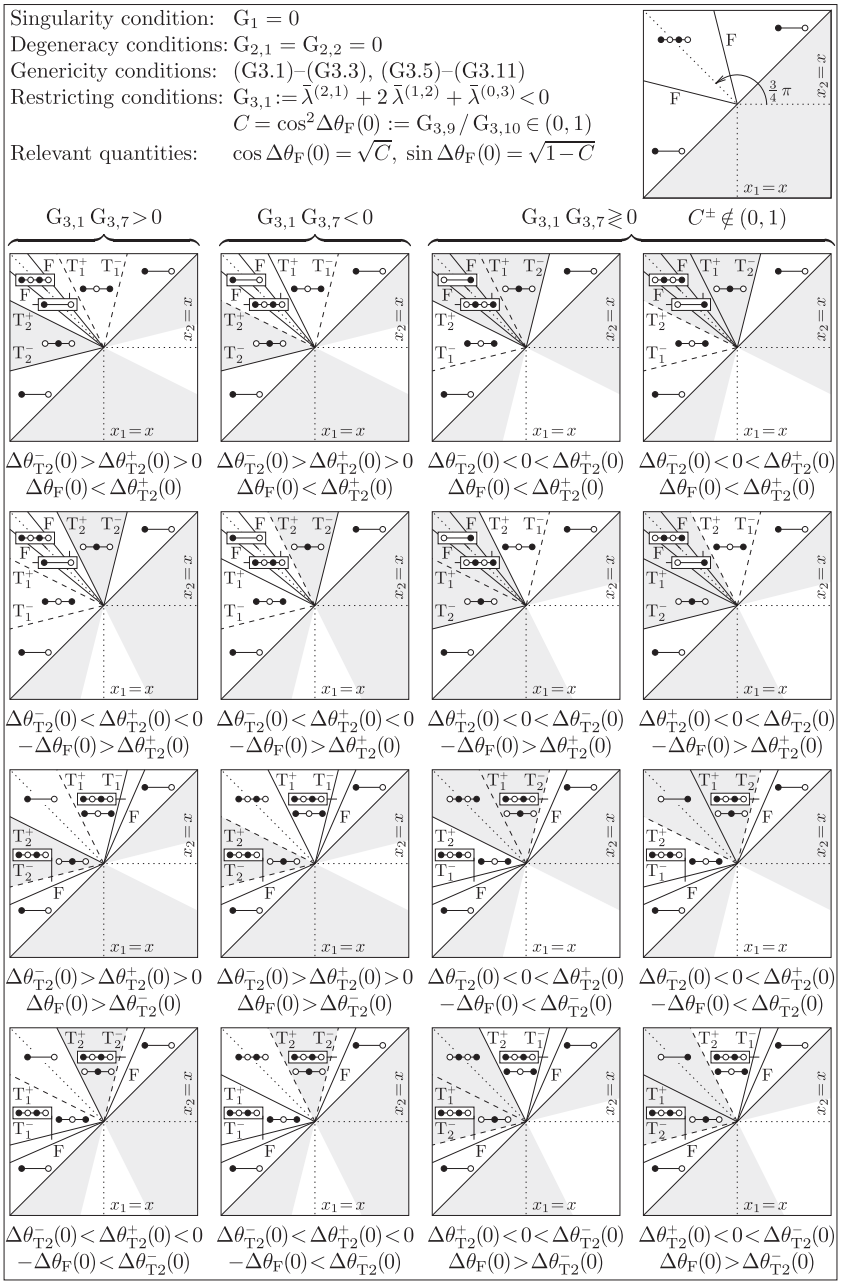

Fig. 10. Classification of the competition scenarios that are generically possible close to a singular strategy x with vanishing second-order fitness derivatives. Only the cases with $G_{3,1} < 0$ (selection favors smaller strategy values on both sides of x) and $C = \cos^2 \Delta\theta_F(0) \in (0, 1)$ (two saddle-node bifurcations) are shown. The cases with $G_{3,1} > 0$ can be obtained by reversing the stability of all equilibria. The cases with $C \notin (0, 1)$ (no saddle-node bifurcations) are reported in Fig. 9.

$(\lambda(x_1, x_2) > 0)$ and by resident invasion close to the monomorphic equilibrium $(n_1, n_2, N) = (0, \hat{n}(x_2), N(x_2))$ $(\lambda(x_2, x_1) > 0)$. Thus the gray–gray areas of the MIP are those in which resident–invader coexistence is protected.

Fig. 5 shows that only the four classical Lotka–Volterra competition scenarios can generically occur when the resident and invader strategies are nearly singular. As it is well known from the first classification of singular strategies (Metz et al., 1996; Geritz et al., 1997, 1998), there are eight possible PIP configurations, that can be discriminated in terms of the second pure-derivatives of the invasion fitness (see the top-right panel, adapted from Geritz et al. (1998), where the genericity conditions (G2.1) and (G2.2) are also graphically interpreted). The four configurations a–d are characterized by $G_{2,2} < 0$, i.e., selection favors larger/smaller invader strategies when the resident x_1 is smaller/larger than x (convergence to the singular strategy in a one-dimensional adaptive dynamics), whereas $G_{2,2} > 0$ in cases e–h (divergence from the singular strategy). Note that cases e–h can be, respectively, obtained from cases a–d by reversing the stability of all equilibria and, consequently, the type of transcritical bifurcations and the gray–white filling. Cases b–e are *evolutionarily stable* (the singular strategy is locally protected against invasion; Maynard Smith and Price, 1973; Maynard Smith, 1982), cases f–a are not.

For each PIP configuration, the bifurcation boundaries separating different competition scenarios in the strategy plane (x_1, x_2) are drawn, locally to the singular point (x,x), only for $x_1 < x_2$ (above the diagonal $x_1 = x_2$). Of course the bifurcation boundaries extend below the diagonal in the same direction and, due to the symmetry of the resident–invader model (1), the competition scenario for $x_1 > x_2$ (below the diagonal) is obtained from the scenario at point (x_2, x_1) (above the diagonal) by exchanging x_1 with x_2 and n_1

with n_2 (i.e., by horizontally flipping the r-sketch). As discussed in Section 3.2, the bifurcation boundaries technically correspond to transcritical bifurcations at which the internal equilibrium collides (and exchanges stability) with the monomorphic equilibrium $(n_1, n_2, N) = (0, \pi(x_2), \overline{N}(x_2))$ ($n_1 = 0$ and $r = 1$) at the bifurcation $\underline{T}_1$ or with the monomorphic equilibrium $(n_1, n_2, N) = (\pi(x_1), 0, N(x_1))$ ($n_2 = 0$ and $r = 0$) at the bifurcation T_2. The bifurcation curves T_1 and T_2 are symmetric w.r.t. to the diagonal (again due to the symmetry of model (1)) and emanate from the point (x,x) with directions given by the angles $\theta_{T1}(0)$ and $\theta_{T2}(0)$, that are also expressed in terms of the second pure-derivatives of the invasion fitness. The bifurcations are non-catastrophic if the internal equilibrium is stable (solid lines in cases g–b characterized by $G_{2,1} < 0$). This means that crossing the bifurcation curve, along with gradual changes in some model parameters, does not involve a radical change in the asymptotic state of model (1). Conversely, the bifurcations are catastrophic (dashed line in cases c–f with $G_{2,1} > 0$) if the internal equilibrium is unstable.

Note that the invasion fitness $\lambda(x_1, x_2) > 0$ vanishes along the bifurcation curve T_2, so that T_2 defines the boundary of the PIP (above and below the diagonal). Further note that only four configurations are distinguishable from the point of view of bifurcation analysis, since the fact that the angle of a bifurcation curve goes through $\frac{1}{2}\pi$ (e.g., from case a to b) does not qualitatively change the unfolding of the competition scenarios locally to (x,x). However, the distinction is biologically relevant, as the singular strategy changes evolutionarily stability.

As it follows from the analysis of Sections 3.2 and 3.3.1 (both assuming $G_{2,1} < 0$), when along with parameter changes the quantity in (G2.2) vanishes, the cone of resident–invader coexistence becomes wider and approaches the diagonal. Generically, i.e., by further assuming (G3.1), two singular strategies (one for which $G_{2,2} > 0$ and one for which $G_{2,2} < 0$) collide and disappear, as sketched in Fig. 6. Note that this is not a bifurcation of model (1), but rather a bifurcation of the Adaptive Dynamics resulting from repeated invasions, first graphically discussed in Geritz et al.(1999). At the bifurcation, generically, four PIP configurations can occur. The two that are characterized by $G_{3,1} < 0$ (selection favors smaller strategy values on both sides of x) are shown in Fig. 7. The other two are obtained by reversing the stability of all equilibria, and hence the type of the transcritical bifurcation and the gray–white filling.

Close to the other codimension-one-degenerate singular strategy, at which (G2.1) fails under (G2.2), the number of different generic configurations of the competition scenarios gets up to 24. Half of the cases are shown in Fig. 8 under $G_{2,2} < 0$ (selection favors larger/smaller invader strategies when the resident x_1 is smaller/larger than x), that now also implies evolutionary stability, recall that $G_{2,2} = \lambda^{(0,2)}$, so that $\lambda(x_1, x_1 + \varepsilon) < 0$ for small ε. The remaining 12 cases can be obtained by reversing the stability of all equilibria, and hence the type of the transcritical bifurcation and the gray–white filling. Moreover, note that only four cases are distinguishable from the point of view of bifurcation analysis, as the four configurations in each column present the same unfolding of the competition scenarios (the order in which bifurcations are encountered by increasing θ is the same). The additional distinc-tions might however be evolutionarily relevant, though the evo-lutionary scenarios close to degenerate singularities are still uninvestigated.

Table 3
Genericity conditions.

$$G_1 := \overline{\lambda}^{(0,1)} \neq 0 \quad \text{(G1)}$$

$$G_{2,1} := \overline{\lambda}^{(1,1)} \neq 0 \quad \text{(G2.1)}$$

$$G_{2,2} := \overline{\lambda}^{(1,1)} + \overline{\lambda}^{(0,2)} = \tfrac{1}{2}\left(\overline{\lambda}^{(0,2)} - \overline{\lambda}^{(2,0)}\right) \neq 0 \quad \text{(G2.2)}$$

$$G_{3,1} := \overline{\lambda}^{(2,1)} + 2\,\overline{\lambda}^{(1,2)} + \overline{\lambda}^{(0,3)} \neq 0 \quad \text{(G3.1)}$$

$$G_{3,2} := 3\,\overline{\lambda}^{(2,1)} + \overline{\lambda}^{(0,3)} \neq 0 \quad \text{(G3.2)}$$

$$\begin{aligned} G_{3,3} \overset{*}{:=}\ & -\overline{\lambda}^{(2,1)} + \overline{\phi}_{2,1}^{(0,0,0,1)}\overline{n} \\ & - \tfrac{1}{\det M}\left(\overline{g}^{(0,0,1,0,0,1)}\tilde{F}^{(1,0,0,0,0)} + \overline{g}^{(1,0,0,0,0,1)}\tilde{g}^{(1,0,0,0,0,0)}\right)\left(\overline{\lambda}^{(0,2)} + \overline{\phi}_{2,1}\,\overline{n}\right) \\ & - \tfrac{1}{\det M}\left(\overline{g}^{(0,0,1,0,0,1)}\tilde{F}^{(0,0,1,0,0)} + \overline{g}^{(1,0,0,0,0,1)}\tilde{g}^{(0,0,1,0,0,0)}\right)\overline{\psi}_{2,1}\overline{n} \neq 0 \ (P > 0) \end{aligned} \quad \text{(G3.3)}$$

$$G_{3,3} \overset{*}{:=} -\overline{\lambda}^{(2,1)} + \overline{\phi}_{2,1}^{(0,0,1)}\overline{n} - \tfrac{\overline{g}^{(1,0,0,0,1)}}{\overline{g}^{(1,0,0,0,0)}}\left(\overline{\lambda}^{(0,2)} + \overline{\phi}_{2,1}\,\overline{n}\right) \neq 0 \quad (P = 0) \quad \text{(G3.3)}$$

$$G_{3,4} \overset{*}{:=} \tfrac{1}{3}G_{3,2} + G_{3,3} \neq 0 \quad \text{(G3.4)}$$

$$G_{3,5} := \overline{\lambda}^{(2,1)} + \overline{\lambda}^{(1,2)} \neq 0 \quad \text{(G3.5)}$$

$$G_{3,6} := 3\left(\overline{\lambda}^{(1,2)}\right)^2 - 2\left(2\,\overline{\lambda}^{(2,1)} + \overline{\lambda}^{(1,2)}\right)\overline{\lambda}^{(0,3)} - \left(\overline{\lambda}^{(0,3)}\right)^2 \neq 0 \quad \text{(G3.6)}$$

$$\begin{aligned} G_{3,7}^{\pm} := & \tfrac{1}{3}\sin\,\Delta\theta_{T2}^{\pm}(0)\cos\,\Delta\theta_{T2}^{\pm}(0)\left(3\overline{\lambda}^{(1,2)} + \overline{\lambda}^{(0,3)}\right) \\ & - \tfrac{1}{2}\left(\sin^2\Delta\theta_{T2}^{\pm}(0) - \cos^2\Delta\theta_{T2}^{\pm}(0)\right)G_{3,5} \neq 0 \end{aligned} \quad \text{(G3.7)}$$

$$G_{3,8}^{\pm} \overset{*}{:=} \cos^2\Delta\theta_{T2}^{\pm}(0)G_{3,3} - \sin\,\Delta\theta_{T2}^{\pm}(0)\cos\,\Delta\theta_{T2}^{\pm}(0)G_{3,5} \neq 0 \quad \text{(G3.8)}$$

$$G_{3,9} \overset{*}{:=} G_{3,5}^2 + G_{3,3}G_{3,1} \neq 0 \quad \text{(G3.9)}$$

$$G_{3,10} \overset{*}{:=} G_{3,5}^2 + G_{3,3}\left(-G_{3,3} + 2\,\overline{\lambda}^{(1,2)} + \tfrac{2}{3}\overline{\lambda}^{(0,3)}\right) \neq 0 \quad \text{(G3.10)}$$

$$G_{3,11} \overset{*}{:=} G_{3,1} + G_{3,3} - 2\,\overline{\lambda}^{(1,2)} - \tfrac{2}{3}\overline{\lambda}^{(0,3)} \neq 0 \quad \text{(G3.11)}$$

$$G_4 := \tfrac{G_{3,2}G_{3,5}}{6\sqrt{2}\,G_{2,2}} - \tfrac{\sqrt{2}}{12}\left(\overline{\lambda}^{(3,1)} + \overline{\lambda}^{(1,3)}\right) \neq 0 \quad \text{(G4)}$$

Table 4
Graphical notation and bifurcation boundaries in Figs. 4–10.

Symbol	Equation	Line style	Description
T_1	$\theta = \theta_{T1}(\varepsilon)$	Solid (non-catastrophic) dashed (catastrophic)	Transcritical bifurcation at which an internal equilibrium collides with the resident monomorphic equilibrium $(n_1, n_2, N) = (0, \overline{n}(x_2), \overline{N}(x_2))$ ($n_1 = 0$ and $r = 1$ at the bifurcation)
T_2	$\theta = \theta_{T2}(\varepsilon)$	Solid (non-catastrophic) dashed (catastrophic)	Transcritical bifurcation at which an internal equilibrium collides with the invader monomorphic equilibrium $(n_1, n_2, N) = (\overline{n}(x_1), 0, \overline{N}(x_1))$ ($n_2 = 0$ and $r = 0$ at the bifurcation)
$T_1^{\pm}$	$\theta = \frac{3}{4}\pi + \Delta\theta_{T1}^{\pm}(\varepsilon)$	Solid (non-catastrophic) dashed (catastrophic)	Transcritical bifurcations at $(n_1, n_2, N) = (0, \overline{n}(x_2), \overline{N}(x_2))$ ($n_1 = 0$ and $r = 1$)
$T_2^{\pm}$	$\theta = \frac{3}{4}\pi + \Delta\theta_{T2}^{\pm}(\varepsilon)$	Solid (non-catastrophic) dashed (catastrophic)	Transcritical bifurcations at $(n_1, n_2, N) = (\overline{n}(x_1), 0, \overline{N}(x_1))$ ($n_2 = 0$ and $r = 0$)
F	$\theta = \theta_F(\varepsilon)$ $\theta = \frac{3}{4}\pi \pm \Delta\theta_F(\varepsilon)$	Solid (catastrophic)	Saddle-node (fold) bifurcations at which two internal equilibria (one stable, one unstable) collides and disappear
–	$\theta = \frac{1}{4}\pi$, $x_1 = x_2$	Solid	The diagonal is a degenerate transcritical bifurcation at which a segment of critically stable equilibria connects the monomorphic states
–	$\theta = \frac{3}{4}\pi$, $x_1 + x_2 = 2x$	Dotted	Anti-diagonal, no bifurcation occurs
Filled dots			Unstable (saddle) equilibria
Empty dots			Unstable (saddle) equilibria
r-sketches from Fig. 1			Resident–invader relative dynamics
Gray region			Invader invasion, $\lambda(x_1, x_2) > 0$
White dots			Invader extinction, $\lambda(x_1, x_2) < 0$

The results of Section 3.3.2 show that when along with parameter changes a negative fitness cross-derivative vanishes under (G2.2), the cone of resident–invader coexistence narrows in a cuspwise manner around the anti-diagonal $\theta=\frac{3}{4}\pi$. Generically, more specifically by also assuming (G3.2)–(G3.4) and (G4), there are three distinct bifurcation boundaries separating the different competition scenarios that can occur locally to the singular point (x,x), all emanating from (x,x) in the direction of the anti-diagonal. Two are the (symmetric) transcritical bifurcations curves T_1 and T_2 (respectively, involving the monomorphic equilibria with $n_1=0$ and $n_2=0$) that are bended to the same side of the anti-diagonal (the two first-order curvatures $\theta^{(1)}_{T1}(0)$ and $\theta^{(1)}_{T2}(0)$ being equal) and indeed distinct (under (G4) the two second-order curvatures $\theta^{(2)}_{T1}(0)$ and $\theta^{(2)}_{T2}(0)$ are nonzero and opposite). The third bifurcation boundary is a saddle-node (or fold) bifurcation involving two internal equilibria. It can be bended to either side of the anti-diagonal (under (G3.3) its first-order curvature $\theta^{(1)}_{F}(0)$ is different from that of the transcritical curves) and it delimits, together with one of the two transcritical bifurcations, the region of resident mutant coexistence (defined as the set of (x_1,x_2)−combinations allowing a stable internal equilibrium).

Of the two internal equilibria involved in the saddle-node bifurcation, one is stable and one is not, and this makes coexistence unprotected (see Fig. 1e and f). We have therefore shown that unprotected coexistence is always possible close to a singular strategy that is degenerate only in the fitness cross-derivative. Of course our results hold generically, i.e., provided all genericity conditions in Table 3 are satisfied. However, the concept of genericity depends on the universe of discourse. For example, the internal equilibria in Lotka–Volterra models are defined by linear equations in the population densities, so that either one or no solution is present away from bifurcations. Indeed, in Section 5.2 we show that condition (G3.3) systematically fails in Lotka–Volterra competition models, and (G3.3) is exactly the condition for the existence of the saddle-node bifurcation (see Section 3.3.2 for details). Note that our approach immediately extends to any degenerate situation, by simply assuming the desired degeneracies and considering the leading order in the expansion of the resident–invader relative dynamics (see Eq. (10)).

Finally, the number of different local configurations of the competition scenarios becomes 52 close to the codimension-two-degenerate singular strategies at which (G2.1) and (G2.2) both fail (i.e., all fitness second derivatives vanish at x) under the genericity conditions (G3.1)–(G3.3), (G3.5)–(G3.11). Half of the cases (those characterized by $G_{3,1}<0$, selection favoring smaller strategies on both sides of x) are shown in Figs. 9 and 10, and all represent qualitatively different unfoldings of the competition scenarios. The other half are obtained by reversing the stability of all equilibria, and hence the type of the transcritical bifurcation and the gray–white filling.

As it follows from the analysis in Section 3.3.3, locally to this double-degenerate singularity, the region of resident mutant coexistence is again conical, but not symmetric w.r.t. to the anti-diagonal and can even be composed of several sectors delimited, case by case, by a different mixture of transcritical and saddle-node bifurcations. The (symmetric) transcritical bifurcations at the monomorphic equilibria with $n_1=0$ and $n_2=0$ are either absent (if $C^{\pm}$ are both outside $(0,1)$) or each of them occur on a pair of curves (if $C^{\pm}$ are both in $(0,1)$), denoted T_i^+ and T_i^- and locally characterized by angles $\theta^+_{Ti}(0)>\theta^-_{Ti}(0)$. The saddle-node bifurcation is also either absent (if $C\notin(0,1)$, see Fig. 9) or present on a pair of curves (if $C\in(0,1)$, see Fig. 10), symmetric w.r.t. the anti-diagonal and with local directions, $\frac{3}{4}\pi+\Delta\theta_F(0)$ and $\frac{3}{4}\pi-\Delta\theta_F(0)$ $(0<\Delta\theta_F(0)<\frac{1}{2}\pi)$, that generically differ from those of the transcritical bifurcations. Note that unprotected coexistence is possible even in the absence of saddle-node bifurcations (Fig. 9). Also note the PIPs, that are locally composed of several sectors with positive (gray) and negative (white) fitness (delimited by the transcritical bifurcations $T_2^{\pm}$ and by the diagonal).

5. Examples

We now apply our formulas to two examples. In the first one we consider a model for the evolution of cannibalism (Dercole and Rinaldi, 2002; Dercole, 2003), in which the three degenerate singular strategies considered in Sections 3.3.1–3.3.3 all occur for particular values of the model parameters. We do not exemplify the formulas that apply away from singularity and close to a generic singular strategy, as they have been available in the literature for some years (Metz et al., 1996; Geritz et al., 1997, 1998; Dercole and Rinaldi, 2008) and extensively tested (see again Dercole and Rinaldi, 2002; Dercole, 2003; Dercole et al., 2003, but also, e.g., Dercole, 2005; Dercole et al., 2006, 2008, 2010a,b; Der-cole and Rinaldi, 2010, for testing on particular examples, and Landi et al., 2013; Della Rossa et al., 2015, for a systematic analysis of the ESS-branching transition of adaptive dynamics).

In the second example we show the manner in which a Lotka–Volterra resident–invader model is degenerate.

5.1. A model for the evolution of cannibalism

In Dercole and Rinaldi (2002) and Dercole (2003), the (non-negative) strategy x measures the cannibalistic tendency of the individual, assumed to increase with adult body size. The g-function is

$$g(n_1,n_2,N,x_1,x_2,x') := e\frac{a_0(x')N+a(x',x_1)n_1+a(x',x_2)n_2}{1+a_0(x')h(x')N+a(x',x_1)h(x')n_1+a(x',x_2)h(x')n_2} - \frac{a(x_1,x')n_1}{1+a_0(x_1)h(x_1)N+a(x_1,x_1)h(x_1)n_1+a(x_1,x_2)h(x_1)n_2} - \frac{a(x_2,x')n_2}{1+a_0(x_2)h(x_2)N+a(x_2,x_1)h(x_2)n_1+a(x_2,x_2)h(x_2)n_2} - c(n_1+n_2), \tag{38}$$

where N is the density of a zooplankton resource, harvested by both types of cannibals. The density N is later considered constant (so we apply the formulas for $P=0$), though we leave the argument N in g for consistency of notation and also for suggesting a new example (with $P=1$) with a dynamical N (e.g., chemostat or logistic). For an individual with strategy x', the first term in the right-hand side of (38) describes consumption, consisting of the harvesting of N and cannibalism on the resident populations; the second and third terms describe deaths due to cannibalism; the final term describes intra-specific competition for space and other limiting resources.

The energy conversion factor e and the competition coefficient c are treated as constant parameters, while the attack rate coefficients on zooplankton and conspecifics and the handling time are trait-dependent according to the following functions:

$$a_0(x) := \frac{2A_0}{\left(\frac{x}{x^0}\right)^{\alpha}+\left(\frac{x^0}{x^0}\right)^{\alpha}}, \tag{39a}$$

$$a(x_1,x_2) := A\frac{2}{\left(\frac{p\,x_1}{x_2}\right)^{\beta}+\left(\frac{x_2}{p\,x_1}\right)^{\beta}}\frac{x_1^{\gamma}}{\overline{x}^{\gamma}+x_1^{\gamma}}\left(1-\frac{x_1^{\delta}}{\overline{x}^{\delta}+x_1^{\delta}}\right), \tag{39b}$$

$$h(x) := w_1 x^{-w_2}. \tag{39c}$$

Harvesting zooplankton is effective only around a lower strategy x^0 (small body size, see (39a)), while cannibalism gets significant

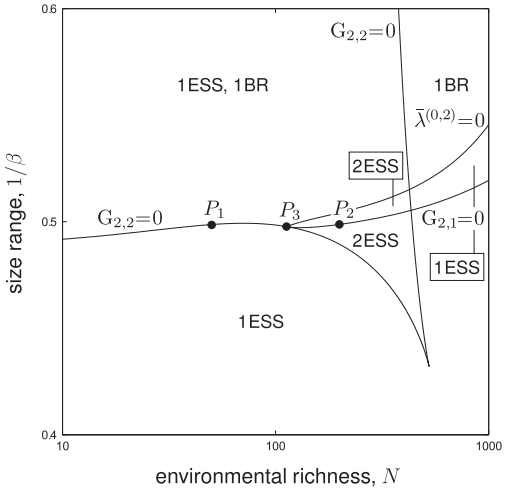

Fig. 11. Arrangements of the singular strategies of the *g*-function (38) w.r.t. parameters N and $1/\beta$ (reproduced from Dercole and Rinaldi, 2002, Fig. 3; parameter values: $c=1$, $e=0.6$, $A_0=1$, $x^0=0.1$, $\alpha=2$, $A=10$, $p=0.2$, $\underline{x}=0.5$, $\overline{x}=5$, $\gamma=8$, $\delta=2$, $w_1=0.1$, $w_2=0.25$; diagram obtained numerically with the package AUTO, Doedel et al., 2007).

only at larger strategies ($x>\overline{x}$, and up to a physically limiting strategy $\overline{x}$), with size preference for the victim given by the fraction $p\in(0,1)$ of the individual size (see (39b)). Handling time per unit of ingested food (39c) is decreasing with body size (see Dercole and Rinaldi, 2002, for a more detailed description).

Depending on the parameter values, there can be either one or two convergence-stable singular strategies, the larger of which can lead to evolutionary branching. This is shown in Fig. 11 in the plane of parameters N and $1/\beta$. While N describes the quality of the environment, in terms of food richness, $1/\beta$ is a surrogate for the juvenile-to-adult size range in the population (a larger $1/\beta$ results in a higher attack rate toward individuals of the same strategy, and this is possible only if the population size range is wider). Below we use the larger singular value as the reference strategy x close to which we unfold the resident–invader competition scenarios.

The transition from one to two singularities is the saddle-node AD bifurcation described in Section 3.3.1, at which condition (G2.2) fails. It occurs along the two boundaries of the cusp region in Fig. 11. Along the nearly vertical boundary, a repelling singularity collides and disappears with the non-reference (lower) convergence-stable singular strategy, whereas the repelling singularity collides and disappears with strategy x along the other boundary. Focusing on the reference singular strategy x, no other degeneracy occurs at point P_1 (i.e., condition (G2.1) is satisfied at P_1), whereas (G2.1) also fails at point P_3 (i.e., all fitness second derivatives vanish at P_3). Moreover, starting from point P_3, we can follow the curve corresponding to the other codimension-one degeneracy, along which (G2.1) fails while (G2.2) does not, point $P2$ being an example. Points P_1–P_3 therefore correspond to the degenerate singular strategies studied in Sections 3.3.1–3.3.3, respectively. Note that from point P_3 it is also possible to follow the curve corresponding to the (codimension-one) ESS-branching transition (along which $\bar{\lambda}^{(0,2)}=0$ under (G2.1) and (G2.2)).

We now unfold the bifurcations of the resident–invader dynamics for strategies x_1 and x_2 close to the singular value x and for parameters $(N,1/\beta)$ at points P_1–P_3 of Fig. 11. The genericity conditions and the relevant quantities for the classification of the singularity are reported in Table 5, according to which we expect (counting left-to-right/top-to-bottom) case 1 of Fig. 7 at point P_1, case 4 of Fig. 8 at point P_2, and case 5 of Fig. 9 at point P_3. The numerically obtained bifurcation diagrams (locally to the singular point (x,x) in the $(x_1,x_2)-$plane) are reported in Fig. 12 and confirm the classification.

Table 5
Relevant quantities and genericity conditions at points P_1, P_2, and P_3 in Fig. 11.

Quantity	P_1	P_2	P_3
N	50.0	200.0	112.55
β	2.0054	2.0050	2.0093
x	0.6101	0.7919	0.6345
$\overline{n}$	0.9849	1.8032	1.6588
$G_{2,1}$	-2.9516	–	–
$G_{2,2}$	–	-0.7575	–
$G_{3,1}$	-28.6660	–	-24.360
$G_{3,2}$	–	72.677	110.07
$G_{3,3}$	–	2.3538	5.3888
$G_{3,4}$	–	26.579	
$G_{3,5}$	–	–	-24.479
$G_{3,6}$	–	–	4478.9
$G^{+}_{3,7}$	–	–	-91.731
$G^{-}_{3,7}$	–	–	75.307
$G^{+}_{3,8}$	–	–	14.663
$G^{-}_{3,8}$	–	–	-7.5244
$G_{3,9}$	–	–	467.93
$G_{3,10}$	–	–	241.18
$G_{3,11}$	–	–	42.078
G_4	–	119.523	–
$\theta^{(1)}_{T2}(0)$	3.4337	-11.306	–
$\theta^{(2)}_{T2}(0)$	–	-223.12	–
$\theta^{(1)}_{F}(0)$	–	-12.404	–
$\Delta\theta^{+}_{T2}(0)$	–	–	$0.3352\,\frac{\pi}{2}$
$\Delta\theta^{-}_{T2}(0)$	–	–	$-0.7655\,\frac{\pi}{2}$
$C=\cos^2\Delta\theta_F(0):=G_{3,9}/G_{3,10}$		–	$\notin(0,1)$

5.2. Lotka–Volterra competition models

Lotka–Volterra resident–invader competition is described by the *g*-function:

$$g(n_1,n_2,x_1,x_2,x') := r(x')\left(1-\frac{\alpha(x',x_1)}{K(x')}n_1-\frac{\alpha(x',x_2)}{K(x')}n_2\right), \tag{40}$$

where $r(x)$ is the *intrinsic growth rate* (per-capita) of the species, $K(x)$ the *carrying capacity*, and $\alpha(x_1,x_2)$ the competition function, with

$$\alpha(x,x)=1. \tag{41}$$

No other intra- or inter-specific interactions are considered (i.e., $P=0$ and argument N is omitted in g).

The *g*-function being linear in the resident and invader densities n_1 and n_2, the right-hand side of Eq. (10) is linear in r, i.e., all functions $R_{i,j}$, $i<j$,arenullfori≥ 2(seeTable 1). Consequently, there cannot be two distinct internal equilibria for the relative invader density r and the saddle-node bifurcations generically expected in the analysis of Sections 3.3.2 (case (3.2): vanishing fitness cross-derivative) and 3.3.3 (case (3.3): vanishing all fitness second deriva-tives) cannot occur. In both cases (3.2) and (3.3), the saddle-node bifurcations occur under the genericity (transversality) condition (G3.3) (see the expression of (G3.3) for $P=0$in Table 3). We now show that $G_{3,3}=0$fortheg-function in (40) at a singular strategy x characterized by vanishing fitness cross-derivative.

Let us start from the invasion fitness

$$\lambda(x,x')=r(x')\left(1-\alpha(x',x)\frac{K(x)}{K(x')}\right),$$

where $\overline{n}(x)=K(x)$ is the resident monomorphic equilibrium. Taking the constraint (41) into account (together with its x-derivatives, e.g., $\alpha^{(1,0)}(x,x)+\alpha^{(0,1)}(x,x)=0$ at first order), the singularity

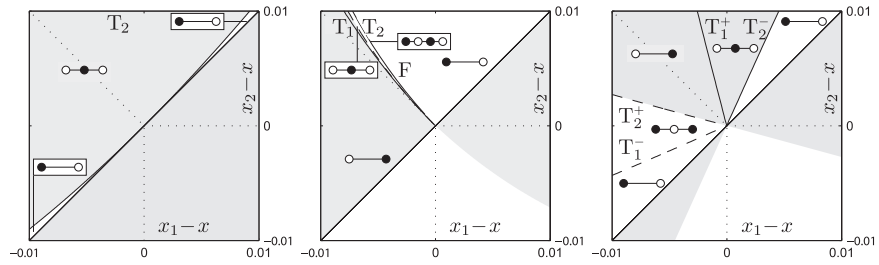

Fig. 12. Bifurcation diagrams of the resident–invader dynamics induced by the g-function (38) w.r.t. strategies (x_1, x_2) close to the singular point (x,x). From left to right, panels correspond to points P_1, P_2, and P_3 in Fig. 11 (diagrams obtained numerically with the package AUTO Doedel et al., 2007).

condition

$$\overline{\lambda}^{(0,1)} = \frac{r(x)}{K(x)}\Big(K^{(1)}(x) - K(x)\alpha^{(1,0)}(x,x)\Big) = 0$$

imposes

$$K^{(1)}(x) = K(x)\alpha^{(1,0)}(x,x), \tag{42}$$

whereas the degeneracy of the fitness cross-derivative

$$\overline{\lambda}^{(1,1)} = -r(x)\Big(\alpha^{(1,0)}(x,x)^2 + \alpha^{(1,1)}(x,x)\Big) = 0$$

imposes

$$\alpha^{(1,1)}(x,x) = -\alpha^{(1,0)}(x,x)^2. \tag{43}$$

Now, taking Eqs. (41)–(43) into account, we compute

$$\overline{\lambda}^{(0,2)} = \frac{r(x)}{K(x)}\Big(K^{(2)}(x) - K(x)\alpha^{(2,0)}(x,x)\Big) \tag{44}$$

and

$$\begin{aligned}\overline{\lambda}^{(2,1)} = &-\frac{r^{(1)}(x)}{K(x)}\Big(K^{(2)}(x) - K(x)\alpha^{(2,0)}(x,x)\Big)\\ &+r(x)\Big(2\alpha^{(1,0)}(x,x)^3 - \alpha^{(1,0)}(x,x)\alpha^{(2,0)}(x,x) - \alpha^{(1,2)}(x,x)\Big),\end{aligned} \tag{45}$$

whereas, from the g-function in (40), we have

$$\phi_{2,1}(n,x,x') = -\frac{r(x')}{K(x')}\alpha^{(0,2)}(x',x),$$

$$\overline{\phi}_{2,1} = -\frac{r(x)}{K(x)}\alpha^{(0,2)}(x,x) \overset{(2),(4)}{=} -\frac{r(x)}{K(x)}\Big(2\alpha^{(1,0)}(x,x)^2 - \alpha^{(2,0)}(x,x)\Big), \tag{46}$$

$$\begin{aligned}\overline{\phi}^{(0,0,1)}_{2,1} &= \frac{1}{K(x)}\Big(r(x)\Big(\alpha^{(1,0)}(x,x)\alpha^{(0,2)}(x,x) - \alpha^{(1,2)}(x,x)\Big) - r^{(1)}(x)\alpha^{(0,2)}(x,x)\Big)\\ &\overset{(2),(4)}{=} \frac{1}{K(x)}\Big(r(x)\Big(\alpha^{(1,0)}(x,x)\Big(2\alpha^{(1,0)}(x,x)^2 - \alpha^{(2,0)}(x,x)\Big) - \alpha^{(1,2)}(x,x)\Big)\\ &\quad - r^{(1)}(x)\Big(2\alpha^{(1,0)}(x,x)^2 - \alpha^{(2,0)}(x,x)\Big)\Big),\end{aligned} \tag{47}$$

$$\overline{g}^{(1,0,0,0,1)} = -\frac{r^{(1)}(x)}{K(x)}, \tag{48}$$

and

$$\overline{g}^{(1,0,0,0,0)} = -\frac{r(x)}{K(x)}. \tag{49}$$

Substituting Eqs. (44)–(49) into the expression for $G_{3,3}$ in Table 3 (for $P=0$), it is then trivial to check that all terms cancel out.

Note that all other conditions in Table 3 are generically satisfied, so the results of Sections 3.3.2 and 3.3.3 can be still applied, simply removing the saddle-node bifurcations from the diagrams in Figs. 8–10. However, further degeneracies can be obtained with particular choices for functions r, K, and α. For example, if

(i) resident–invader competition is assumed symmetric, i.e., $\alpha(x_1,x_2) = \alpha(x_2,x_1)$,

(ii) and determined by the strategy difference, i.e., $\alpha(x_1,x_2) = \alpha_0(x_1 - x_2)$, with function α_0 even ($\alpha^{(k)}(0) = 0$ for odd k) due to the symmetry assumed at point (i) and $\alpha_0(0) = 1$,

(iii) and the carrying capacity symmetrically peaks at the singular strategy x ($K^{(k)}(x) = 0$ for odd k and $K^{(2)}(x) < 0$)

(see, e.g., the competition model in Doebeli and Dieckmann, 2000, under symmetric competition), then it is not difficult to see that condition $G_{3,2}$ also vanishes.

In Section 3.3.2 (case (3.2)), $G_{3,2} = 0$ implies that the curvature of the transcritical bifurcations T_1 and T_2 is determined by the second-order derivative $\theta^{(2)}_{T2}(0) = -\theta^{(2)}_{T1}(0)$ (the two equal first-order curvatures $\theta^{(1)}_{T1}(0) = \theta^{(1)}_{T2}(0)$ vanish with $G_{3,2}$, see Eq. (25)). Thus, in the plane of the strategies (x_1,x_2), the two bifurcation curves symmetrically emanate from the singular point (x,x) on opposite sides of anti-diagonal. In Section 3.3.3 (case (3.3)), the assumptions (i)–(iii) also imply $G_{3,5} = 0$ and a fourth-order analysis is required in the expansion in (10). This is not done here, but our methodological approach can in principle deal with any degeneracy.

Finally, note that even though resident–invader competition is of Lotka–Volterra type (i.e., described as in (40) by linear density dependencies in the g-function) in most of applications (see Dercole and Rinaldi, 2008, and references therein), the model easily results generic (i.e., satisfying all genericity conditions in Table 3) if nonlinear density dependencies are present due to other intra- or inter-specific interactions. E.g., because of Allee effects describing spatial or mating structures or because resident and invader are prey or predator populations and harvesting is characterized by a nonlinear functional response.

6. Discussion and future directions

We have systematically investigated the competition between two similar one-dimensional strategies x_1 and x_2. We did that in the restricted but classical context of unstructured and asexual populations varying in continuous time in an isolated, homogeneous, and constant abiotic environment, and with intra- as well as inter-specific interactions described in the vicinity of a stationary regime.

The classification of the possible competition scenarios is made possible by a fundamental assumption on the growth rates of the interacting populations—property P4 of Section 2.1 (recently introduced by Dercole, 2015). Property P4 generalizes the classical mass-action principle that leads, in its original formulation, to linearly density-dependent per-capita growth rates (Lotka–Volterra demographic models). The generalization consists in allowing pairwise interactions in which the concurrent activities of the interacting individuals are also taken into consideration, and this induces a particular structure in the possible nonlinearities. Property P4 has two major technical consequences. One is that the expansion of the dynamics of invasion, w.r.t. the distance ε between point (x_1,x_2) in the strategy plane and the reference point (x,x) of interest, is composed of terms evaluated at the resident

equilibrium. This is a desirable feature in applications that is later discussed. The other consequence is that, up to order k in the expansion, the internal equilibria of the resident–invader dynamics are given by the roots of a polynomial of degree $(k-1)$.

We have unfolded the competition scenarios by increasing level of degeneracy in the corresponding invasion fitness. When the first-order fitness derivatives are not vanishing—i.e., away from a singular strategy—then $k=1$ is enough to characterize the dynamics of invasion, so there are no internal equilibria and we reobtained the "invasion implies substitution" theorem (after Geritz, 2005; Meszéna et al., 2005; Dercole and Rinaldi, 2008). When the second-order fit-ness cross-derivative is not vanishing at a singular strategy—condition (G2.1)—then $k=2$ is enough and, as a result, coexistence is protected whenever possible and it occurs at a unique internal equilibrium. Condition (G2.1) therefore characterizes generic singular strategies and competition in their vicinity is of Lotka–Volterra type: either stable coexistence, or mutual exclusion, or the dominance of one of the two types. Our results here retrace the original classifi-cation of singular strategies (Metz et al., 1996; Geritz et al., 1997, 1998), clarifying the role of the fitness cross-derivative.

Completely new results are obtained close to singular strategies with vanishing fitness cross-derivative. There, a third-order analysis is required ($k=3$) and unprotected coexistence is possible (with two internal equilibria, one stable and one not, see Fig. 1e and f). Two cases (with single and double degeneracy—codimension-one and -two) complete the classification of degeneracies caused by the second-order fitness derivatives. The first (codimension-one) is the case in which the second pure-derivatives are nonvanishing (Section 3.3.2). Then, resident–invader coexistence is confined in cusp regions in the plane of the two strategies (Fig. 8). In the second case (codimension-two), pure-derivatives are also null (Section 3.3.3) and the coexistence region is again conical (as in the generic case), though composed by multiple sectors (Figs. 9 and 10). In both situations there might be multiple cusp (resp. conical) regions characterized by different coexistence scenarios, some of which are unprotected. An important result here is that the stable equilibrium of coexistence is unique in each region, so there is only one way in which evolution can proceed. Alternative stable equilibria of coexistence require at least three internal equilibria (two stable and one not), that is possible only with fitness degeneracies up to third order (i.e., leading terms of order $k=4$ in the dynamics of invasion).

The arrangement of the bifurcation boundaries separating the different competition scenarios that can occur for strategies (x_1, x_2) close to the singular point (x,x) has been locally derived in each case. This analysis answers, among other things, an important question in the adaptive dynamics (AD) modeling framework (Metz et al., 1992, 1996; Dieckmann and Law, 1996; Geritz et al., 1997, 1998; Dercole and Rinaldi, 2008). That is: it shows how the region of validity of the "invasion implies substitution" theorem shrinks while approaching a singular strategy.

All our results hold in the limit $\varepsilon \to 0$, i.e., for the two competing strategies being sufficiently similar. In this limit, the dynamics of the total density of residents and invaders—the variable s—are much faster than the changes in the relative density r of invaders, and the results follow from standard time-scale separation techniques. Our results are therefore local to the reference point (x,x) in the strategy plane and complement those of Priklopil (2012) on the global structure of the bifurcation boundaries of the resident–invader coexistence region. However, by a continuity argument, we can conclude that the competition scenarios that we see close to degenerate singular strategies (e.g., unprotected coexistence in Sections 3.3.2 and 3.3.3) are also possible close to a generic, though nearly degenerate, singularity, provided the difference between resident and invader strategies is not too small.

That coexistence, whenever possible, generically occurs at a unique internal equilibrium was already known from Geritz (2005), Meszéna et al. (2005), and Durinx et al. (2008). These three contributions consider a single-species model, with the same ecological setting considered here (though the model is physiologically structured in Durinx et al. (2008), and nonstationary coexistence is also discussed in Meszéna et al., 2005).

Geritz (2005)assumes a "linear and finite-dimensional environmental feedback," meaning, in the present context, that only density-independent functions $\phi_{d_1,1}$ are present in property P4 (all others being null) and that a special product structure $\phi_{d_1,1}(x, x') = \phi'_{d_1,1}(x)\phi''_{d_1,1}(x')$ is assumed (the notion of "environmental feedback" was introduced in Metz and Diekmann, 1986 in the context of physiologically structured population models; see also Diekmann et al., 2001; Metz and Gyllenberg, 2001; see Dercole, 2015 for a discussion in the context of unstructured models). Geritz (2005) then show the uniqueness of the internal equilibrium of coexistence by exploiting the two-dimensionality of the resident-mutant demographic space.

A more general approach, making use of the time-scale separation between the aggregated density of the species and the relative densities of the different strategies, is taken in Mes-zéna et al. (2005) and in Durinx et al. (2008). Durinx et al. (2008) also assume a finite-dimensional environment (the product structure in the (x, x')−dependence of functions ϕ's) and allow for nonlinear density dependencies (without however being explicit on the structure of the allowed nonlinearities). They focus on extending the AD framework to physiologically structured population models and show, as a byproduct, that for sufficiently similar resident and invader strategies the model equilibria cor-respond to those of an appropriately chosen Lotka–Volterra model.

The focus in Meszéna et al. (2005) is on the joint demographic dynamics of a cloud of similar strategies. The fitness of the invader is defined as a functional over the density distribution of the resident strategies, the latter composed of a set of Dirac peaks in the strategy space. This approach has properties P1–P3 built-in, however, property P4 was not assumed. Although any functional accounting for individual birth and death processes and pairwise (or group) interactions also implies property P4 (Dercole, 2015), no restriction on the functional was considered. Meszéna et al. (2005) instead define an ad-hoc concept of functional derivative w.r.t. a distribution, through which they show P4 only up to first derivatives. Their main message is that mutations should not necessarily be infrequent to apply the AD framework. Even if several mutant types concomitantly compete, only the fittest generically wins, so the mutation-substitution picture of AD remains valid. Only close to a singular strategy the coexistence of similar strategies is possible and Meszéna et al. (2005) show that there is generically a unique equilibrium of coexistence.

With respect to the above contributions, we further show that the genericity condition for the uniqueness of the equilibrium of coexistence is the nonvanishing of the fitness cross-derivative (G2.1), and we do this in a multi-species context.

Besides our new results, and our refinements of previously known facts, our main contribution is the general methodological approach that allows the analysis of competition scenarios characterized by any order of degeneracies in the invasion fitness. Most importantly, the genericity conditions that are derived at each order, as well as the quantities discriminating among the competition scenarios that are possible case by case, can all be tested at the resident monomorphic equilibrium, i.e., before the appearance of the invader type. In fact, most of the genericity conditions (summarized in Table 3) are expressed in terms of the derivatives of the invasion fitness $\lambda(x_1, x_2)$ at the reference point (x,x). When this is not possible (see the stars over the equal sign in Table 3), the conditions are in any case expressed in terms of the "bar"-

evaluations of functions g and F (and their derivatives, including functions ϕ's and ψ of property P4 and their derivatives). These "bar"-evaluations do not require the full knowledge of functions g and F, defining the resident–invader model (1), but only the knowledge of functions g_1 and F_1 of property P1. That is, only the resident demographic equilibrium (defined by g_1 and F_1 in (2)) and a model for the invader dynamics locally to this equilibrium (that is the invasion fitness defined by g_1 in (3)) are necessary and sufficient to draw global conclusion on the resident–invader dynamics. This is very important in applications, where a model for the initial invader dynamics can be easily identified, theoreti-cally and/or experimentally, at the regime of the resident strate-gies. Hence, the potential of similar invaders can be tested without simulating and/or waiting for the full invasion transient.

Moving to future directions of research, further degenerate singular strategies (i.e., with degeneracies up to third or higher order) or ad-hoc degeneracies could be studied. The interest comes from both applications, where modeling assumptions and symmetries make models degenerate, and theory, to fully classify the competition scenarios that are possible for each type of degeneracy. For example, as discussed in Section 5.2, Lotka–Volterra models assume linear density dependencies in the functions g and F and, consequently, fail to satisfy the genericity conditions that require nonlinearities.

And not only the ecological dynamics should be unfolded, but also the evolutionary dynamics locally to the singular strategies allowing resident–invader coexistence. In particular, the well-known branching conditions of Geritz et al. (1997) and Geritz et al. (1998) are given in terms of the second-order fitness derivatives, but little is known (see a comment in Kisdi, 1999) if the evolutionary dynamics are dominated by third- (or higher-) orders in the fitness expansion. The analysis of degenerate evolutionary dynamics requires the third- (or higher-) order expansion of the dimorphic fitness—the invasion potential of a strategy in the environment set by two incipient branching strategies. Though an attempt appeared in Durinx (2008), the task is definitely nontrivial due to the nonsmoothness of the dimorphic fitness at the singular strategy (essentially due to the presence of a continuum of critically stable equilibria of model (1) if $x_1 = x_2 = x$). The case of the ESS-branching transition—vanishing second-pure-derivative $\lambda^{(\theta,2)}$–has already been discussed (Della Rossa et al., 2015), but the cases with vanishing fitness cross-derivative are still waiting. Again property P4 plays a crucial role in allowing the derivation of a proper expansion of the dimorphic fitness. If the expansion is taken to a sufficiently high order, it should give a theoretical base to interesting and unexpected evolutionary scenarios, like the evolutionary branching at an attracting ESS numerically observed by Doebeli and Ispolatov (2010).

Finally, all the results here discussed on the ecological and evolutionary dynamics between similar strategies should be extended to the context of structured populations, characterized by multi-dimensional (vector-valued) strategies. According to the analyses in Durinx (2008) and Durinx et al. (2008), analogous results are expected.

Acknowledgments

We thank Hans Metz for many nice and fruitful discussions and we acknowledge the help of Fabio Della Rossa in the use of the Mathematica package. This work was supported mainly by the Italian Ministry for University and Research (under Contract FIRB RBFR08TIA4) and partly by the Academy of Finland.

Appendix A. Derivatives of the resident equilibrium

Differentiating Eqs. (2a) and (2b) w.r.t. x_1 at $x_1 = x$ and solving for the derivatives $(\overline{n}^{(d)}(x), \overline{N}^{(d)}(x))$, $d \geq 1$, of the resident equilibrium, one gets the results of Table A1, where the $(P+1) \times (P+1)$ matrix M is the same of Table 1 and is here reported for the reader's convenience.

Matrix M is invertible thanks to the hyperbolicity of the resident equilibrium ($\tilde{M}$ being the adjugate matrix, i.e., the transpose of the matrix of cofactors of M). In fact, the Jacobian of model ((1)a, c) with $n_2 = 0$ and $x_1 = x$ is nothing but M with the first row multiplied by $\overline{n}$. If the $P \times P$ matrix $\overline{F}^{(0,0,1,0,0)}$ is invertible, then we have

$$\det M = (\overline{g}^{(1,0,0,0,0,0)} - \overline{g}^{(0,0,1,0,0,0)}(\overline{F}^{(0,0,1,0,0)})^{-1}\overline{F}^{(1,0,0,0,0)}) \det \overline{F}^{(0,0,1,0,0)},$$

$$\tilde{g}^{(1,0,0,0,0,0)} = \det \overline{F}^{(0,0,1,0,0)},$$

$$\tilde{g}^{(0,0,1,0,0,0)} = -\overline{g}^{(0,0,1,0,0,0)} \det \overline{F}^{(0,0,1,0,0)} (\overline{F}^{(0,0,1,0,0)})^{-1},$$

$$\tilde{F}^{(1,0,0,0,0)} = -\det \overline{F}^{(0,0,1,0,0)} (\overline{F}^{(0,0,1,0,0)})^{-1} \overline{F}^{(1,0,0,0,0)},$$

$$\tilde{F}^{(0,0,1,0,0)} = (\overline{F}^{(0,0,1,0,0)})^{-1} (\det M I_P + \overline{F}^{(1,0,0,0,0)} \overline{g}^{(0,0,1,0,0,0)} \det \overline{F}^{(0,0,1,0,0)} (\overline{F}^{(0,0,1,0,0)})^{-1}),$$

but this needs not to be the case.

Table A1
Derivatives of the resident equilibrium $(\overline{n}(x), \overline{N}(x))$.

$$\overline{n}^{(d)} = \frac{1}{\det M}\left(\tilde{g}^{(1,0,0,0,0,0)}\overline{q}_d + \tilde{g}^{(0,0,1,0,0,0)}\overline{Q}_d\right)$$

$$\overline{N}^{(d)} = \frac{1}{\det M}\left(\tilde{F}^{(1,0,0,0,0)}\overline{q}_d + \tilde{F}^{(0,0,1,0,0)}\overline{Q}_d\right)$$

$$M := \begin{bmatrix} \overline{g}^{(1,0,0,0,0,0)} & \overline{g}^{(0,0,1,0,0,0)} \\ \overline{F}^{(1,0,0,0,0)} & \overline{F}^{(0,0,1,0,0)} \end{bmatrix}, \quad \tilde{M} := \begin{bmatrix} \tilde{g}^{(1,0,0,0,0,0)} & \tilde{g}^{(0,0,1,0,0,0)} \\ \tilde{F}^{(1,0,0,0,0)} & \tilde{F}^{(0,0,1,0,0)} \end{bmatrix}, \quad \tilde{M}M = M\tilde{M} = \det M\, I_{1+P}$$

$$-\overline{q}_1 := \overline{g}^{(0,0,0,1,0,0)} + \overline{g}^{(0,0,0,0,0,1)}$$

$$-\overline{Q}_1 := \overline{F}^{(0,0,0,1,0)}$$

$$\begin{aligned} -\overline{q}_2 :=\ & \overline{g}^{(2,0,0,0,0,0)}(\overline{n}^{(1)})^2 + 2\,\overline{g}^{(1,0,1,0,0,0)}\overline{n}^{(1)}\overline{N}^{(1)} + \overline{g}^{(0,0,2,0,0,0)}[\overline{N}^{(1)}, \overline{N}^{(1)}] \\ & + 2\,\overline{g}^{(1,0,0,1,0,0)}\overline{n}^{(1)} + 2\,\overline{g}^{(1,0,0,0,0,1)}\overline{n}^{(1)} + 2\,\overline{g}^{(0,0,1,1,0,0)}\overline{N}^{(1)} + 2\,\overline{g}^{(0,0,1,0,0,1)}\overline{N}^{(1)} \\ & + \overline{g}^{(0,0,0,2,0,0)} + 2\,\overline{g}^{(0,0,0,1,0,1)} + \overline{g}^{(0,0,0,0,0,2)} \end{aligned}$$

$$\begin{aligned} -\overline{Q}_2 :=\ & \overline{F}^{(2,0,0,0,0)}(\overline{n}^{(1)})^2 + 2\,\overline{F}^{(1,0,1,0,0)}\overline{n}^{(1)}\overline{N}^{(1)} + \overline{F}^{(0,0,2,0,0)}[\overline{N}^{(1)}, \overline{N}^{(1)}] \\ & + 2\,\overline{F}^{(1,0,0,1,0)}\overline{n}^{(1)} + 2\,\overline{F}^{(0,0,1,1,0)}\overline{N}^{(1)} + \overline{F}^{(0,0,0,2,0)} \end{aligned}$$

$$\begin{aligned} -\overline{q}_3 :=\ & 3\,\overline{g}^{(2,0,0,0,0,0)}\overline{n}^{(1)}\overline{n}^{(2)} + 3\,\overline{g}^{(1,0,1,0,0,0)}\left(\overline{n}^{(2)}\overline{N}^{(1)} + \overline{n}^{(1)}\overline{N}^{(2)}\right) \\ & + 3\,\overline{g}^{(1,0,0,1,0,0)}\overline{n}^{(2)} + 3\,\overline{g}^{(1,0,0,0,0,1)}\overline{n}^{(2)} + 3\,\overline{g}^{(0,0,2,0,0,0)}[\overline{N}^{(1)}, \overline{N}^{(2)}] \\ & + 3\,\overline{g}^{(0,0,1,1,0,0)}\overline{N}^{(2)} + 3\,\overline{g}^{(0,0,1,0,0,1)}\overline{N}^{(2)} + \overline{g}^{(3,0,0,0,0,0)}(\overline{n}^{(1)})^3 \\ & + 3\,\overline{g}^{(2,0,1,0,0,0)}(\overline{n}^{(1)})^2\overline{N}^{(1)} + 3\,\overline{g}^{(2,0,0,1,0,0)}(\overline{n}^{(1)})^2 + 3\,\overline{g}^{(2,0,0,0,0,1)}(\overline{n}^{(1)})^2 \\ & + 3\,\overline{g}^{(1,0,2,0,0,0)}[\overline{N}^{(1)}, \overline{N}^{(1)}]\overline{n}^{(1)} + 6\,\overline{g}^{(1,0,1,1,0,0)}\overline{n}^{(1)}\overline{N}^{(1)} + 6\,\overline{g}^{(1,0,1,0,0,1)}\overline{n}^{(1)}\overline{N}^{(1)} \\ & + 3\,\overline{g}^{(1,0,0,2,0,0)}\overline{n}^{(1)} + 6\,\overline{g}^{(1,0,0,1,0,1)}\overline{n}^{(1)} + 3\,\overline{g}^{(1,0,0,0,0,2)}\overline{n}^{(1)} \\ & + \overline{g}^{(0,0,3,0,0,0)}[\overline{N}^{(1)}, \overline{N}^{(1)}, \overline{N}^{(1)}] + 3\,\overline{g}^{(0,0,2,1,0,0)}[\overline{N}^{(1)}, \overline{N}^{(1)}] + 3\,\overline{g}^{(0,0,2,0,0,1)}[\overline{N}^{(1)}, \overline{N}^{(1)}] \\ & + 3\,\overline{g}^{(0,0,1,2,0,0)}\overline{N}^{(1)} + 6\,\overline{g}^{(0,0,1,1,0,1)}\overline{N}^{(1)} + 3\,\overline{g}^{(0,0,1,0,0,2)}\overline{N}^{(1)} + \overline{g}^{(0,0,0,3,0,0)} \\ & + 3\,\overline{g}^{(0,0,0,2,0,1)} + 3\,\overline{g}^{(0,0,0,1,0,2)} + \overline{g}^{(0,0,0,0,0,3)} \end{aligned}$$

$$\begin{aligned} -\overline{Q}_3 :=\ & 3\,\overline{F}^{(2,0,0,0,0)}\overline{n}^{(1)}\overline{n}^{(2)} + 3\,\overline{F}^{(1,0,1,0,0)}\left(\overline{n}^{(2)}\overline{N}^{(1)} + \overline{n}^{(1)}\overline{N}^{(2)}\right) \\ & + 3\,\overline{F}^{(1,0,0,1,0)}\overline{n}^{(2)} + 3\,\overline{F}^{(0,0,2,0,0)}[\overline{N}^{(1)}, \overline{N}^{(2)}] \\ & + 3\,\overline{F}^{(0,0,1,1,0)}\overline{N}^{(2)} + \overline{F}^{(3,0,0,0,0)}(\overline{n}^{(1)})^3 \\ & + 3\,\overline{F}^{(2,0,1,0,0)}(\overline{n}^{(1)})^2\overline{N}^{(1)} + 3\,\overline{F}^{(2,0,0,1,0)}(\overline{n}^{(1)})^2 \\ & + 3\,\overline{F}^{(1,0,2,0,0)}[\overline{N}^{(1)}, \overline{N}^{(1)}]\overline{n}^{(1)} + 6\,\overline{F}^{(1,0,1,1,0)}\overline{n}^{(1)}\overline{N}^{(1)} \\ & + 3\,\overline{F}^{(1,0,0,2,0)}\overline{n}^{(1)} + \overline{F}^{(0,0,3,0,0)}[\overline{N}^{(1)}, \overline{N}^{(1)}, \overline{N}^{(1)}] + 3\,\overline{F}^{(0,0,2,1,0)}[\overline{N}^{(1)}, \overline{N}^{(1)}] \\ & + 3\,\overline{F}^{(0,0,1,2,0)}\overline{N}^{(1)} + \overline{F}^{(0,0,0,3,0)} \end{aligned}$$

Table A2
Derivatives of the resident equilibrium $\overline{n}$ for $P=0$ (recall that $\overline{g}^{(1,0,0,0,0)}<0$ due to the hyperbolic stability of the equilibrium).

$$\overline{n}^{(d)} = \frac{\overline{q}_d}{\overline{g}^{(1,0,0,0,0)}}$$

$$-\overline{q}_1 := \overline{g}^{(0,0,1,0,0)} + \overline{g}^{(0,0,0,0,1)}$$

$$-\overline{q}_2 := \overline{g}^{(2,0,0,0,0)}(\overline{n}^{(1)})^2 + 2\left(\overline{g}^{(1,0,1,0,0)} + \overline{g}^{(1,0,0,0,1)}\right)\overline{n}^{(1)} + \overline{g}^{(0,0,2,0,0)} + 2\,\overline{g}^{(0,0,1,0,1)} + \overline{g}^{(0,0,0,0,2)}$$

$$-\overline{q}_3 := 3\,\overline{g}^{(2,0,0,0,0)}\overline{n}^{(1)}\overline{n}^{(2)} + 3\left(\overline{g}^{(1,0,1,0,0)} + \overline{g}^{(1,0,0,0,1)}\right)\overline{n}^{(2)} + \overline{g}^{(3,0,0,0,0)}(\overline{n}^{(1)})^3 + 3\left(\overline{g}^{(2,0,1,0,0)} + \overline{g}^{(2,0,0,0,1)}\right)(\overline{n}^{(1)})^2 + 3\left(\overline{g}^{(1,0,2,0,0)} + 2\,\overline{g}^{(1,0,1,0,1)} + \overline{g}^{(1,0,0,0,2)}\right)\overline{n}^{(1)} + \overline{g}^{(0,0,3,0,0)} + 3\,\overline{g}^{(0,0,2,0,1)} + 3\,\overline{g}^{(0,0,1,0,2)} + \overline{g}^{(0,0,0,0,3)}$$

In case the resident and invader populations have no other intra- or inter-specific interaction, i.e., the case $P=0$, the expressions in Table A1 simplify as in Table A2 (obtained by taking conditions (13a)–(13d) into account and removing the argument N from function g).

Appendix B. Expansion of the fast-equilibrium manifold

The fast-equilibrium manifold $\{s_f(r,\varepsilon,\theta), N_f(r,\varepsilon,\theta),\ r\in[0,1]\}$ is defined by the equilibrium condition for Eqs. (7a) and (7c) (including the $O(\varepsilon)$-terms!), after using the substitutions in (9), i.e.,

$$0 = (1-r)g((1-r)s_f(r,\varepsilon,\theta), rs_f(r,\varepsilon,\theta), N_f(r,\varepsilon,\theta), x+\varepsilon\cos\theta, x+\varepsilon\sin\theta, x+\varepsilon\cos\theta) + rg((1-r)s_f(r,\varepsilon,\theta), rs_f(r,\varepsilon,\theta), N_f(r,\varepsilon,\theta), x+\varepsilon\cos\theta, x+\varepsilon\sin\theta, x+\varepsilon\sin\theta), \tag{B.1a}$$

$$0 = F((1-r)s_f(r,\varepsilon,\theta), rs_f(r,\varepsilon,\theta), N_f(r,\varepsilon,\theta), x+\varepsilon\cos\theta, x+\varepsilon\sin\theta). \tag{B.1b}$$

By expanding both equations in (B.1) around $\varepsilon=0$, taking the results of Table A1 into account, and separately solving the terms of order $k=0,\ldots,3$ for $s_f^{(0,k,0)}(r,0,\theta)$ and $N_f^{(0,k,0)}(r,0,\theta)$, we get the results in Table B1 (where the $(P+1)\times(P+1)$ nonsingular matrix M is the same of Tables 1 and A1, see Supplementary Data).

As anticipated in Section 2.3, the derivatives $s_f^{(0,k,0)}(r,0,\theta)$ and $N_f^{(0,k,0)}(r,0,\theta)$, $k\geq 1$, characterize the ε-perturbations of the fast-equilibrium manifold from the zero-order solution $(s_f(r,0,\theta),\ N_f(r,0,\theta)) = (\overline{n},\overline{N})$. They are given by polynomial expressions in r with degree equal to the order of differentiation and coefficients that are ultimately functions of the reference strategy x and of the perturbation angle θ.

Recall that only the derivatives $s_f^{(0,k,0)}(r,0,\theta)$ and $N_f^{(0,k,0)}(r,0,\theta)$ up to order $k-1$ are needed to determine functions $R_{i,k}$ in Table 1. This is due to the fact that only g-derivatives with at least one order of differentiation w.r.t. the last argument (the invader strategy) matter in Eq. (7b). Thus, only first and second derivatives are needed to derive the results in Table 1, whereas the third derivatives are used to derive the expression of $\overline{R}_{0,4}$ in Table 2, that is used to evaluate (G4).

Finally, the expressions in Table B1 simplify as in Table B2 (taking conditions ((2)a–d) into account and removing the argument N from functions g and ϕ's), if the resident and invader populations have no other intra- or inter-specific interaction (the case $P=0$).

Table B1
ε-Expansion of the fast-equilibrium manifold $\{s_f(r,\varepsilon,\theta),\ N_f(r,\varepsilon,\theta),\ r\in[0,1]\}$.

$$s_f^{(0,k,0)}(r,0,\theta) = ((1-r)\cos\theta + r\sin\theta)^k\overline{n}^{(k)} + \frac{1}{\det M}\left(\tilde{g}^{(1,0,0,0,0,0)}q_{f,k} + \tilde{g}^{(0,0,1,0,0,0)}Q_{f,k}\right)$$

$$N_f^{(0,k,0)}(r,0,\theta) = ((1-r)\cos\theta + r\sin\theta)^k\overline{N}^{(k)} + \frac{1}{\det M}\left(\tilde{F}^{(1,0,0,0,0)}q_{f,k} + \tilde{F}^{(0,0,1,0,0)}Q_{f,k}\right)$$

$$q_{f,0} = Q_{f,0} = q_{f,1} = Q_{f,1} := 0$$

$$-q_{f,2} := r(1-r)(\sin\theta - \cos\theta)^2\left(\overline{g}^{(0,0,0,0,0,2)} + \overline{\phi}_{2,1}\,\overline{n}\right)$$

$$-Q_{f,2} := r(1-r)(\sin\theta - \cos\theta)^2\,\overline{\psi}_{2,1}\,\overline{n}$$

$$\begin{aligned}
-q_{f,3} :=\ & r(1-r)(\sin\theta-\cos\theta)^2((2-r)\cos\theta+(1+r)\sin\theta)\left(\overline{g}^{(0,0,0,0,0,3)} + \overline{\phi}_{3,1}\,\overline{n}\right)\\
&+3r(1-r)(\sin\theta-\cos\theta)^2((1-r)\cos\theta+r\sin\theta)\left(\overline{g}^{(0,0,0,1,0,2)} + \overline{g}^{(1,0,0,0,0,2)}\overline{n}^{(1)}\right.\\
&\left.+\overline{g}^{(0,0,1,0,0,2)}\overline{N}^{(1)} + \overline{\phi}_{2,1}\,\overline{n}^{(1)} + \overline{\phi}_{2,1}^{(1,0,0,0)}\overline{n}\overline{n}^{(1)} + \overline{\phi}_{2,1}^{(0,1,0,0)}\overline{n}\overline{N}^{(1)} + \overline{\phi}_{2,1}^{(0,0,0,1)}\overline{n}\right)\\
&+r(1-r)\left((1-r)\cos^3\theta+(3r-2)\cos^2\theta\sin\theta+(1-3r)\cos\theta\sin^2\theta+r\sin^3\theta\right)\overline{\phi}_{3,2}\,\overline{n}^2\\
&-3((1-r)\cos\theta+r\sin\theta)\left(\overline{g}^{(1,0,1,0,0,0)}\overline{N}^{(1)} + \overline{g}^{(2,0,0,0,0,0)}\overline{n}^{(1)} + \overline{g}^{(1,0,0,1,0,0)} + \overline{g}^{(1,0,0,0,0,1)}\right)\\
&\times\left(((1-r)\cos\theta+r\sin\theta)^2\overline{n}^{(2)} - s_f^{(0,2,0)}(r,0,\theta)\right)\\
&-3((1-r)\cos\theta+r\sin\theta)\left(\overline{g}^{(1,0,1,0,0,0)}\overline{n}^{(1)} + \overline{g}^{(0,0,1,1,0,0)} + \overline{g}^{(0,0,1,0,0,1)}\right)\\
&\times\left(((1-r)\cos\theta+r\sin\theta)^2\overline{N}^{(2)} - N_f^{(0,2,0)}(r,0,\theta)\right)\\
&-3((1-r)\cos\theta+r\sin\theta)\overline{g}^{(0,0,2,0,0,0)}[\overline{N}^{(1)}, \left(((1-r)\cos\theta+r\sin\theta)^2\overline{N}^{(2)} - N_f^{(0,2,0)}(r,0,\theta)\right)]
\end{aligned}$$

$$\begin{aligned}
-Q_{f,3} :=\ & r(1-r)(\sin\theta-\cos\theta)^2((2-r)\cos\theta+(1+r)\sin\theta)\overline{\psi}_{3,1}\,\overline{n}\\
&+3r(1-r)(\sin\theta-\cos\theta)^2((1-r)\cos\theta+r\sin\theta)\left(\overline{\psi}_{2,1}\,\overline{n}^{(1)} + \overline{\psi}_{2,1}^{(1,0,0)}\overline{n}\overline{n}^{(1)} + \overline{\psi}_{2,1}^{(0,1,0)}\overline{n}\overline{N}^{(1)}\right)\\
&+r(1-r)\left((1-r)\cos^3\theta+(3r-2)\cos^2\theta\sin\theta+(1-3r)\cos\theta\sin^2\theta+r\sin^3\theta\right)\overline{\psi}_{3,2}\,\overline{n}^2\\
&-3((1-r)\cos\theta+r\sin\theta)\left(\overline{F}^{(1,0,1,0,0)}\overline{N}^{(1)} + \overline{F}^{(2,0,0,0,0)}\overline{n}^{(1)} + \overline{F}^{(1,0,0,1,0)}\right)\\
&\times\left(((1-r)\cos\theta+r\sin\theta)^2\overline{n}^{(2)} - s_f^{(0,2,0)}(r,0,\theta)\right)\\
&-3((1-r)\cos\theta+r\sin\theta)\left(\overline{F}^{(1,0,1,0,0)}\overline{n}^{(1)} + \overline{F}^{(0,0,1,1,0,0)}\right)\\
&\times\left(((1-r)\cos\theta+r\sin\theta)^2\overline{N}^{(2)} - N_f^{(0,2,0)}(r,0,\theta)\right)\\
&-3((1-r)\cos\theta+r\sin\theta)\overline{F}^{(0,0,2,0,0)}[\overline{N}^{(1)}, \left(((1-r)\cos\theta+r\sin\theta)^2\overline{N}^{(2)} - N_f^{(0,2,0)}(r,0,\theta)\right)]
\end{aligned}$$

Table B2
ε-Expansion of the fast-equilibrium manifold $\{s_f(r,\varepsilon,\theta),\ r\in[0,1]\}$ for $P=0$ (recall that $\overline{g}^{(1,0,0,0,0,0)}<0$ due to the hyperbolic stability of the equilibrium).

$$s_f^{(0,k,0)}(r,0,\theta) = ((1-r)\cos\theta + r\sin\theta)^k\overline{n}^{(k)} + \frac{q_{f,k}}{\overline{g}^{(1,0,0,0,0,0)}}$$

$$q_{f,0} = q_{f,1} := 0$$

$$-q_{f,2} := r(1-r)(\sin\theta - \cos\theta)^2\left(\overline{g}^{(0,0,0,0,0,2)} + \overline{\phi}_{2,1}\,\overline{n}\right)$$

$$\begin{aligned}
-q_{f,3} :=\ & r(1-r)(\sin\theta-\cos\theta)^2((2-r)\cos\theta+(1+r)\sin\theta)\left(\overline{g}^{(0,0,0,0,0,3)} + \overline{\phi}_{3,1}\,\overline{n}\right)\\
&+3r(1-r)(\sin\theta-\cos\theta)^2((1-r)\cos\theta+r\sin\theta)\\
&\times\left(\overline{g}^{(0,0,1,0,0,2)} + \overline{g}^{(1,0,0,0,0,2)}\overline{n}^{(1)} + \overline{\phi}_{2,1}\,\overline{n}^{(1)} + \overline{\phi}_{2,1}^{(1,0,0)}\overline{n}\overline{n}^{(1)} + \overline{\phi}_{2,1}^{(0,0,1)}\overline{n}\right)\\
&+r(1-r)\left((1-r)\cos^3\theta+(3r-2)\cos^2\theta\sin\theta+(1-3r)\cos\theta\sin^2\theta+r\sin^3\theta\right)\overline{\phi}_{3,2}\,\overline{n}^2\\
&-3((1-r)\cos\theta+r\sin\theta)\left(\overline{g}^{(2,0,0,0,0,0)}\overline{n}^{(1)} + \overline{g}^{(1,0,1,0,0)} + \overline{g}^{(1,0,0,0,1)}\right)\\
&\times\left(((1-r)\cos\theta+r\sin\theta)^2\overline{n}^{(2)} - s_f^{(0,2,0)}(r,0,\theta)\right)
\end{aligned}$$

Appendix C. Supplementary data

Supplementary data associated with this paper can be found in the online version at http://dx.doi.org/10.1016/j.jtbi.2015.11.032.

References

Bulmer, M.G., 1980. The Mathematical Theory of Quantitative Genetics. Oxford University Press, New York.

Della Rossa, F., Dercole, F., Landi, P., 2015. The branching bifurcation of adaptive dynamics. Int. J. Bifurcat. Chaos 25, 1540001.

Dercole, F., 2003. Remarks on branching-extinction evolutionary cycles. J. Math. Biol. 47, 569–580.

Dercole, F., 2005. Border collision bifurcations in the evolution of mutualistic interactions. Int. J. Bifurcat. Chaos 15, 2179–2190.

Dercole, F., 2015. The ecology of asexual pairwise interactions: the generalized law of mass action. Theor. Ecol., http://dx.doi.org/10.1007/s12080-015-0287-3, in press.

Dercole, F., Dieckmann, U., Obersteiner, M., Rinaldi, S., 2008. Adaptive dynamics and technological change. Technovation 28, 335–348.

Dercole, F., Ferrière, R., Rinaldi, S., 2002. Ecological bistability and evolutionary reversals under asymmetrical competition. Evolution 56, 1081–1090.

Dercole, F., Ferrière, R., Rinaldi, S., 2010a. Chaotic Red Queen coevolution in three-species food chains. Proc. R. Soc. Lond. B: Biol. 277, 2321–2330.

Dercole, F., Gragnani, A., Ferrière, R., Rinaldi, S., 2006. Coevolution of slow-fast populations: evolutionary sliding, evolutionary pseudo-equilibria and complex Red Queen dynamics. Proc. R. Soc. Lond. B: Biol. 273, 983–990.

Dercole, F., Irisson, J.O., Rinaldi, S., 2003. Bifurcation analysis of a prey–predator coevolution model. SIAM J. Appl. Math. 63, 1378–1391.

Dercole, F., Prieu, C., Rinaldi, S., 2010b. Technological change and fisheries sustainability: the point of view of adaptive dynamics. Ecol. Model. 221, 379–387.

Dercole, F., Rinaldi, S., 2002. Evolution of cannibalistic traits: scenarios derived from adaptive dynamics. Theor. Popul. Biol. 62, 365–374.

Dercole, F., Rinaldi, S., 2008. Analysis of Evolutionary Processes: The Adaptive Dynamics Approach and its Applications. Princeton University Press, Princeton, NJ.

Dercole, F., Rinaldi, S., 2010. Evolutionary dynamics can be chaotic: a first example. Int. J. Bifurcat. Chaos 20, 3473–3485.

Dieckmann, U., Law, R., 1996. The dynamical theory of coevolution: a derivation from stochastic ecological processes. J. Math. Biol. 34, 579–612.

Diekmann, O., Gyllenberg, M., Huang, H., Kirkilionis, M., Metz, J.A.J., Thieme, H.R., 2001. On the formulation and analysis of general deterministic structured population models. II. Nonlinear theory. J. Math. Biol. 43, 157–189.

Doebeli, M., Dieckmann, U., 2000. Evolutionary branching and sympatric speciation caused by different types of ecological interactions. Am. Nat. 156, 77–101. Doebeli, M., Ispolatov, I., 2010. Continuously stable strategies as evolutionary branching points. J. Theor. Biol. 266, 529–535.

Doedel, E.J., Champneys, A.R., Dercole, F., Fairgrieve, T.F., Kuznetsov, Yu.A., Oldeman, B., Paffenroth, R.C., Sandstede, B., Wang, X.J., Zhang, C.H., 2007. AUTO-07p: Continuation and Bifurcation Software for Ordinary Differential Equations. Department of Computer Science, Concordia University, Montreal, QC.

Durinx, M., 2008. Life Amidst Singularities (Doctoral thesis). Institute of Biology, Leiden University. The Netherlands.

Durinx, M., Metz, J.A.J., Meszéna, G., 2008. Adaptive dynamics for physiologically structured population models. J. Math. Biol. 56, 673–742.

Fenichel, N., 1979. Geometric singular perturbation theory for ordinary differential equations. J. Differ. Equ. 31, 53–98.

Gause, G.F., 1934. The Struggle for Existence. Williams and Wilkins, Baltimore.

Geritz, S.A.H., 2005. Resident–invader dynamics and the coexistence of similar strategies. J. Math. Biol. 50, 67–82.

Geritz, S.A.H., Gyllenberg, M., Jacobs, F.J.A., Parvinen, K., 2002. Invasion dynamics and attractor inheritance. J. Math. Biol. 44, 548–560.

Geritz, S.A.H., Kisdi, E., Meszéna, G., Metz, J.A.J., 1998. Evolutionarily singular strategies and the adaptive growth and branching of the evolutionary tree. Evol. Ecol. 12, 35–57.

Geritz, S.A.H., Kisdi, E., van der Meijden, E., Metz, J.A.J., 1999. Evolutionarily dynamics of seed size and seedling competitive ability. Theor. Popul. Biol. 55, 324–343.

Geritz, S.A.H., Metz, J.A.J., Kisdi, E., Meszéna, G., 1997. The dynamics of adaptation and evolutionary branching. Phys. Rev. Lett. 78, 2024–2027.

Gintis, H., 2000. Game Theory Evolving. Princeton University Press, Princeton, NJ.

Grossman, G.M., Helpman, E., 1991. Innovation and Growth in the Global Economy. MIT Press, Cambridge, MA.

Hardin, G., 1960. The competitive exclusion principle. Science 131, 1292–1298.

Hek, G., 2010. Geometric singular perturbation theory in biological practice. J. Math. Biol. 60, 347–386.

Hofbauer, J., Sigmund, K., 2003. Evolutionary games dynamics. Bull. Am. Math. Soc. 40, 479–519.

Hoppensteadt, F., 1966. Singular perturbations on the infinite interval. Trans. Am. Math. Soc. 123, 521–535.

Kisdi, E., 1999. Evolutionary branching under asymmetric competition. J. Theor. Biol. 197, 149–162.

Kuznetsov, Yu.A., 2004. Elements of Applied Bifurcation Theory, 3rd ed.. Springer-Verlag, Berlin.

Landi, P., Dercole, F., Rinaldi, S., 2013. Branching scenarios in eco-evolutionary prey–predator models. SIAM J. Appl. Math. 73, 1634–1658.

Lotka, A.J., 1920. Analytic note on certain rhythmic relations in organic systems. Proc. Natl. Acad. Sci. 6, 410–415.

Maynard-Smith, J., 1982. Evolution and the Theory of Games. Cambridge University Press, Cambridge, UK.

Maynard-Smith, J., 1993. The Theory of Evolution, 3rd ed.. Cambridge University Press, Cambridge, UK.

Maynard Smith, J., Price, J., 1973. The logic of animal conflicts. Nature 246, 15–18.

Mayr, E., 1982. The Growth of Biological Thought. Harvard University Press, Cambridge, MA.

Meijer, H.G.E., Dercole, F., Oldeman, B.E., 2009. Numerical bifurcation analysis. In: Meyers, R.A. (Ed.), Encyclopedia of Complexity and System Science. Springer-Verlag, Berlin, pp. 6329–6352.

Meszéna, G., Gyllenberg, M., Jacobs, F.J., Metz, J.A.J., 2005. Link between population dynamics and dynamics of Darwinian evolution. Phys. Rev. Lett. 95, 078105.

Metz, J.A.J., Diekmann, O., 1986. The Dynamics of Physiologically Structured Populations. Lecture Notes in Biomathematics, vol. 68. Springer-Verlag, Berlin.

Metz, J.A.J., Geritz, S.A.H., Meszéna, G., Jacobs, F.J.A., van Heerwaarden, J.S., 1996. Adaptive dynamics: a geometrical study of the consequences of nearly faithful reproduction. In: van-Strien, S.J., Verduyn-Lunel, S.M. (Eds.), Stochastic and Spatial Structures of Dynamical Systems. Elsevier Science, Burlington, MA, pp. 183–231.

Metz, J.A.J., Gyllenberg, M., 2001. How should we define fitness in structured metapopulation models? Including an application to the calculation of evolutionarily stable dispersal strategies. Proc. R. Soc. Lond. B: Biol. 268, 499–508. Metz, J.A.J., Nisbet, R.M., Geritz, S.A.H., 1992. How should we define fitness for general ecological scenarios? Trends Ecol. Evol. 7, 198–202.

Mylius, S.D., Diekmann, O., 2001. The resident strikes back: on the evolutionary jumping between population dynamical attractors. J. Theor. Biol. 211, 297–311.

Priklopil, T., 2012. On invasion boundaries and the unprotected coexistence of two strategies. J. Math. Biol. 64, 1137–1156.

Sutton, R.S., Barto, A.G., 1998. Reinforcement Learning: An Introduction. MIT Press, Cambridge, MA.

Vincent, T.L., Brown, J.S., 2005. Evolutionary Game Theory, Natural Selection, and Darwinian Dynamics. Cambridge University Press, Cambridge, UK.

Volterra, V., 1926. Variazioni e fluttuazioni del numero d'individui in specie animali conviventi. Mem. Accad. Naz. Lincei 2, 31–113 (in Italian).

Ziman, J. (Ed.), 2000. Technological Innovation as an Evolutionary Process. Cambridge University Press, Cambridge, UK.